Characterization of PfFNT – a lactate transporter in *Plasmodium falciparum*

Dissertation

zur Erlangung des Doktorgrades

der Mathematisch-Naturwissenschaftlichen Fakultät

der Christian-Albrechts-Universität zu Kiel

vorgelegt von

Janis Rambow

Kiel 2015

Erster Gutachter:	Prof. Dr. Eric Beitz
Zweiter Gutachter:	Prof. Dr. Christian Peifer
Tag der mündlichen Prüfung:	13.02.2015
Zum Druck genehmigt:	13.02.2015

gez. Prof. Dr. Wolfgang Duschl, Dekan

To my parents.

Maxima enim est hominum semper patientia virtus.

–

Cato

Table of content

Abbreviations

Amp	Ampicillin
Ady2	Acetate transporter in *Saccharomyces cerevisiae*
AUC	Area under the curve
BLAST	Basic local alignment search tool
Bq	Becquerel
cDNA	complementary deoxyribonucleic acid
Ci	Curie
FNT	Formate nitrite transporter
DAPI	4',6-diamidino-2-phenylindole
DEPC	Diethylpyrocarbonate
dNTP	Deoxynucleoside triphosphate
DMSO	Dimethylsulfoxide
DNA	Deoxyribonucleic acid
E. coli	*Escherichia coli*
EPM	Erythrocyte plasma membrane
Fps1	*S. cerevisiae* glycerol facilitator
G418	Geneticin
GFP	Green fluorescent protein
g	Gravity
HA-tag	Human influenza hemagglutinin-tag
HEPES	2-(4-(2-hydroxyethyl)-piperazin-1-yl)-ethanesulfonic acid
HRP	Horseradish peroxidase
IC_{50}	Inhibitory concentration for a half-maximal effect
Jen1	Lactate transporter in *Saccharomyces cerevisiae*
LB medium	Luria-Bertani medium
LDH	Lactate-dehydrogenase
MCT	Monocarboxylate transporter
MES	2-(N-morpholino)ethanesulfonic acid
M-TBS-T	Milk powder and Tween 20-containing TRIS buffered saline
NAD^+	Nicotinamide adenine dinucleotide (oxidized)
NADH	Nicotinamide adenine dinucleotide (reduced)
NTC	Nourseothricin
OD_{600}	Optical density at 600 nm
PAGE	Polyacrylamide gel electrophoresis

PBS	Phosphate buffered saline
PEG	Polyethylene glycol
PfAQP	*Plasmodium falciparum* aquaglyceroporin
PPM	Parasite plasma membrane
PV	Parasitophorous vacuole
PVM	Parasitophorous vacuole membrane
PVDF	Polyvinylidene difluoride
RBC	Red blood cell
r.m.s.ds	Root Mean Square - Delay Spread
rpm	Rounds per minute
S. cerevisiae	*Saccharomyces cerevisiae*
SD medium	Synthetic defined medium
SDS	Sodium dodecyl sulfate
TRIS	Tris(hydroxymethyl)aminomethane
pCMBS	para-chloromercuribenzene sulfonate
P. falciparum or Pf	*Plasmodium falciparum*
v/v	Volume per volume
w/v	Weight per volume
wt	Wild-type
X. laevis	*Xenopus laevis*
YNB	Yeast nitrogen base
YPD	Yeast peptone dextrose

Summary

A distinctive character of the mature intraerythrocytic form of the malaria parasite, *Plasmodium falciparum*, is a high glycolytic flow rate to fulfill its energetic requirements. This action produces two mole of lactic acid per mole of glucose as the anaerobic end product resulting in large quantities that need to be removed from the parasite cytosol. On its way out into the bloodstream lactate has to cross three different phospholipid bilayers, the parasite plasma membrane, the parasitophorous vacuole membrane and the red blood cell membrane. Although transport characteristics have been described for lactate in *P. falciparum* the molecular identity of the underlying permease(s) is still unknown. Here the discovery of a gene, PfFNT, responsible for the peptide that facilitates lactate transport over the parasite plasma membrane is described. It is a member of the formate nitrite transporter family (FNT) with high sequence similarities to microbial FNTs. For characterization of the protein a *Saccharomyces cerevisiae* knock out strain was employed that has lost the ability to transport monocarboxylates. Using this system PfFNT lactate/proton symport was found. This was confirmed by a direct proportionality of L-lactate transport to the prevailing pH gradient. Moreover when this gradient was abolished by proton decouplers, i.e. carbonylcyanide-3-chlorophenylhydrazone (CCCP) and 2,4-dinitrophenol (DNP), transport ceased. The PfFNT facilitated substrate pattern fits microbial FNTs, with acetate exhibiting the highest permeability followed by formate, L-lactate, D-lactate and pyruvate in decreasing order. The dicarboxylate malonate was excluded showing selectivity of monovalent anions over multivalent anions which is also a common feature shared by all FNTs discovered so far. The non-charged molecule glycerol, which is similar in size to lactate, was also excluded. Moreover facilitation features, such as transport rates and inhibition profile, match earlier findings from measurements performed in isolated living parasites *in vitro* hinting at a central position of PfFNT in parasite metabolism. For this the antiplasmodial compounds phloretin, furosemide, and cinnamate derivatives where tested revealing IC_{50} values around 1 mM. Inhibition requires a negative moiety though, since the uncharged cinnamamide had no effect. Notably the organomercurial p-chloromercuribenzene sulfonate (pCMBS), an inhibitor of human lactate transport, did not alter transport rates of PfFNT. This, taken together with the fact that there are no FNT homologs apparent in the human genome indicates PfFNT as a novel promising antimalarial drug target. Additionally PfFNT is the only transporter of the plasmodial glycolytic pathway for which structure information is available from crystals of homologous proteins predisposing it to further design of high affinity inhibitors.

Zusammenfassung

Ein herausragendes Merkmal des intraerythrozytären Malariaerregers, *Plasmodium falciparum,* ist eine hohe glykolytische Flussrate um seinen Energiebedarf zu decken. Bei diesem Vorgang werden aus einem Molekül Glukose zwei Moleküle Laktat gebildet, welches als metabolisches Endprodukt in hohen Mengen anfällt und aus dem parasitären Zytosol ausgeschleust werden muss. Auf seinem Weg ins Blut muss das Laktat drei Phospholipid Doppelmembranen überwinden, die parasitäre Plasmamembran, die parasitäre Vakuolen Membran und die Membran der Erythrozyten. Obwohl diese Transportprozesse in *P. falciparum* bereits beschrieben wurden, konnte die molekulare Identität der zugrunde liegenden Permease(n) bis jetzt nicht geklärt werden. In dieser Arbeit wurde das Gen, PfFNT, identifiziert das für das Peptid codiert, welches für die Laktatleitung über die Parasiten Membran verantwortlich ist. Es gehört zur Familie der Formiat Nitrit Transporter (FNT) und besitzt ähnliche Transporteigenschaften wie mikrobielle FNTs. Zur Charakterisierung des Proteins wurde ein *Saccharomyces cerevisiae* knock-out Stamm verwendet, welcher nicht dazu befähigt ist Monocarboxylate zu transportieren. In diesem System wurde gezeigt, dass PfFNT Laktat in Symport mit Protonen leitet. Dieses wurde durch eine direkt zum vorherrschenden pH-Wert proportionale Transportrate belegt. Zudem konnte der Transport gestoppt werden, indem der pH-Gradient durch Protonenentkoppler, wie Carbonylcyanid-3-chlorophenylhydrazon (CCCP) und 2,4-Dinitrophenol (DNP) zerstört wurde. Das durch PfFNT geleitete Subtratspektrum entspricht dem der bisher beschriebenen mikrobiellen FNTs. Dabei zeigt das Acetat Molekül die höchste Permeabilität, gefolgt von Formiat, L-Laktat, D-Laktat und Pyruvat in absteigender Reihenfolge. Das zweifach negativ geladene Malonat wurde nicht transportiert, was ebenfalls zu der Selektivität der bisher beschriebenen FNTs passt, die alle nur einfach geladene Anionen leiten. Das ungeladene Glycerol, welches eine ähnliche Größe zum Laktat Molekül aufweist, wurde ebenfalls nicht transportiert. Des Weiteren passen die Transporteigenschaften, wie Transportrate und Inhibitionsprofil zu denen, welche aus Daten gewonnen wurden, die in lebenden isolierten Parasiten *in vitro* gemessen wurden. Dieses deutet auf eine zentrale Rolle von PfFNT im parasitären Metabolismus hin. Hierfür wurden die antiplasmodial wirkenden Substanzen Phloretin, Furosemid und Zimtsäurederivate getestet, welche alle IC_{50} Werte um 1 mM zeigen. Inhibition erfordert zudem eine einzelne negative Ladung da das ungeladene Zimtsäureamid keine Wirkung auf die Transportrate hat. Bemerkenswert ist, dass die Organoquecksilber-Verbindung p-Chloromercuribenzensulfonat (pCMBS), ein bekannter Inhibitor des menschlichen Laktat Transports, den Transport durch PfFNT nicht verändert. Dies, zusammengenommen mit der Tatsache, dass es keine homologen Gene zu FNTs im menschlichen Genom gibt, deutet auf eine potentielle Rolle von PfFNT als

neues Wirkstoffziel zur Behandlung von Malaria hin. Zusätzlich ist PfFNT der einzige Transporter des plasmodialen glykolytischen Stoffwechsels für den Strukturdaten aus Proteinkristallisationen in hoher Auflösung verfügbar sind. Daher ist PfFNT prädispositioniert für ein Design von hochaffinen Inhibitoren.

1 Introduction

The human malaria parasite *Plasmodium falciparum* is absolutely dependent on the acquisition of host glucose for fulfilling its energetic needs while it resides inside human erythrocytes. The main waste product out of this metabolic pathway is lactate that needs to be removed from the cells in order to keep them viable. Although the biochemical properties of this transport have been characterized, the molecular identity of the parasite encoded lactate transporter has remained unknown.

1.1 Malaria

The species of the genum *Plasmodium* are the causative agents of malaria. Their highly specialized life cycle is divided between an *Anopheles* mosquito vector and a vertebrate host, which, depending on the parasite species, ranges from reptiles to birds, rodents and primates. To date there are five species that are able to infect man, *P. malariae*, *P. ovale*, *P. vivax*, *P. knowlesi* and *P. falciparum*. The latter causes the most severe form of the disease, *Malaria tropica*. The estimated cases are worldwide about 200 million while in 2012 over 600000 deaths occurred, with approximately half of the victims being among children under the age of five which live in the poorest countries of the world. [World Malaria Report 2013]

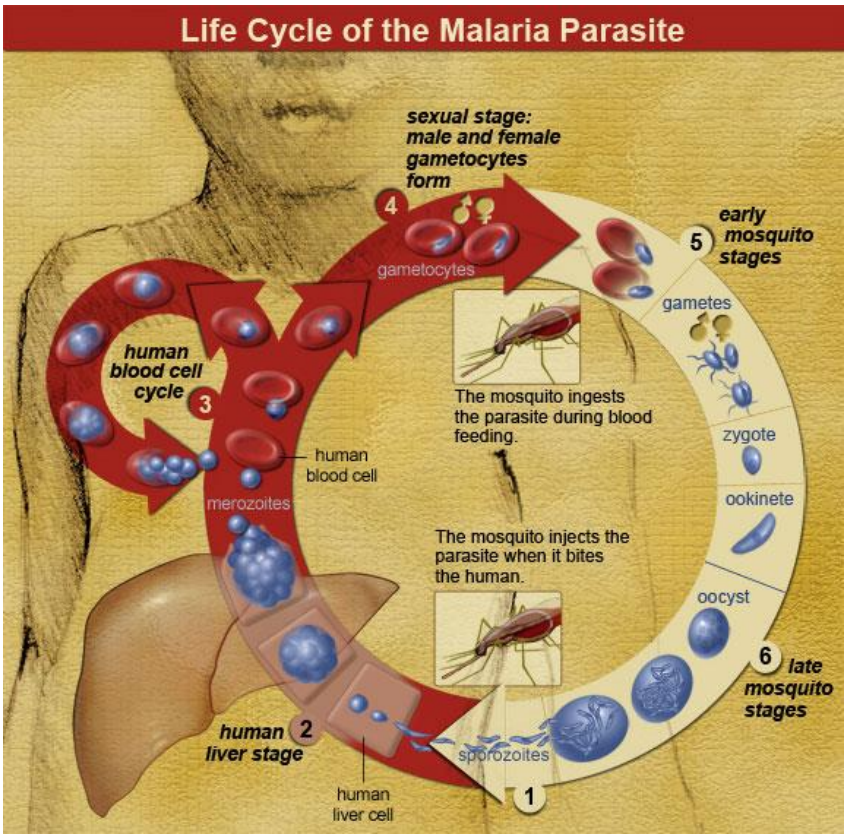

Figure 1.1 | Life cycle of the malaria parasite. Displayed are the different developmental stages of the parasite during its transition from its mosquito host to human. [National Institute of Allergy and Infectious Diseases (NIAID)]

The parasite undergoes a complex life cycle, which includes the development of a zygote, meiosis and subsequent asexual replication in mosquitoes (figure 1.1). Mosquitoes of the genum *Anopheles* are the primary host, which inject the infectious form of the parasite called sporozoites to the secondary host being vertebrates, e.g. humans [Smith et al. *Mem Inst Oswaldo Cruz.* 2014]. Here, sporozoites begin the extraerythrocytic development by invading liver cells (figure 1.1). In this state the parasite not only vastly multiplies to form up to 30,000 merozoites out of one single cell but also, in the case of *P. ovale* and *P. vivax*, is able to form resistant dormant bodies, called hypnozoites. They are the cause for recrudescence of clinical malaria even after years of convalescence [Markus *Parasitol Res.* 2011]. Furthermore the released merozoites go on to invade differentiated red blood cells. In this asexual replicating cycle, known as schizogony, one merozoite forms up to 32 new merozoites which in turn reinvade new RBC's resulting in a burden of millions of infected erythrocytes (figure 1.2) [Francia et al. *Nat Rev Microbiol.* 2014].

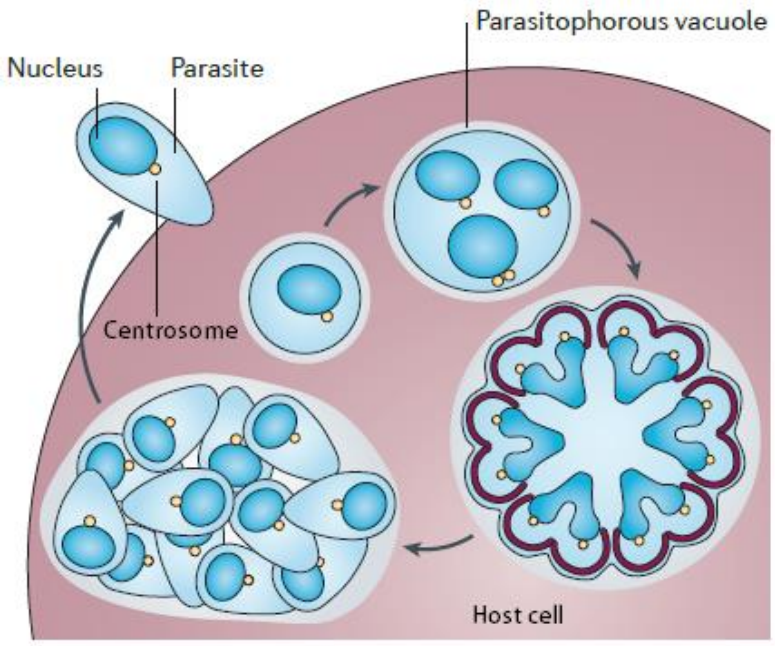

Figure 1.2 | Replication cycle of *P. falciparum* inside RBCs. During invasion the parasite is encapsuled inside a parasitophorous vacuole. Within nuclei replicate mitotically, first asynchronous, later synchronous. Ultimately new merozoites are released from the red cell completing the circle of schizogony. [Francia et al. *Nat Rev Microbiol.* 2014]

This infection of, and replication within the red cells is the cause of the clinical symptoms of malaria. These symptoms differ in their periodicity depending on which of the five species infected the host and ultimately result in the outcome of the disease. The most deadly form is caused by *P. falciparum* [Francia et al. *Nat Rev Microbiol.* 2014]. This species targets a protein to the erythrocyte cell surface, *P. falciparum* erythrocyte membrane protein 1 (PfEMP1), which mediates binding of infected erythrocytes to the endothelial lining of blood vessels [Crabb et al. *Cell* 1997; Miller et al. *Mol Biochem Parasitol.* 1993]. Most likely this process leads to cerebral malaria, a major cause of malaria related deaths [Wassmer et al. *Ann N Y Acad Sci.* 2003]. Eventually, out of this replication cycle, merozoites develop into the sexual form, which are called male and female gametocytes. These circle the blood stream and can be taken up again by a mosquito during its blood meal completing the parasitic development cycle [Francia et al. *Nat Rev Microbiol.* 2014]. *P. falciparum* belongs to phylum *Apicomplexa* which are generally characterised by a polar apical complex, a morphologically distinctive structure consisting of specialized organelles [Waller et al. *Curr. Issues Mol. Biol.* 2005]. Such are the micronemes, rhoptries and the conoid which are all located at one pole of the respective

invasive form. A common feature of most apicomplexans is that they are obligatory intracellular pathogens, while their extracellular stages inside their respective hosts are of short period. Another morphologically distinctive feature shared by many apicomplexans is a rudimentary plastid, the apicoplast, which is thought of being the result of a secondary endosymbiosis event between a free-living ancestor of these parasites and a red alga [Waller et al. *Curr. Issues Mol. Biol.* 2005]. Although being non-photosynthetic, the apicoplast is nevertheless essential for parasite survival, reasoned by several biosynthetic pathways, which are located within [Fichera et al. *Nature* 1997; Soldati *Parasitol Today*. 1999; Goodman et al. *Curr Drug Targets.* 2007; Lizundia et al. *Antimicrob Agents Chemother.* 2009].

1.2 *Plasmodial* carbon metabolism

During its asexual intra-erythrocytic developmental phases *P. falciparum* absolutely relies on glucose fermentation to fulfill its energetic needs [McKee et al. *J Exp Med.* 1946]. In this situation the infected RBC's consume glucose at rates up to two magnitudes higher than uninfected red blood cells [McKee et al. *J Exp Med.* 1946]. By this, lactate is generated at the amount of 18 mmol l^{-1} min^{-1} that needs to be removed in order to keep the cells viable [Ginsburg *Trends Parasitol*. 2002]. On its way out of the cell, lactate must cross 3 phospholipid bilayers, the parasite cell membrane, the parasitophorous membrane and the host cell membrane. How and by which permeases this is accomplished is still elusive (figure 1.3).

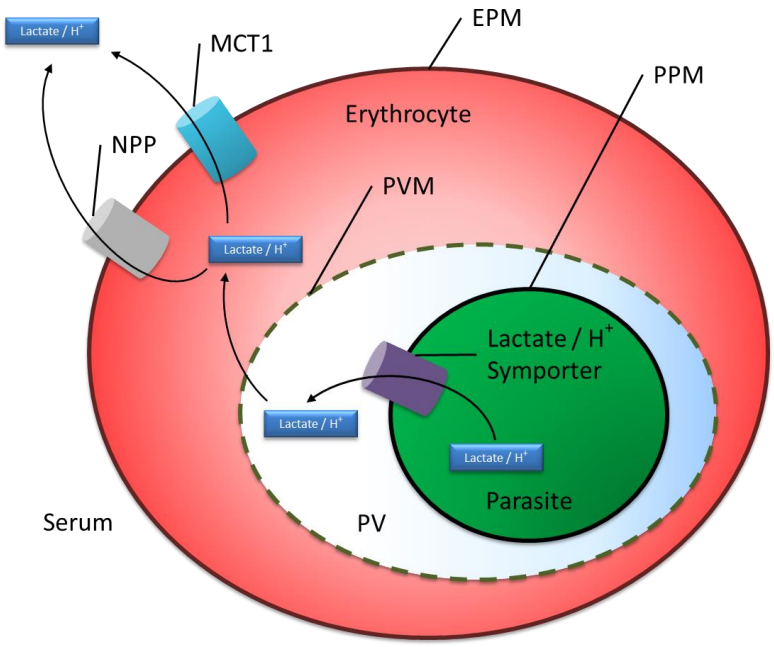

Figure 1.3 | Lactate's way out of the parasite. Lactate has to cross 3 different membranes on its way to the blood serum. Since it is charged at physiological pH and therefore membrane impermeable, permeases need to be involved. Crossing of the parasite plasma membrane (PPM) is thought of being accomplished by an unknown lactate/proton symporter. The parasitophorous vacuole membrane (PVM) is either fenestrated or equipped with high-capacity, low-selectivity channels. Either way it is freely permeable to low molecular-weight solutes [Desai et al. *Nature* 1993]. Finally, the erythrocyte plasma membrane (EPM) is overcome via the human MCT1 and the new permeation pathways (NPP) [Ginsburg et al. *Mol. Biochem. Parasitol.* 1983].

If lactate is not exported the result would be an intracellular drop in pH due to high amounts of protons generated by ATP depletion together with huge osmotic stress caused by doubling of the molar mass inside the parasite (net equation: 1 mol glucose -> 2 mol lactate, figure 1.4).

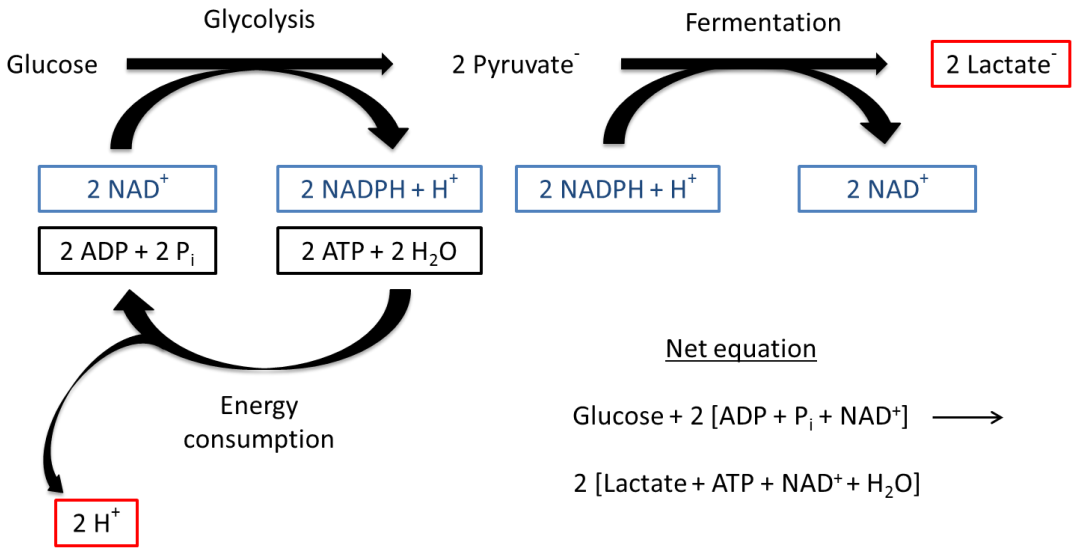

Figure 1.4 | Glycolytic pathway in *Plasmodium*. Protons are not generated during homolactic glucose fermentation since this process is none acidifying as can be seen in the net equation. When energy is freed from ATP hydrolysis by ATPases protons are produced in a 1:1 stoichiometry. Throughout glycolysis ATP is generated from oxidizing glucose to pyruvate. In order to restore consumed redox equivalents pyruvate is further reduced to lactate by fermentation. Major metabolic end-products are displayed in red rectangles.

Intriguingly *Plasmodium* and its host cell share the same carbohydrate metabolism, principally the Embden–Meyerhof–Parnas pathway of glycolysis. For the red blood cell this is clear due to absent mitochondria and a strongly reduced set of metabolic enzymes [Roigas et al. *Folia Haematol* 1965; Worthington et al. *Eur J Biochem.* 1976; Otto et al. *Acta Biol Med Ger.* 1977; Morelli et al. *Proc Natl Acad Sci U S A*, 1978]. For the parasite the situation is a little bit different since plasmodia are known to have a single mitochondrion and encode for all necessary glycolytic enzymes [Rudzinska *Int Rev Cytol.* 1969; Aikawa *Am J Trop Med Hyg.* 1966; van Dooren et al. *FEMS Microbiol Rev.* 2006; Torrentino-Madamet *Curr Mol Med.* 2010]. Nevertheless only a very small fraction of the consumed glucose is completely oxidized to CO_2 which is in line with the fact that *in vitro* cultures of *P. falciparum* require microaerophilic culture conditions for optimal growth while they are inhibited by atmospheric O_2 concentrations [Krungkrai et al. *Southeast Asian J Trop Med Public Health.* 1999; Scheibel et al. *Exp Parasitol* 1979]. During glycolysis energy is generated in the form of ATP. For this glucose is oxidized to pyruvate. This action consumes 2 moles of reduction equivalents, being NAD^+. In order to keep glycolysis running and when O_2 as the terminal electron acceptor is absent

pyruvate is further reduced to lactate. By this, lactate fermentation restores NAD^+ as redox equivalent. The abundance and tightly regulated glucose concentration in the host blood serum together with the red cells reduced metabolism are thought of having led to this quite inefficient (e.g. oxidative phosphorylation produces up to 38 mol ATP out of 1 mol glucose vs. 2 mol ATP for 1 mol glucose via glycolysis) but tightly host-cell-adopted metabolism of the parasites. But there is another argument for fermentation over oxidative respiration in *Plasmodium*. To gain amino acids the parasite consumes the host cell's hemoglobin in large amounts. This is of fundamental importance since *P. falciparum* has entirely lost the ability of *de novo* amino acid synthesis [Liu et al. *Proc Natl Acad Sci U S A* 2006]. During hemoglobin degradation iron atoms of the heme groups are released which are known to produce oxidative stress, e.g. in the form of oxygen radicals [Kumar et al. *Toxicol Lett.* 2005]. Anaerobic conditions may prevent cell damage by this mechanism which indeed results in the need for an alternative way to produce energy in the absence of oxygen as ultimate electron acceptor – fermentation. It has been known for years that *Plasmodium* gets rid of the waste product lactate and at the same time deals with its proton burden through one combined mechanism, a lactate/proton symporter that acts in a 1:1 stoichiometry [Kanaani et al. *Cell. Physiol.* 1991; Cranmer et al. *J. Biol. Chem.* 1995; Elliott et al. *Biochem. J.* 2001]. Till now the molecular identity of this permease has escaped discovery.

Comprehensively the following facts are of major interest in the malaria causing microbe *P. falciparum*:

- Glucose is the prime energy source
- Lactate is the major metabolic end product derived by fermentation
- Protons are plentifully generated by ATP depletion
- Lactate and protons need to be removed from the cell

1.3 Lactate transport in the host: MCTs

Monocarboxylates such as lactate, pyruvate and ketone bodies play key roles in the human energy metabolism and must be transported across cell membranes [Poole et al. *Am. J. Physiol.* 1993]. For this objective a family of proton-linked monocarboxylate transporters (MCTs) has evolved with specialized transport properties and distinct tissue distribution. So far four members were discovered in the human genome and have been studied intensively [Halestrap *Mol Aspects Med.* 2013]. Common to all family members are predicted 12 transmembrane helices (TMs) with C- and N-termini facing intracellular and a large cytosolic loop between TMs 6 and 7. Topology has been confirmed for MCT1 (figure 1.5) by labeling

studies and proteolytic digestion and a three-dimensional structure has been modelled that suggests a reasonable molecular transport mechanism [Manoharan et al. *Mol. Membr. Biol.* 2006; Wilson et al. *J. Biol. Chem.* 2009]. For correct trafficking to the plasma membrane and also activity MCTs1-4 require association with an accessory peptide, basigin or embigin. These are glycoproteins that share the features of a single TM and 2 to 3 extracellular immunoglobulin domains.

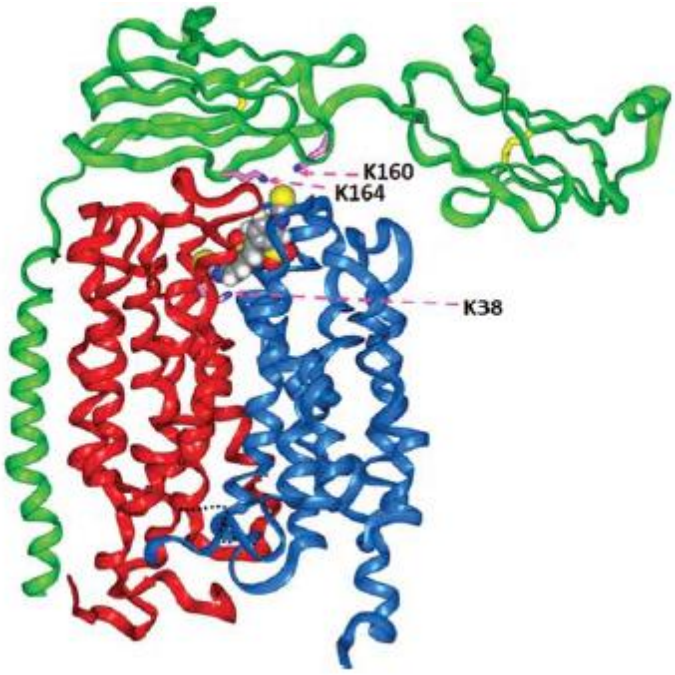

Figure 1.5 | Proposed structure of MCT1 in association with embigin. For correct expression and functionality MCTs need to be associated with a chaperone peptide, embigin or basigin. DIDS (grey molecule) is an inhibitor of monocarboxylate transport via MCTs. It's binding to MCT1 and embigin occurs through lysine residues in both proteins (marked with arrows) [Halestap *IUBMB Life* 2011].

Intriguingly it has been recently discovered that basigin is an essential receptor for erythrocyte invasion by *P. falciparum* [Crosnier et al. *Nature* 2011]. Further MCTs belong to the SLC16 family, whose members are involved in a wide range of metabolic pathways including energy metabolism of the brain, skeletal muscle, heart, gluconeogenesis, T-lymphocyte activation, bowel metabolism, spermatogenesis and drug transport [Halestrap

Mol Aspects Med. 2013; Kobayashi et al. *Int J Pharm.* 2006]. For example MCTs take a central position in the Cori cycle. In this MCT4 acts as a lactate exporter, e.g. in type II skeletal fiber cells, while MCT1, that is highly expressed in heart and liver, acts as a lactate exporter. These properties arise from differences in substrate affinities between the two peptides. In tissue that is highly glycolytic but at the same time under anaerobic conditions, e.g. white skeletal muscles under high tension, lactate is fermented in order to restore reduction equivalents in the form of NAD^+ consumed by glycolysis and thereby keep ATP generation running. This lactate is shuttled to tissue that has the appropriate enzymatic setting and sufficient supply with oxygen. Here, it can be either further oxidized to CO_2 leading to a complete energy yield out of this substrate or used to rebuild glucose again (figure 1.6) [Cori *Physiol. Rev* 1931; Brooks *J Physiol.* 2009].

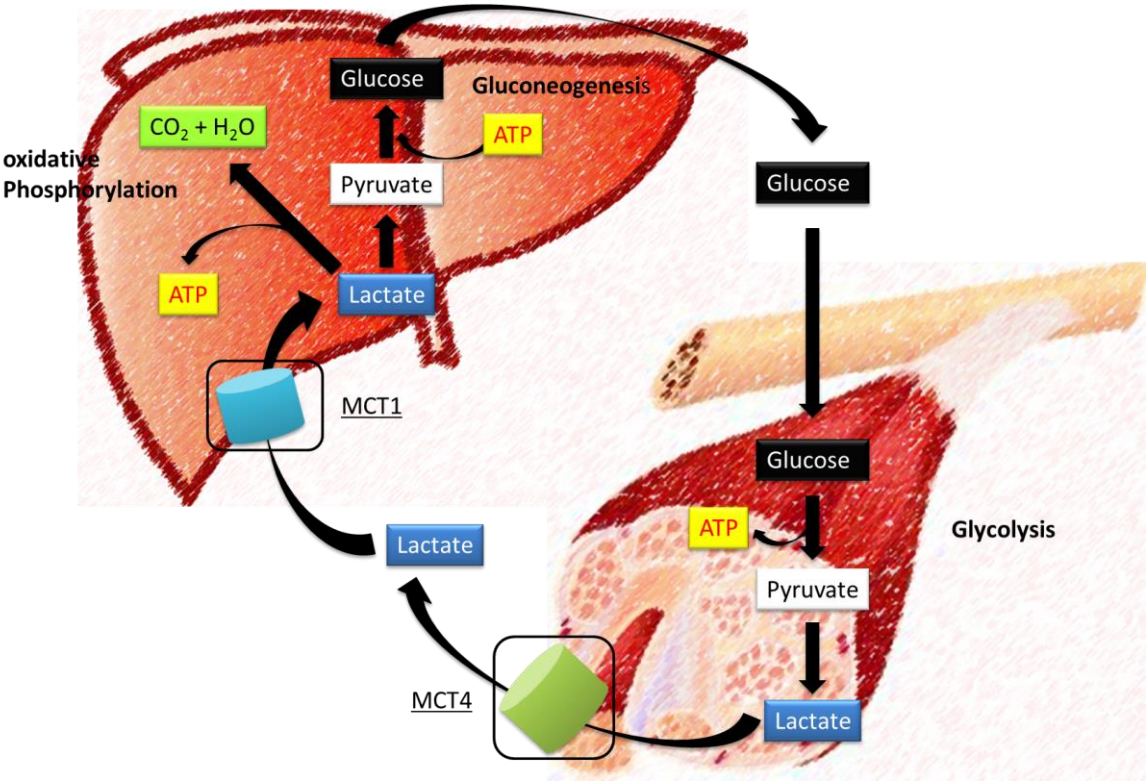

Figure 1.6 | The lactate shuttle. Shown is the Cori cycle. Glucose is metabolized in glycolytic tissue, e.g. white fiber muscle cells to lactate. This is exported via MCT4 to the blood stream and imported by MCT1 in the respective organs for further metabolism. There, lactate can be a) used in gluconeogenesis to build up new glucose or b) oxidized in mitochondria to CO_2 to get maximum energy yield.

Certain interest has aroused on these permeases some years ago since MCT play a key role in cancer metabolism and are therefore promising drug targets in cancer chemotherapy [Dimmer et al. *Biochem J.* 2000; Manning Fox et al. *J Physiol.* 2000].

The prevailing hypothesis is that lactate is facilitated via MCT homologues in *P. falciparum* [Elliott et al. *Biochem. J.* 2001; Cranmer et al. *J. Biol. Chem.* 1995]. Due to a certain degree of sequence similarity there are two putative plasmodial MCT genes annotated (PFB0465c and PFI1295c; PlasmoDB.org). Moreover experiments on permeabilized infected RBCs revealed lactate transport characteristics and an inhibitor pattern both comparable to human lactate transporters, i.e. MCTs [Kanaani et al. *Cell. Physiol.* 1991; Cranmer et al. *J. Biol. Chem.* 1995; Elliott et al. *Biochem. J.* 2001]. Noteworthy to say that the only known lactate transporter in the RBC membrane, MCT1, is most likely not capable of coping with the vastly elevated lactate levels inside the infected erythrocyte cytosol [Kanaani et al. *Cell. Physiol.* 1991]. Also *P. falciparum* produces 6-7% of its total lactate in the form of the D-enantiomer which is about three times slower transported by the stereoselective MCT1 compared to the L-enantiomer [Vander Jagt et al. *Mol. Biochem. Parasitol.* 1990; Broer et al. *Biochem. J.* 1998]. These facts suggest that if lactate is shuttled over the erythrocyte membrane via plasmodial MCT homologues at least their substrate affinities have to be different to those of human MCTs.

1.4 Lactate transport in lower organisms: Formate-nitrite transporters

Recently a new class of lactate permeases has been discovered, the formate nitrite transporter family (FNT), which mediate monocarboxylate transport in prokaryotes and lower eukaryotes. This peptide family was originally found in bacteria and knowledge on transport characteristics spread quickly accompanied by obtainment of numerous high resolution protein crystal structures [Waight et al. *Curr Opin Struct Biol* 2013].

While eukaryotes, especially mammals, are homolactic fermenters, prokaryotes use a wide range of compounds as terminal electron acceptors under anaerobic conditions, including carbon dioxide, oxidized sulfur and nitrogen substances [Clegg et al. *Mol Microbiol* 2002; Kabil et al. *J Biol Chem* 2010]. These respiration products are tightly regulated by numerous enzymes, ion channels and transporters due to the fact that they have a detrimental potential when present at higher concentrations [Stephenson et al. *Biochem J* 1932]. Nevertheless cells can benefit by the redox potential of these anions. Under anaerobic conditions mixed acid fermentation results in temporary metabolic end products being mainly

formate and acetate. Similar to this nitrite and hydrosulfide are produced [Stokes *J Bacteriol* 1949; Sawers *Microbiology* 2006]. To deal with transport of these compounds across lipid bilayers the family of formate nitrite transport channels (FNTs) has emerged [Suppmann et al. *Mol Microbiol* 1994; Sawers *Antonie Van Leeuwenhoek* 1994]. This family can further be divided into three subfamilys, the formate channels (FocA) [Suppmann et al. *Mol Microbiol* 1994], the nitrite channels (NirC) [Jia et al. *Biochem J* 2009] and the hydrosulfide channels (HSC) [Czyzewski et al. *Nature* 2012]. The overall protein structure of this family is well known since plentiful data on 3-d high resolution crystals has been collected. These peptides form homomeric pentamers in the phospholipid membrane as functional units (figure 1.7 1)). These, although sharing absolutely no sequence similarities, have a similar tertiary structure as aquaporins, a phenomenon referred to as molecular mimicry (figure 1.7 2) and 3)) [Wang et al. *Nature* 2009].

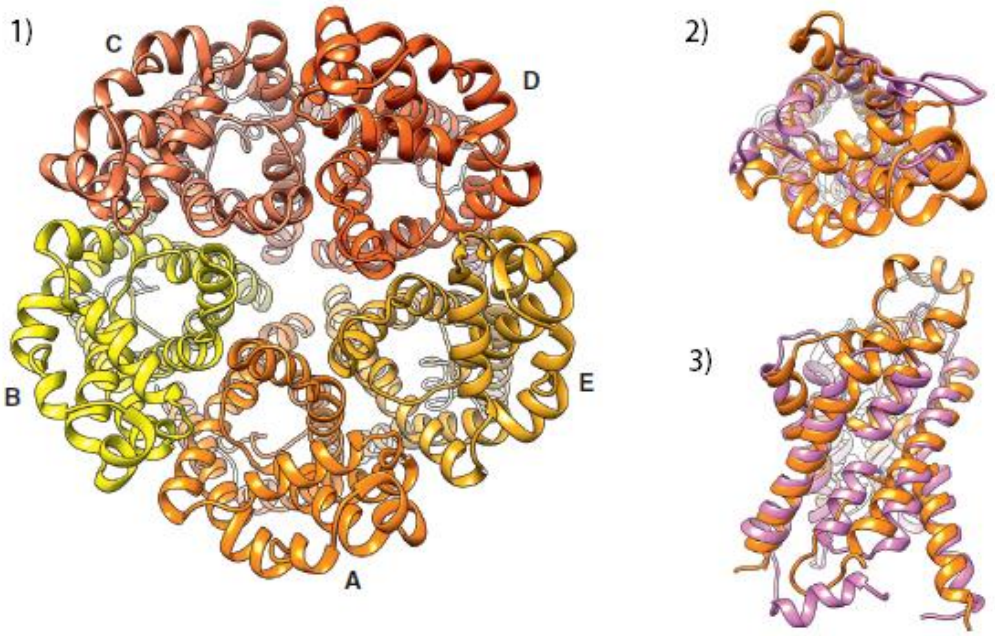

Figure 1.7 | FNT structure and comparison to aquaporins. Shown is 1) the pentameric structure of FocA from *Vibrio cholera* [Waight et al. *Nat Struct Mol Biol* 2010] and its superposition with bovine AQP1 [Sui et al. *Nature* 2001], 2) top view from the extracellular side, 3) side view from within the membrane. FocA = orange, AQP1 = purple [Waight et al. *Curr Opin Struct Biol* 2013].

The protomers are each composed of six tilted transmembrane α-helices and two half helices forming a right-handed bundle that surrounds a 15-Å long narrow pore, which is believed to be the permeation pathway for anions (figure 1.7 2)). The overall structures of the FNT subfamilies show only minor differences, resulting in a high degree of similarity between them. This is reflected in the conduction profile of FNTs: they transport monovalent anions, ranging from small inorganic compounds such as nitrite to larger organic molecules like acetate [Czyzewski et al. *Nature* 2012; Lü et al. *Proc Natl Acad Sci U S A* 2012]. Albeit having a polyspecific anion substrate pattern FNTs are non-conductive for cations and multivalent anions [Wang et al. *Nature* 2009; Lü et al. *Science* 2011; Whaigt et al. *Nat. Struct. Mol. Biol* 2010; Lü et al. *Proc. Natl. Acad. Sci. USA* 2012; Czyzewski et al. *Nature* 2012].

Notably the FNT family is widely distributed among enteric bacteria such as *Escherichia* and *Salmonella* species [Saier et al. *Biochim. Biophys. Acta* 1999]. With the fact that many of these cause severe human illnesses, FNT proteins may function as valuable drug targets. In fact they might hold the potential to lead to the discovery of a novel class of antibiotics.

1.5 Aim of this work

The primary objective of this thesis is to identify and test candidate proteins responsible for lactate transport over the parasite membrane. If a hit is found its transport properties will be characterized. Also a set of known inhibitors for *P. falciparum* lactate transport will be tested. Candidate testing and characterization will be based on a mutant yeast strain, with phenotypic as well as radioactive tests.

2 Materials

2.1 Chemicals and enzymes

AppliChem, Darmstadt
MES, Tween 20, SDS, Streptomycinsulfate, LB-Agar-Powder,
Glycine, LB-Medium-Powder, Phosphoenolpyruvate, Magnesiumacetate

Becton Dickinson and Company, Heidelberg
Bacto Proteose Peptone No. 3, Bacto Agar, Bacto Peptone, Bacto Tryptone, Bacto Yeast Extract

Bio-Rad, Munich
Bio-Rad Protein Assay-Reagent

Fermentas, St.Leon-Rot
Restriction enzymes, dNTPs, T4-DNA Ligase, RiboLock RNase Inhibitor

Genaxxon BioScience, Ulm
Agarose LE, Ampicillin, TEMED

GE Healthcare, Freiburg
PD MidiTrap G25, ECL plus Western-Blotting Detection System, Hybond-P Western Blot-Membranes, Q-Sepharose Fast Flow, Whatman Nuclepore Track-Etch Membranes, Whatman Chromatography Paper 3MM

J.T.Baker, Munich
Methanol, Ethanol, Isopropanol, Acetic acid

Merck, Darmstadt
Glycine, Potassiumchloride, di-Sodiumhydrogenphosphate-dihydrate, Sodiumformate, Saccharose, Dimethyl sulfoxide, G 418 Sulfate

MP Biomedicals, Illkirch, France
Ethidiumbromide

Peqlab, Erlangen
peqGOLD Prestained Protein Marker III

Promega, Mannheim
Wizard Plus SV-Minipreps DNA Purification System

R-biopharm, Darmstadt
Enzytec(TM) L-Milchsäure Test

Roche Diagnostics, Mannheim
cOmplete EDTA-free Protease inhibitor cocktail tablets

Roth, Karlsruhe
Ammoniumperoxodisulfate, Ammoniumsulfate, Boric acid, Glycerol 86 %, Urea, HEPES, di-Potassiumhydrogenphosphate, Potassiumchloride, Lithiumchloride, MOPS, MES, Sodiumdihydrogenphosphate-Monohydrate, Sodiumhydrogencarbonate, TRIS, Tween 20, Triton X 100, Sodiumhydroxide, Sodiumchloride, Kanamycetinsulfate, L-Arginine, L-Leucine, L-Proline, LB-Agar (Lennox), Milkpowder, Bromphenolblue, D(+)-Glucosemonohydrate, LB-Medium (Lennox), D(+)-Saccharose, Rotiphorese Blue R, Calciumchloride, Albumin Fraction V (BSA), Trichloroacetic acid, Ethylenediaminetetraacetic acid, Potassiumacetate, Sodiumazide, Triton X-100, Saccharose, Dithiothreitol, Tris, Boric acid, Pen/Strep-PreMix, 2-Mercaptoethanol

Sigma-Aldrich, Munich
Poly(ethylene glycol) 8000, 2-(N-morpholino)ethanesulfonic acid, Glass beads, Sodiumformate, Sodiumgluconate, Sodiumnitrate, Urea, L-Asparagine Monohydrate, L-Arginine Monohydrochloride, L-Aspartic acid Sodiumsalt Monohydrate, L-Cysteine, L-Glutamic acid Sodiumsalt
Monohydrate, L-Alanine, L-Glutamine, L-Histidine Monohydrochloride Monohydrate, L-Isoleucine, L-Methionine, L-Lysine Monohydrochloride, L-Phenylalanine, L-Tryptophan, L-Tyrosine, L-Threonine, L-Valine, Hepes, Imidazole, Potassium-D-gluconate, L-Serine, L-Proline, Acetylphosphate, ATP, CTP, GTP, UTP

Stratagene, La Jolla, USA
PfuTurbo DNA Polymerase

Südlaborbedarf, Gauting
High Yield PCR Clean-Up & Gel-Extraction Kit

Thermo Fischer Scientific, Waltham, USA
First Strand cDNA Synthesis kit

Zinsser Analytic, Frankfurt
Scintillation cocktail Quicksafe A

2.2 Equipment

Adolf Wolf SANOclav, Bad Überkingen-Hausen
Autoclave for sterilization

Agilent Technologies, Waldbronn
UV/Vis-Spectrometer Varian Cary 50 UV-Vis

Beckman Coulter, Krefeld
Optima XL-80K Ultracentrifuge, SW 60 Ti Rotor Swinging Bucket, 50.2 Ti, Centrifuge Tubes Microfuge Tube Polyallomer 1.5ml

Bio-Rad, Munich
Power Pac 2000, Transblot SD semidry transfer cell

Clemens, Waldbüttelbronn
PCR-machine Primus advanced HT2X and HT Manager Software

Eppendorf, Hamburg
Photometer BioPhotometer, Centrifuge 5415R

Grant-bio, Hillsborough, USA
Rotator Mixer PTR-30

Heraeus Instruments, Osterode
Centrifuge Multifuge 1S-R, Microcentrifuge Biofuge pico

Infors, Bottmingen, Swizzerland
Incubation board Infors

Kern & Sohn, Balingen
Special accuracy weighing machine ABS 120-4

New Brunswick Scientific, Wesseling-Berzdorf
Deep-freeze cabinet U535 innova

Osram, Augsburg
Halogen lamp "64607 EFM", 8 V 50 W, for "Bioscreen" (ordered via iLF bioserve, Germany, from Oy Growth Curves, Finland)

Oy Growth Curves, Helsinki, Finland
Combined incubation shaker and turbidometer "Bioscreen C microbiology reader"
100-well plates "Honeycomb 2"
Software "EZExperiment"

Peqlab, Erlangen
SDS-gel-casting stand and –running chamber

Raytest, Straubenhardt
Gel-documentation-dystem IDA

Roche Diagnostics, Mannheim
Picture-documentation-system Lumi Imager F1

Savant Instruments, Farmingoale, USA
DNA SpeedVac R110 Vakuumcentrifuge

Schott Instruments, Mainz
pH-Meter Lab 850

Scientific-Industries, Bohemia, USA
Vortex Genie 2

SG Wasseraufbereitung und Regenerierstation, Barsbüttel

Ultrapure water system

WTB Binder Labortechnik, Tuttlingen

Hot-air steriliser, Incubator

PerkinElmer Inc., Waltham, USA

Packard TriCarb liquid scintillation counter

2.3 Plasmids used

Plasmid structures were generated using the PlasMapper software (version 2.0).

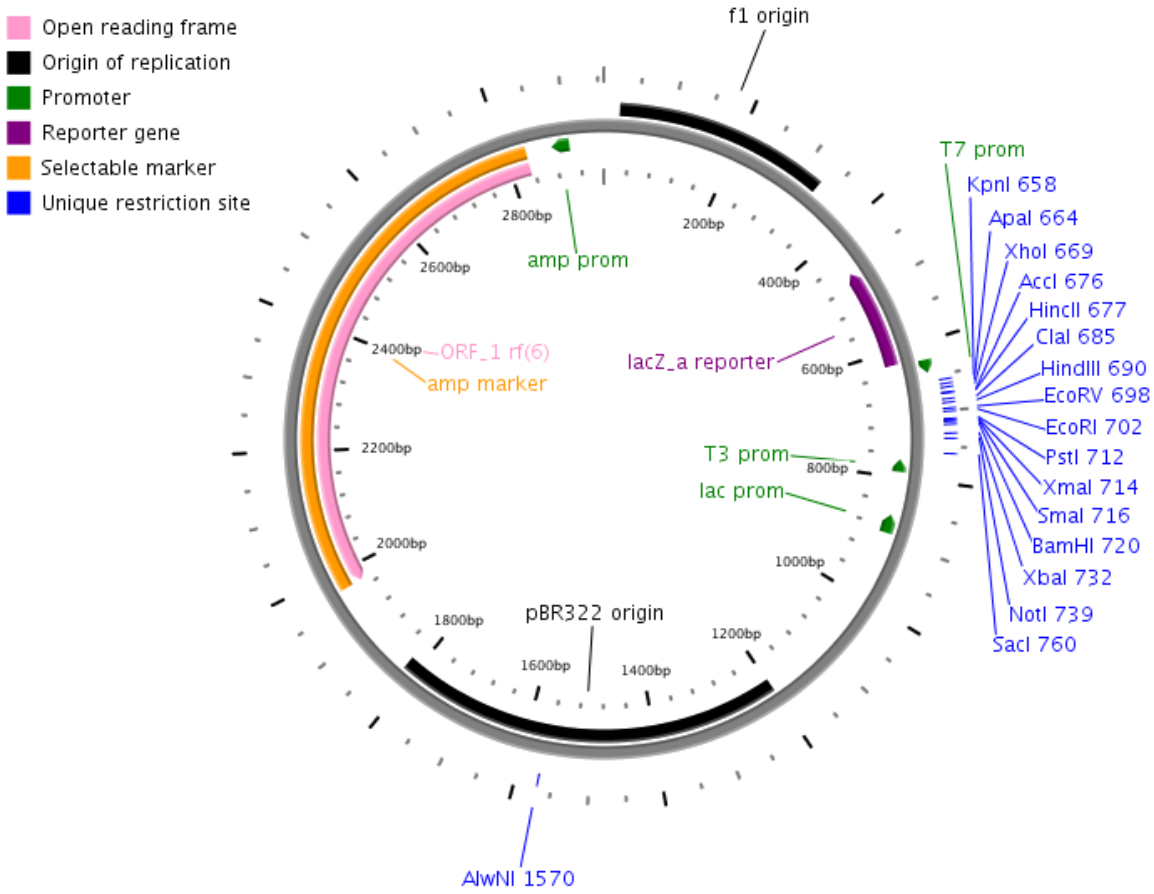

Figure 2.1 | pBluesript II SK(-). Cloning vector used for site directed mutagenesis in *E. coli*.

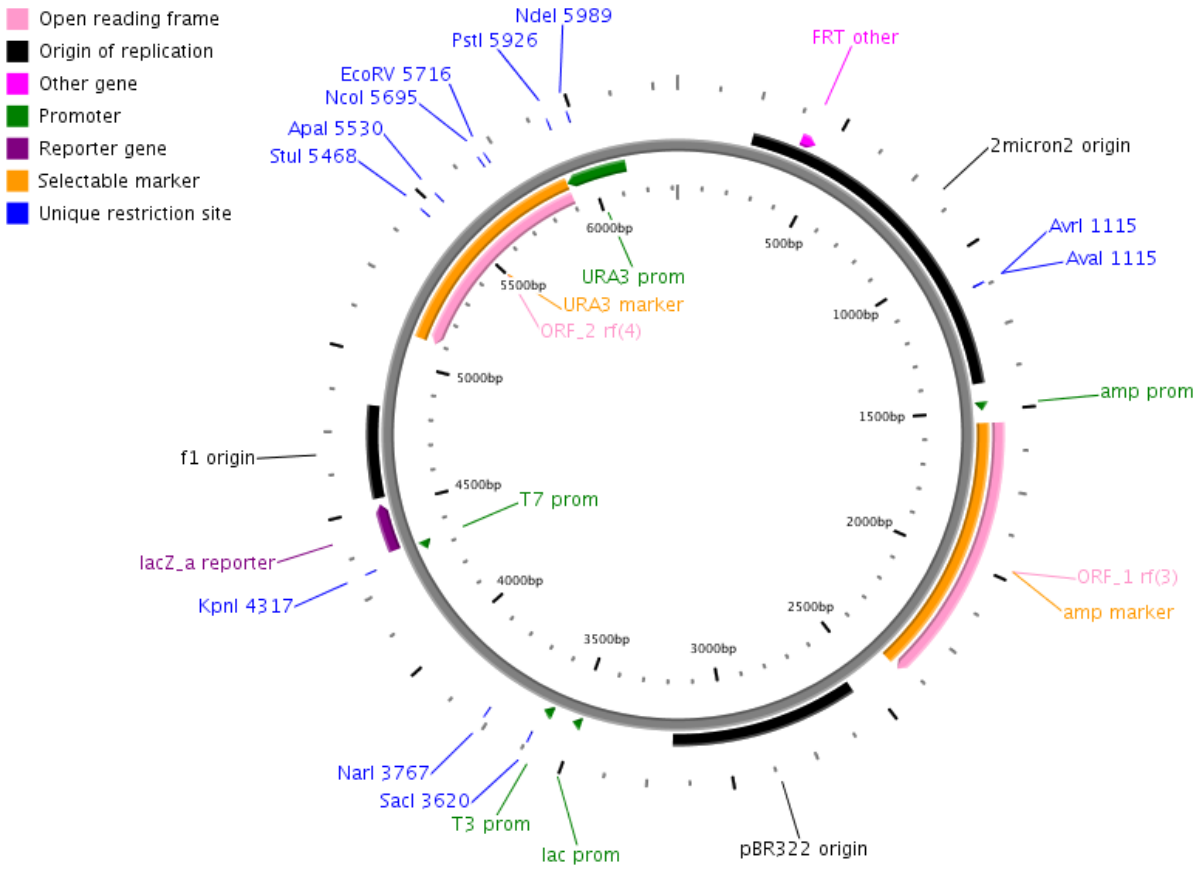

Figure 2.2 | pHA426MET25r. Yeast high copy shuttle vector. Used in *E. coli* and *S. cerevisiae*

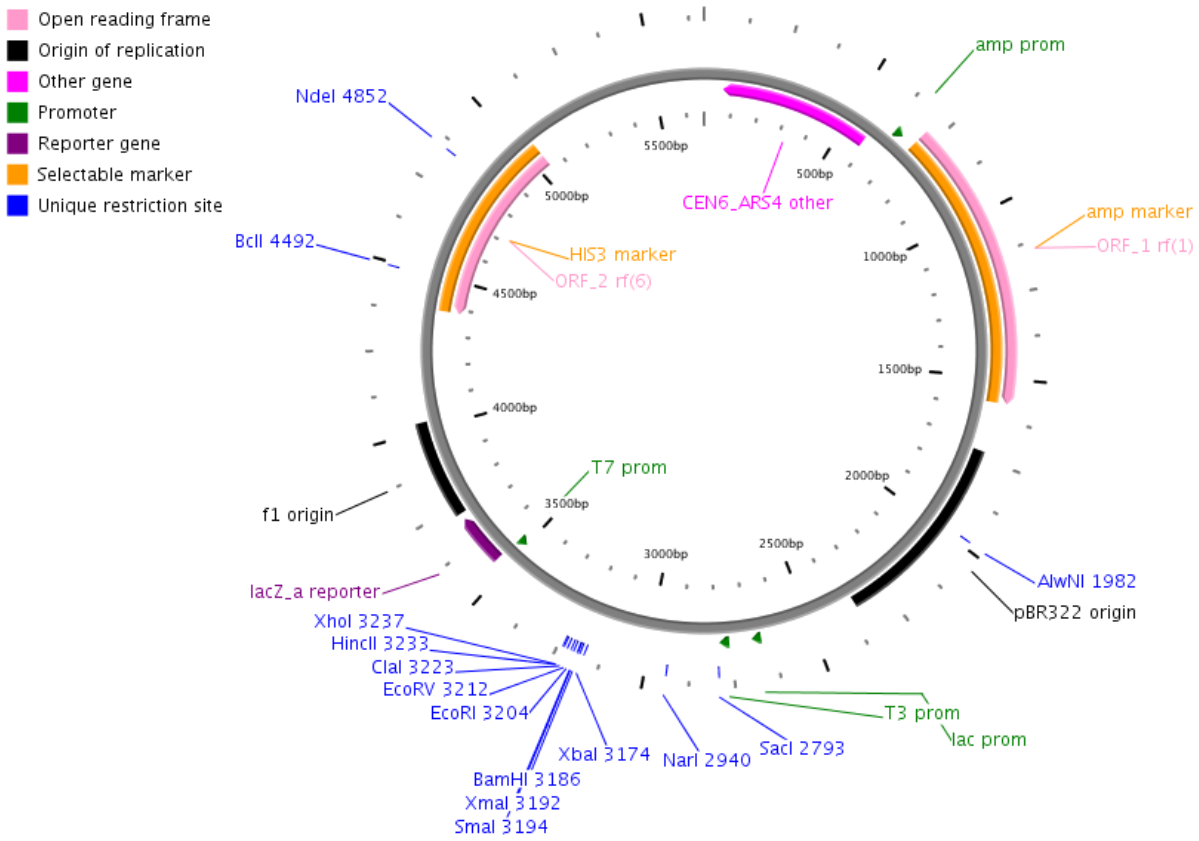

Figure 2.3 | pRS413(met25). Yeast high copy shuttle vector. Used in *E. coli* and *S. cerevisiae.* Derived from pBluesript II SK(-).

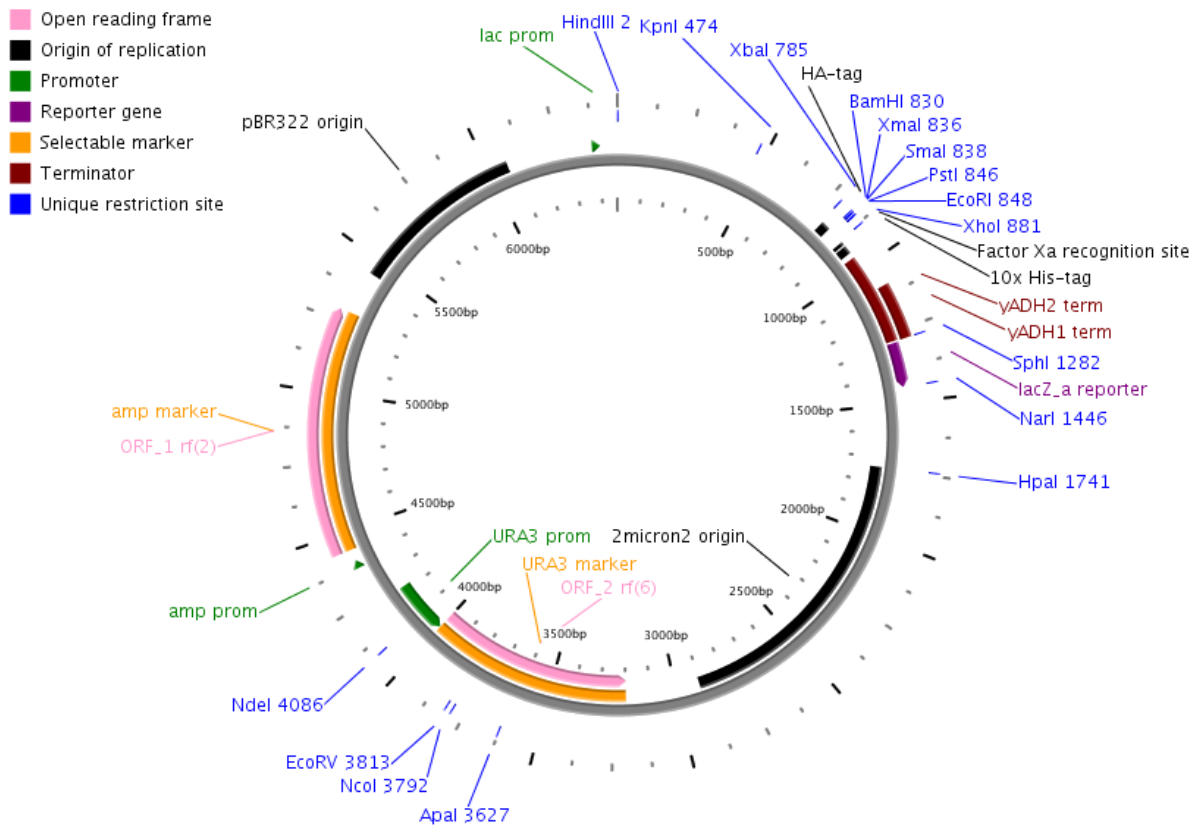

Figure 2.4 | pDRTXa. Yeast high copy shuttle vector. Used in *E. coli* and *S. cerevisiae.* Has a N-terminal HA- and a C-terminal 10x His-tag, with the latter being cleavable due to an upstream factor Xa recognition site.

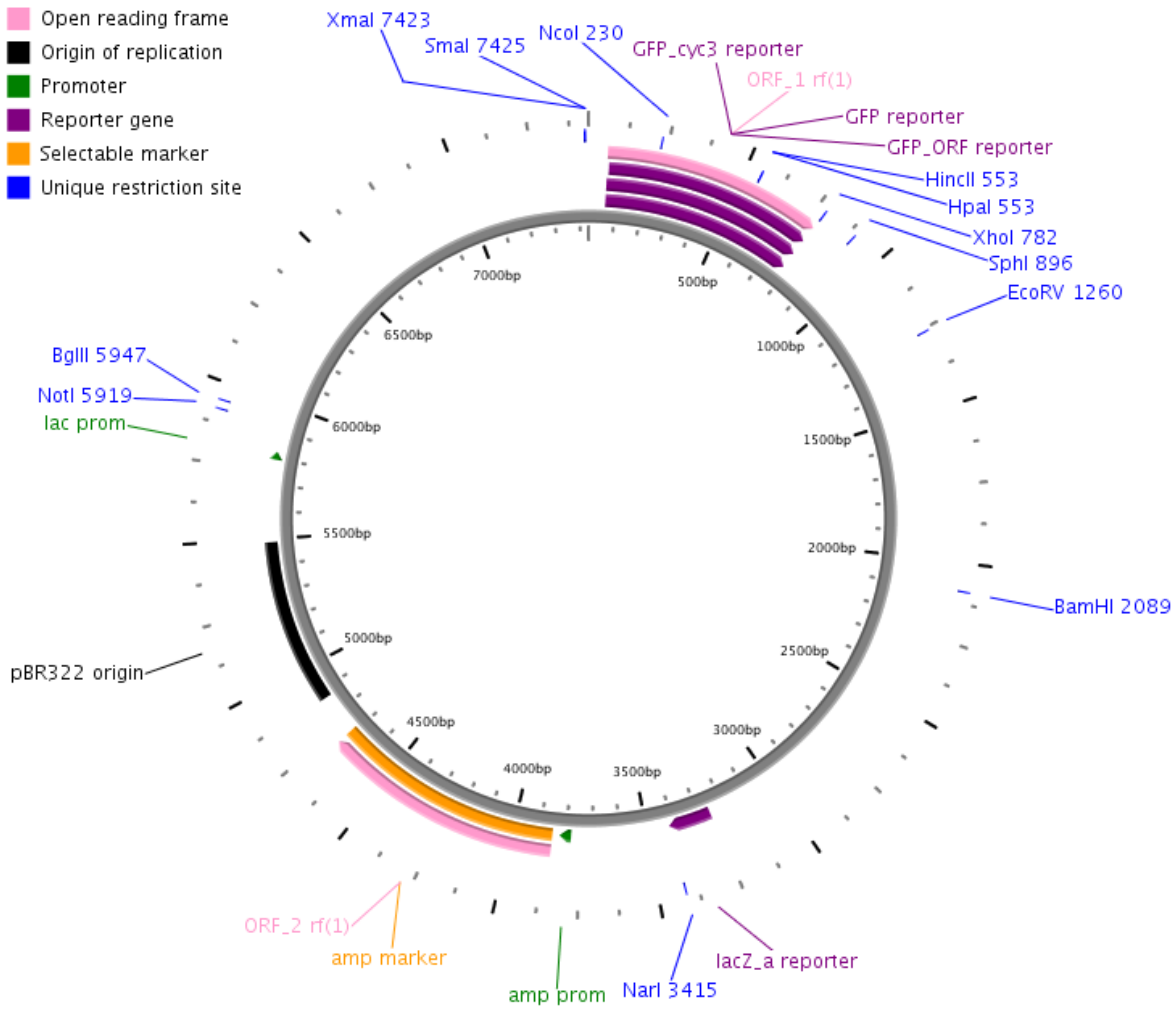

Figure 2.5 | pARL1-GFP. Expression vector in *P. falciparum* with a C-terminal GFP-tag.

2.4 Primer and oligonucleotides used

Primer name	Sequence
T7 sequencing primer	TAA TAC GAC TCA CTA TAG GG
T3 sequencing primer	GTG TAA GTT GGT ATT ATG TAG
PMA5‘ sequencing primer	CTCTCTTTTATACACACATTC
ADH3‘ sequencing primer	CATAAATCATAAGAAATTCGC
rMCT1-F(Spe)	gagagaACTAGTATGCCACCTGCGATTGGCGGGCCAGTG
rMCT1-rv(Sal)	gagagaGTCGACGACTGGGCTCTCCTCCTCCGCGGGGTC
rMCT1 ’985 rv sequencing primer	GGCACACTCCATTCGCAACAACAGA
rMCT1 ’599 f sequencing primer	CTCAGCAAGGCAAGGTGGAAAAACTCAAG
hMCT4-F(Bam)	gagagaGGATCCATGGGAGGGGCCGTGGTGGACGAG
hMCT4-rv(Sal)	gagagaGTCGACGACACTTGTTTCCGGGGTGTGAAC
hMCT4 ’1072 Rv sequencing primer	GCCACCGCCTCCATCAGCAGCACCAG
hMCT4 ’549 F sequencing primer	GGGCGGCCTGCTGCTCAACTGCTGCGTGTG
SceJEN1 Rv 3’ (SalI)	TCT gtc gac TTA AAC GGT CTC AAT ATG CTC CTC
SceJEN1 F 5’ (BamHI)	AGA gga tcc ATG TCG TCG TCA ATT ACA GAT GAG
ScJen1 iF sequencing primer	TGC GTT TCA GTA TCA GTC GC
ScJen1 iRv sequencing primer	TCA TAC CCC CAC AAA TAG CAC
Pf70 F 5’ (SalI)	TACGACGTTCCTGACTACGCGGACactagtATGAATATAATACCTTCA ACAGCTGTG
Pf70 Rv 3’ (XhoI)	CCTTACTTATGTGTATCTTGACAAActcgagATCGAGGGAAGGGTCG AGCAC
Pf70 ’563 iF sequencing primer	AAGATGTTTTGAATAGAGT
Pf70 ’646 iRv sequencing primer	TTCTGGATCATTGTCCATTTTAACTTCCATGGTTGC
Pf75 F 5’ (SpeI)	TACGACGTTCCTGACTACGCGGACactagtATGAAAAAAGAGAATAC

	TTCCCTGTTATC
Pf 75 Rv 3' (XhoI)	CAGCATCATGTTAGCACTAGCATTTctcgagATCGAGGGAAGGGTCG AGCAC
PfFNT F 5' (BamHI)	GAGAGAggatccATGCCACCAAATAATTCCAAATATGTTTTAGATC
PfFNT Rv 3' (XhoI)	CTCAAATGAAAAGTTTATCTATAGAATTACGAAATctcgagTCTCTC

2.5 Organisms

2.5.1 *E. coli* strains

Stratagene, Waldbronn
Escherichia coli XL1-blue MRF'

Escherichia coli DH5 F– '80lacZ15M(lacZYA-argF)U169 recA1 endA1 phoA supE44 hsdR17(rk–, mK+)– thi-1 gyrA96 relA1

2.5.2 *S. cerevisiae* strains

Saccharomyces cerevisiae W303-1A Δjen1 Δady2 (MATa, can1-100, ade2-1oc, his3-11-15, leu2-3,-112, trp1-1-1, ura3-1, jen1::kanMX4, ady2::hphMX4) kindly provided by M. Casal

Euroscarf, Frankfurt
Saccharomyces cerevisiae BY4742 (Brachmann et al., 1998)
Saccharomyces cerevisiae BY4742Δfps1 (MATa, his3-1, leu2Δ0, lys2Δ0, ura3Δ0, fps1::kanMX)

Own laboratory
Saccharomyces cerevisiae BY4742Δjen1Δady2Δcyb2 LDH (MATa, his3-1, lys2Δ0, ura3Δ0, Δcyb2+LDH::kanMX, Δady2::NAT, Δjen1::LEU2)
Saccharomyces cerevisiae BY4742Δjen1Δady2Δcyb2Δadh1 LDH (MATa, lys2Δ0, ura3Δ0, Δcyb2+LDH::kanMX, Δady2::NAT, Δjen1::LEU2, Δadh1::HIS3)

2.5.3 *Plasmodium* strain

Plasmodium falciparum 3D7

2.6 Antibodies

Anti HA 12CA5 mouse, monoclonal, Roche 1:5000/ 1:2000 (dilution first/second antibody)
Penta-His mouse, monoclonal, Qiagen 1:5000/ 1:5000 (dilution first/second antibody)
HRP-Conjugated anti-mouse goat, Jackson Immuno Research

2.7 Buffer and media

AppliChem, Darmstadt
LB medium powder (Lennox), LB agar (Lennox)

Becton Dickinson, Heidelberg
Bacto Agar, Bacto Peptone, Bacto Tryptone, Bacto Yeast Extract, Difco Yeast Nitrogen Base w/o Amino Acids and Ammonium (YNB)

Oxoid, Basingstoke, UK
Agar Bacteriological

Roth, Karlsruhe
LB medium powder (Lennox), LB agar (Lennox)

***E. coli* growth media**
1000 x Ampicillin
(ampicillin Na 10 %, -20 °C)

1000 x Tetracyclin
(tetracyclin 1.5 %, -20 °C)

LB medium (Lennox)
(tryptone 1 %, yeast extract 0.5 %, NaCl 0.5 %, or prepared from LB-medium-powder 2 %)

LB agar (Lennox)
(tryptone 1 %, yeast extract 0.5 %, NaCl 0.5 %, Bacto Agar 1.5 %, or prepared from LBagar-powder 3.5 %)

Antibiotic-containing LB media
(ampicillin 100 µg/ml or tetracycline 15 µg/ml, added after autoclaving)

***S. cerevisiae* growth media**
1000 x Histidine
(L-histidine HCl·1H2O 2 %, 4 °C)

200 x Leucine
(L-leucine 2 %)

1000 x Lysine
(L-lysine HCl 2 %, 4 °C)

100x Uracil
(0.2 %)

200x Adenine
(0.5 %)

500x Tryptophan
(0.5 %, 4 °C)

100x L-lactate
(2.5 %)

YPD
(yeast extract 1 %, peptone 2 %, D-glucose 2 %)

SD KHL
(YNB 0.17 %, (NH4)2SO4 0.5 %, D-glucose·H2O 2 %, NaOH → pH 5.6, L-lysine HCl 20 mg/l, L-histidine HCl·1H2O 20 mg/l, L-leucine 100 mg/l)
Amino acids were added after autoclaving.

SLac AHLW

(YNB 0.17 %, (NH4)2SO4 0.5 %, L-lactate 0.25 %, pH was set either with NaOH or HCl to pH 5.0 (buffered with succinate 0.25 mM)/ 6.0 or 6.5 (buffered with MES 20 mM)/ 7.0 or 7.5 (buffered with TRIS 50 mM), adenine 25 mg/l, L-histidine HCl·1H2O 20 mg/l, L-leucine 100 mg/l, L-tryptophan 10 mg/l)

Amino acids and L-lactate were added after autoclaving.

YPD and SD KHL agar

(Oxoid Agar 2 % in the respective media)

***P. falciparum* buffer**

Standard buffer (125 mM NaCl, 5 mM KCl, 20 mM glucose, 25 mM HEPES, 25 mM MES, 1 mM $MgCl_2$, pH 6.8)

L-lactate buffer (125 mM NaCl, 5 mM KCl, 1 mM $MgCl_2$, 20 mM glucose, 25 mM HEPES, 25 mM MES and 5 mM L-lactate sodium salt (final concentration) pH 6.8 and 0.1 µCi/µl)

Oil phase (5:4 Dibutylphthalate/Dioctylphthalate)

3 Methods

3.1 Molecular biology methods

3.1.1 *E. coli* competent cells generation

For the generation of competent *E. coli* cells either the DH5α-strain or the XL1-Blue-strain was used. When DH5α bacteria were used no addition of antibiotics to the growth medium was necessary contrary to XL1-Blue cells, where 15 mg/l tetracycline was added to the LB-medium.

5 ml of medium were inoculated with bacteria and grown overnight (with 200 rpm shaking) at 37 °C. Out of this pre-culture a 100-fold dilution in 100 ml was generated which was incubated at again 37° C with shaking until an OD_{600} of 0.3 - 0.6 was reached. These cells were harvested with centrifugation at 2000 *g* for 10 minutes and kept on ice. The resulting pellet was washed twice with a 0.1 M $CaCl_2$ solution and resuspended in 10 ml of 0.1 M $CaCl_2$ containing 20 % glycerol. Accordingly cells were incubated on ice for at least four hours and aliquotated to 100 µl in 1.5 ml reaction tubes which were stored at -80 °C.

3.1.2 *E. coli* transformation

A 100 µl aliquot of competent *E. coli* cells was taken out of the -80 °C freezer and incubated on ice for about three minutes. Less than 25 µl DNA-solution was pipetted to the cells which were again incubated on ice for 30 minutes. Followed by one minute heat shock at 42 °C, the *E. coli* were kept on ice for another two minutes. Subsequently 900 µl LB medium was added to the cells and incubated for one hour at 37 °C with shaking on a roller drum. After centrifugation of the *E. coli* at 13000 *g* for 15 seconds 900 µl medium was discarded and the cells resuspendend in the remaining 100 µl. The cell suspension was plated on agar plates containing the appropriate antibiotic for selection and incubated over night at 37 °C.

3.1.3 *E. coli* cultivation and generation of permanent cultures

If not indicated elsewise all cultivation of *E. coli* was performed at 37 °C. First cells derived from either transformation or out of glycerol stocks were spread on agar plates and incubated overnight. On the next day single colonies were picked and incubated in 4 ml liquid LB medium for another overnight period. For longer storage of these cultures 0.5 ml cell suspension was mixed with 0.5 ml glycerol 85% in a 1.5 ml reaction tube and frozen at -80 °C.

3.1.4 *E. coli* plasmid DNA isolation

Isolation of *E. coli* plasmid DNA was achieved using a commercial kit Wizard® Plus SV Minipreps (Promega) and executed according to the manufacturers manual.

3.1.5 Purification and determination of DNA concentration

In order to purify DNA for cloning it was processed via a commercial kit the HiYield® PCR Clean-up/Gel Extraction Kit (SLG®) either directly, e.g. if a restriction enzyme digestion was done or after an agarose gel electrophoresis.

For separation of DNA by size agarose gel electrophoresis (1 % agarose in 50 ml TAE buffer with 1 µl ethidiumbromide) was used. Samples were mixed with a loading buffer and separated by electrophoresis at 100 V for 20 minutes. The size and the concentration of the fragments were estimated by comparing them to a size marker consisting of PstI-digested λ-DNA under a UV light at 366 nm (figure 3.1).

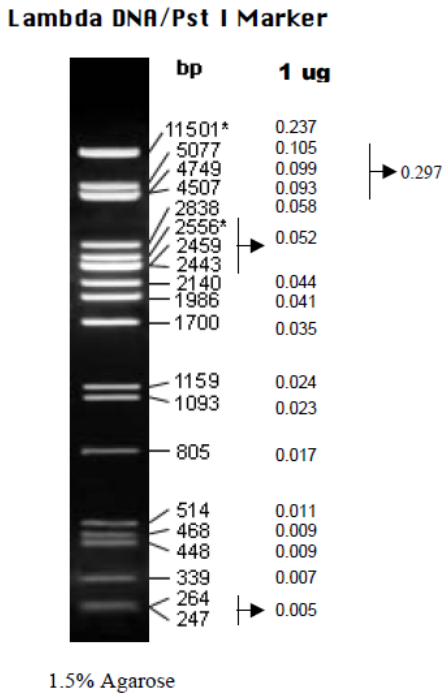

Figure 3.1 | Lambda DNA size marker. The DNA of the phage is digested with PstI [New England Biolabs].

3.1.6 DNA sequencing

Sequencing was accomplished by using a CEQTM 8000 Genetic Analysis System of Beckman Coulter®. Here the DNA was separated by capillary gel electrophoresis and visualized by fluorescence dye labeled didesoxyribonucleoside-triphosphates (ddNTPs) during PCR amplification. For this 50 – 150 fmol dsDNA was used in an optimal DNA to primer ratio of 1:40. 6 µl DNA and primer were mixed with 4 µl "GenomeLab DTCS - Quick Start Master Mix" and the following PCR program was run:

Initial denaturation	96 °C	5 minutes	
Denaturation	96 °C	20 seconds	30x
Annealing	50 °C	20 seconds	
Elongation	60 °C	4 minutes	
Storage	8 °C	Infinite	

After running the PCR to each sample 5 µl stop solution was added containing 2 µl 3 M NaOAc pH 5.2, 2 µl 100 m M EDTA pH 8.0 and 1 µl 20 mg/ml glycogen. Further DNA purification was done by ethanol precipitation where each sample was transferred to a 1.5 ml reaction tube. Here 60 µl ice cold 95% ethanol was added and afterwards immediately centrifugated at 15 000 *g* for 15 minutes. After carefully removing the supernatant the resulting pellet was washed twice with ice cold 70% ethanol followed by drying for 15 minutes in the SpeedVac®. The dry pellets were resuspended in 30 µl "Sample Loading Solution (SLS)" and analyzed in the sequencer.

Results were interpreted using the DNASTAR software.

3.1.7 DNA modification

DNA cloning was done to multiply desired DNA. For this, the gene sequence and a plasmid had to be digested with compatible ends generated by suitable restriction enzymes. The vector was additionally dephosphorylated with Calf Intestine Alkaline Phosphatase (CIAP). Furthermore the DNA was purified by either a commercial kit or by gel purification (see 3.1.5), ligated via the T4 DNA Ligase and transformed into *E. coli* for amplification (see 3.1.2). A control digestion was done verification. After a site directed mutagenesis the modified DNA was sequenced additionally.

3.1.8 Polymerase chain reaction

The PCR is a multi-purpose tool used not only for simple amplification of pieces of DNA but also, if slightly modified, for many other applications, e. g. site directed mutagenesis, generation of single strand copy DNA and sequencing.

For standard PCR the template DNA that had to be amplified was mixed with two sequence specific primers (each 0.5 µM), dNTPs (each 200 µM), 5x One*Taq* Standard Reaction Buffer (NEB) and One*Taq* DNA Polymerase (NEB). The total volume was set with ddH_2O to 50 µl. The temperature settings were adapted to the template DNA, the primers and the length of the generated PCR product. The standard program was as following:

Denaturation	95 °C	5 min	
Denaturation	95 °C	1 min	30x
Annealing	T_m	30 s	
Extension	68 °C	1-3 min	
Final extension	68 °C	10 min	
Storage	8 °C	∞	

The number of cycles was depended on the quality of the template DNA, mostly it was set to 30 times. The annealing temperature T_m was depended on the composition of the primer pair and was calculated with the following formula:

$$T_m = 4 \cdot (GC\%) + 2 \cdot (AT\%)$$

With GC% and AT% being the percentaged concentrations in the primers. The extension time was calculated with:

$$t = 0.06 \cdot base\ pairs\ of\ expected\ product\ lenght$$

Note that this time was never less than 1 minute.

3.1.9 Site directed mutagenesis

This PCR variation was used to mutate specific single amino acids in gene sequences.
For the PCR 50 ng of pBluescript plasmid DNA containing the gene coding sequence was used together with 30 µM of the respective forward and reverse primers which contained the desired sequence alterations. Furthermore dNTPs, the Pfu Turbo® DNA Polymerase AD Puffer and the Pfu Turbo® DNA Polymerase AD were added in a reaction tube and throughoutly mixed. The reaction tube was placed inside a termocycler and the following program was run:

Denaturation	95 °C	2 min	
Denaturation	95 °C	1 min	30x
Annealing	55 °C	1 min	
Extension	68 °C	15 min	
Final extension	68 °C	10 min	
Storage	8 °C	∞	

After running the PCR program the template DNA was digested with *Dpn*I at 37 °C for overnight. On the next day purification of the synthesized DNA was carried out as described in 3.1.5. With the newly generated plasmid *E. coli* competent cells were transformed followed by sequencing to ensure a successful mutation.

3.1.10 Colony PCR

This protocol was designed to quickly screen for positive mutations in the genome of bacteria or yeasts. Parameters of the method were similar to the standard PCR with the exception that instead of purified DNA a lysate of a single clone was used. A clone was picked with a pipette tip and suspended in 20 µl of ddH_2O. This suspension was boiled at 95 °C for 30 seconds and spun down 16,000 *g* for 2 seconds. 5 µl of the supernatant were used as template for PCR (see 3.1.8).

3.1.11 First strand cDNA synthesis

First strand cDNA synthesis was needed to obtain coding DNA without introns from *P. falciparum* RNA. A commercial kit, "First Strand cDNA Synthesis Kit" (Thermo Scientific) was used. Afterwards the generated cDNA was directly used as template for amplification of the desired genes.

3.1.12 *S. cerevisiae* transformation

For transformation the strain was inoculated in 5 ml YPD medium and grown overnight at 29 °C with 200 rpm shaking. The culture was diluted in 50 ml YPD medium to an OD_{600} of 0.2 and incubated at 29 °C with 200 rpm shaking till the OD_{600} reached about 0.6 (being normally about four hours). Cells were collected at 3000 *g* for 5 minutes and washed twice with 25 ml ddH_2O and finally resuspended in 1 ml ddH_2O. For each transformation 100 µl yeast suspension was pipetted into 1.5 ml reaction tubes and centrifuged again at 13000 rpm for another 30 seconds. The supernatant was discarded and 360 ml transformation mix (240 ml PEG3500 (50 %), 36 ml 1 M lithium acetate, 50 ml boiled *single-stranded-carrier* DNA, 34 ml ddH_2O and 0.4 ml plasmid-DNA) were added. Immediately after adding the mix, cells were resuspended by rubbing the reaction tubes over a plastic rack. Thereafter the tubes were

incubated at 42 °C for 1 hour, centrifuged at 13000 rpm for 30 seconds and the supernatant was discarded. The obtained pellet was resuspended in 1 ml ddH_2O. 100 µl were plated onto agar plates containing the appropriate nutritional composition for selection. The plates were incubated at 29 °C for 3 to 5 days.

3.1.13 Yeast glycerol stock generation

500 µl of an overnight culture of *S. cerevisiae* was thoroughly mixed with glycerol 80% and immediately frozen at -80 °C.

3.1.14 Gene knock-out in *S. cerevisiae*

Genetic modification of yeasts was necessary to sustain a strain that was unable to grow on L-lactate as the sole carbon source without a suitable exogenous lactate-facilitator. The method used is a PCR-based gene deletion strategy derived from Baudin et al. (1993).

First, mutation primer had to be designed. They had to be complement to approximately 45 base pairs of the region up- and downstream of the desired gene sequence in the yeast chromosomal genome. With these primers a resistance cassette was amplified by PCR. The product was directly transformed into the selected yeast strain. Transformation was executed (see 3.3.1) with the difference that after the heat shock cells were resuspended in 1 ml YPD medium and incubated for another 2 to 3 hours at 29 °C with 200 rpm shaking. During this incubation homologous recombination occurred (figure 3.2). Afterwards cells were plated and incubated like previously described (see 3.1.12).

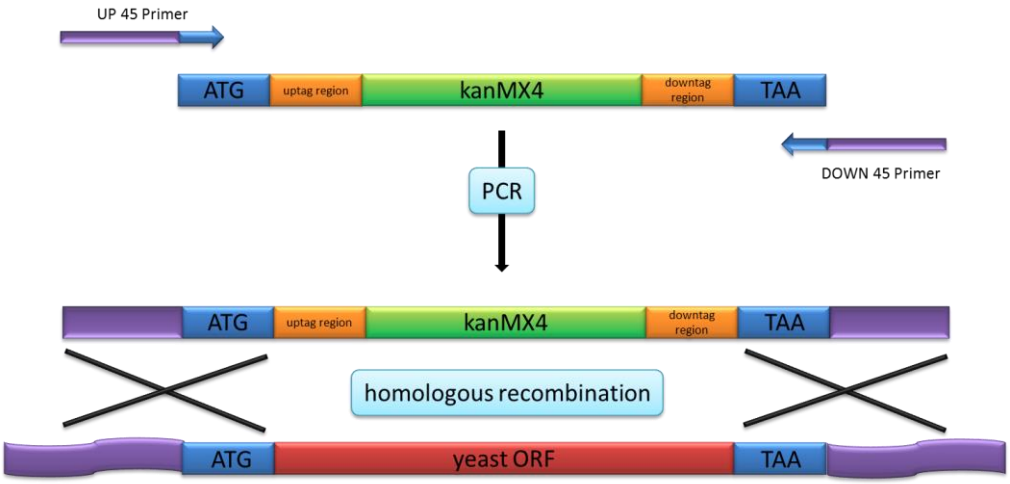

Figure 3.2 | Homologous recombination in yeast. A PCR product is directly used for exchange with a defined chromosomal sequence via homologous recombination in *S. cerevisiae*. Note that the homologous linker arms consist only of about 45 base pairs. ORF = open reading frame, kanMX4 = kanamycin resistance cassette

From the resulting plates 4 single colonies were plated again on selection agar and incubated for another 3 to 5 days at 29 °C. To verify the knock out a colony PCR was performed (see 3.1.10). Positive clones for the intended gene knock were taken for permanent culture generation (see 3.1.13).

3.2 Protein analytics

3.2.1 Protein quantification

In order to estimate the protein concentration of yeast microsomal fractions the Bradford assay was carried out. For this commercial available "Bio-Rad Protein Assay" reagent was used. A calibration curve with bovine serum albumin (BSA) as a standard is inevitable for estimating the protein concentration. For the measurement 0.8 to 8 µl of the sample were diluted in 800 µl distilled water and mixed with 200 µl of the Bio-Rad reagent. After incubation of 5 to 10 minutes at room temperature the sample was measured at 595 nm wave length with distilled water as blank.

3.2.2 SDS PAGE

Sodium lauryl sulfate polyacrylamide gel electrophoresis is a valuable method to separate proteins (mainly) by size. Thereby the anionic detergent SDS denaturizes the peptides and copes the ionic charges of the amino acid residues to an overall negatively charged molecule which is then separated through a gel matrix by its electrophoretic mobility. Since the charge of all peptides is negative due to the SDS treatment smaller molecules are able to move faster to the anode and therefore are separated from the bigger, i. e. longer protein chains. The gel typically consists of a resolving and a stacking unit which are composed as follows:

	Resolving gel		Stacking gel
	12.5%	15%	
ddH_2O	5.25 ml	4.5 ml	2.4 ml
Resolving gel buffer	3.0 ml	3.0 ml	-
Stacking gel buffer	-	-	1.0 ml
Acrylamide (40%)	3.75 ml	4.5 ml	0.6 ml
TEMED	10 µl	10 µl	6 µl
APS (10%)	80 µl	80 µl	25 µl

For denaturation, membrane-proteins were incubated with 4x SDS loading buffer for 30 minutes at 37 °C. The gel was polymerized between two glass plates in a gel caster with a comb on top to generate sample pockets. Once the samples are loaded onto the gel 160 V were applied till the samples had run through the stacking gel. At this point the voltage was increased to 200 V. When the samples had reached to middle of the resolving gel voltage was switched off. After this the gel was either stained with Coomassie-blue or transferred onto a PVDF membrane for Western blotting. For staining, Coomassie Brilliant Blue (“Rotiphorese Blue R”) was used. Here the SDS gel was incubated shakingly at room temperature for one hour. Destaining solution was used untill the background staining had lowered appropriately and bands became visible.

3.2.3 Western-Blotting

Typically Western-Blotting was used to visualize peptides after they have been separated by SDS PAGE. Here proteins are transferred onto a PVDF membrane and specifically detected by antibodies. After gel electrophoresis the SDS gel was placed between six Whatman® papers which had been soaked in transfer buffer solution and a PVDF membrane which had been activated by incubation in methanol for five minutes at room temperature. The proteins were transferred at 17 V for 1 hour to the PVDF membrane. When the blotting was completed the membrane with the transferred proteins was blocked for 1 h in TBS-T solution with 3% milk powder at room temperature. Subsequent the membrane was incubated shakingly with the primary antibody in TBS-T containing 3% milk powder overnight at 4 °C. At the next day non bound antibodies were washed off with TBS-T solution shakingly for 15 minutes at room temperature. This was repeated three times. Afterwards the secondary antibody was added and incubated for one hour at room temperature with shaking. The following washing steps were carried out like done before. To activate the horseradish peroxidase of the secondary antibody it was incubated in a commercially available reaction mix ("ECL Plus Western Blotting Detection System", GE Healthcare) for 5 minutes at room temperature. The resulting chemiluminescence was detected in an imaging and gel documentation system (Lumi-Imager F1™, Roche).

3.2.4 Isolation of the *S. cerevisiae* microsomal fraction

In order to isolate membrane proteins in yeast the following method was applied. A colony of transformed yeast cells was picked from an agar plate and inoculated in 100 ml medium for one to two days at 29 °C with shaking till the OD_{600} reached about 1. After centrifugation at 3000 *g* for 5 minutes cells were washed first with 50 ml water and second with 1 ml precooled extraction buffer. Thereafter the cells were resuspended in 0.5 ml precooled extraction buffer containing 15 µl protease-inhibitor-mix (25×) and kept on ice for the rest of the procedure in 50 ml falcon tubes. An equal volume of acid washed glass beads was added and vortexed for 10 times for 30 seconds with incubation on ice for also 30 seconds in between. Subsequent the yeast cells were collected by centrifugation at 13000 *g* for 5 minutes at 4 °C. The supernatant was kept and transferred to ultracentrifugation tubes. The remaining pellet was again resuspended in 0.5 ml extraction buffer with 15 µl protease-inhibitor-mix (25×) and a final extraction cycle with adjacent centrifugation was executed. The resulting

supernatant was added to the previous one to the ultracentrifugation tubes. Ultracentrifugation was performed at 100000 *g* for 45 minutes at 4 °C under low-pressure. The supernatant was discarded and the pellet in 100 µl storage buffer containing 10 µl protease-inhibitor-mix (25×) resuspended. Samples were stored at -20 °C if not processed immediately.

3.3 Enzymatic L-lactate determination

To measure the L-lactate concentration in yeast medium a commercially available kit "Enzytec(TM) L-Milchsäure Test" (r-biopharm) was used. The manufacturers manual was altered for higher sample number, due to smaller sample volumes. The method underlies the following principles and pipetting scheme:

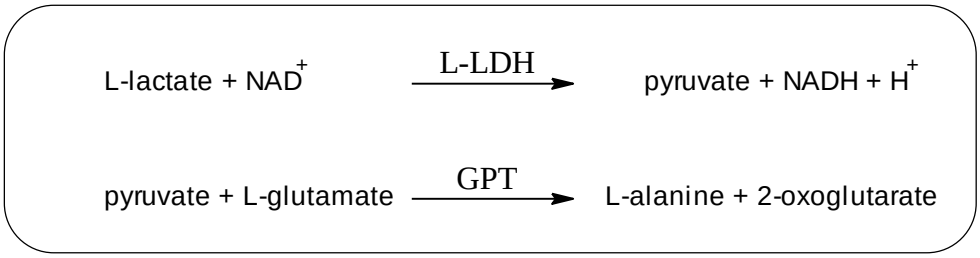

Figure 3.3 | Principle of enzymatic reaction. L-lactate is oxidized to pyruvate while NAD^+ is reduced to NADH. NADH is detected by UV absorption. To ensure a complete conversion and to prevent a back reaction an amino group is transferred from pyruvate to L-glutamate via GPT.

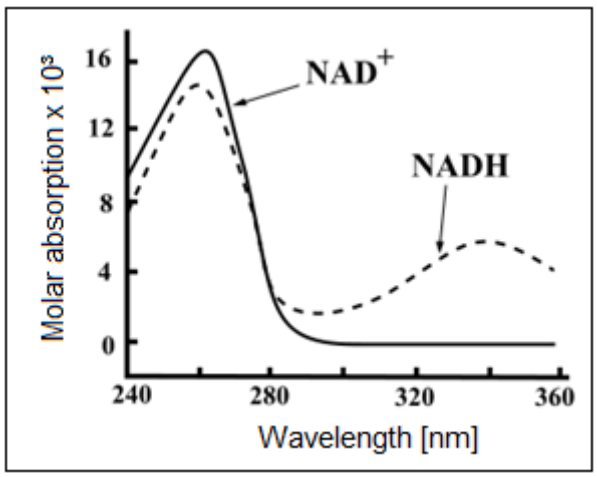

Figure 3.4 | Absorption pattern of NAD⁺/NADH. Generation of NADH is detected at 340 nm. Since the reaction ratio is equimolar the L-lactate concentration in the sample can be calculated [R-Biopharm AG, Darmstadt].

Pipette into 96-well plate:	Blank	Standard	Sample
Glycylglycine Buffer #1	75.89 µl	75.89 µl	75.89 µl
NAD solution # 2	15.18 µl	15.18 µl	15.18 µl
GPT suspension # 3	1.52 µl	1.52 µl	1.52 µl
Sample solution	-	-	75.89 µl
Standard solution	-	75.89 µl	-
Redist. Water	75.89 µl	-	-
--- MIX ---	----------	----------	----------
L-LDH solution	1.52 µl	1.52 µl	1.52 µl
Total volume	170 µl	170 µl	170 µl

Figure 3.5 | Pipetting scheme for enzymatic L-lactate determination. This scheme was altered from the manufacturers' original in order to adopt the measurement to a 96-well plate. Before adding the LDH enzyme the samples had to be thoroughly mixed and incubated for 5 minutes at room temperature. The final volumes of 170 µl lead to a liquid volume of 1 cm width in a single well. This allowed a direct calculation of the L-lactate concentration in the sample.

3.4 Functional characterization in yeast

3.4.1 Phenotypic lactate uptake assay

Basic principle of the lactate uptake assays was that a *S. cerevisiae* knock out strain was used which lacks endogenous lactate transporters and is therefore unable to grow on lactate as the sole carbon source. Introduction of an exogenous lactate transporter restores growth which is why this assay was used for a plasmodial lactate transporter screening.

The yeasts were incubated at 30 °C in YPD or synthetic selective medium containing the appropriate nutritional requirements with 220 rpm shaking in liquid culture or on agar plates. In synthetic selective medium (SD) the sole carbon source was either 2% (wt/vol) glucose or 0.25% (wt/vol) L-lactate sodium salt. Yeast from liquid cultures was harvested at the exponential phase of growth at an OD_{600} of about 0.8 washed twice with water and resuspended in water. The cells were now prepared for further testing depending on the method used.

3.4.1.1 Agar plate assay

The yeast OD_{600} was set to 1 (± 10%) and diluted 1:10, 1:100 and 1:1000. From this suspension 5 µl were pipetted onto a SD agar plate (either 2% glucose or 0.25% L-lactate) which was buffered with 20 mM MES, pH 5.6. The plates were incubated at 30 °C for 5-7 days. Results were documented.

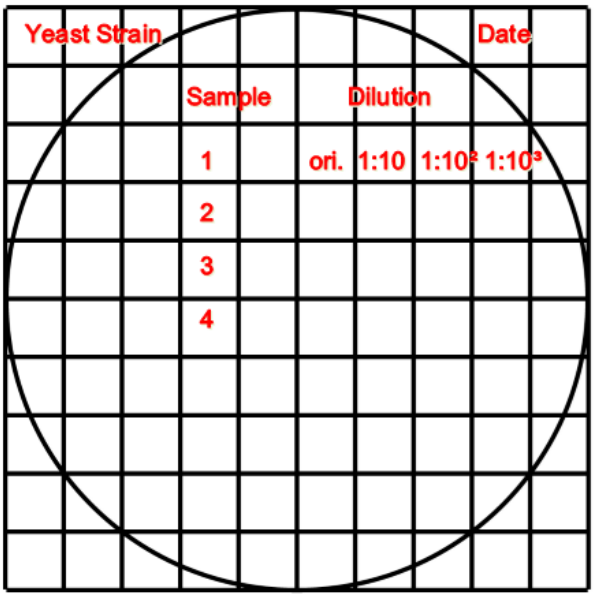

Figure 3.6 | Sample application scheme for plate assay. A grid was placed underneath the agar plate for easier pipetting.

3.4.1.2 Semi-quantitative liquid culture assay

10 µl cell suspension at an OD_{600} of 2 (± 25%) were mixed with 290 µl SD medium again with either 2% glucose or 0.25% L-lactate as the only carbon source. The medium was buffered with either 25 mM succinate (for pH 5.0), 20 mM MES (for pH 6.0 and 6.5) or 50 mM TRIS (for pH 7.0 and 7.5). For the assay multiwell honeycomb micro plates (BioScreen Testing Services, Inc., Torrance, CA) were used and measured in a BioScreen C Analyzer (BioScreen Testing Services, Inc., Torrance, CA) for one week at an incubation temperature of 30 °C. The turbidity was recorded via a wide band filter (420-580 nm).

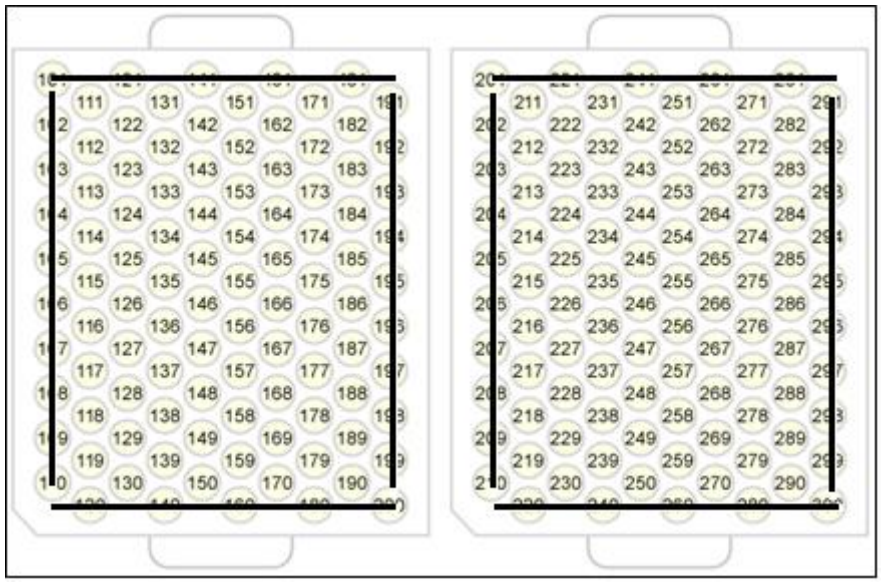

Figure 3.7 | BioScreen C® Honeycomb 100-well plate. According to the manufacturer this rather unconventional geometry provides a uniform temperature across all wells on a plate. Contrary to that more evaporation was observed at the wells on the edges and hence not used.

3.4.2 Radiolabeled substrate transport assays

For direct transport characterization of PfFNT, ^{14}C-radiolabled substrate transport assays with different test parameters were established. ^{14}C-carbon is an unstable isotope of carbon which naturally occurs on earth about one part per trillion out of all carbon in the atmosphere. It has a half-life of 5730 years and is radioactive, i.e. it decays into ^{14}N through beta decay. ^{14}C labeled substrates were detected in a liquid scintillation counter (figure 3.8).

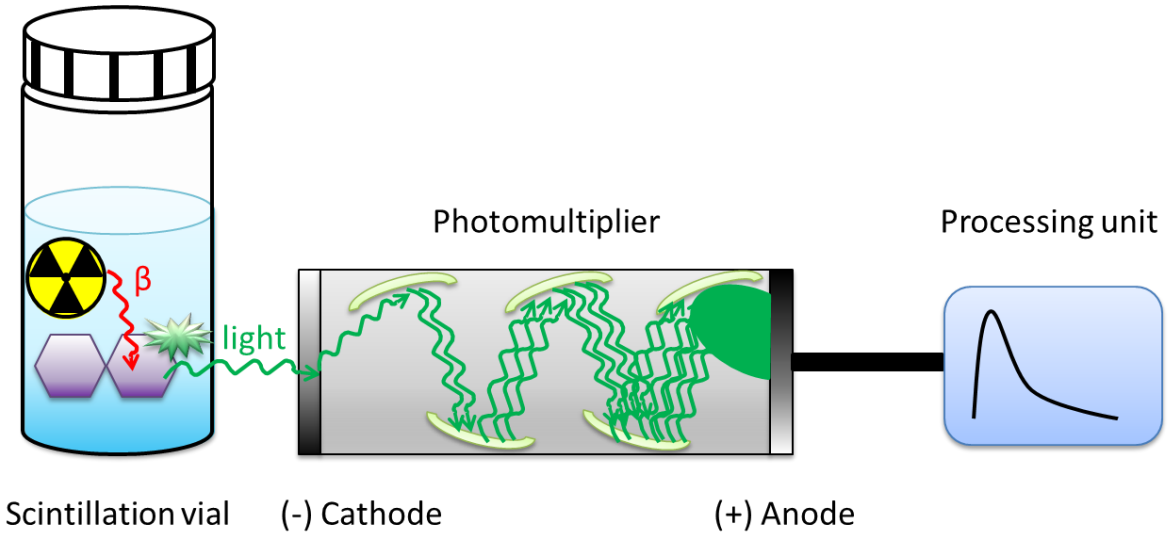

Figure 3.8 | Scheme of liquid scintillation counting. Beta rays induce light emission from aromatic molecules. Light pulses are amplified in a photomultiplier unit. The resulting current is recorded and converted into a spectrum.

For this purpose samples were treated with scintillation cocktail which contained aromatic molecules that have the ability to emit fluorescence when exposed to beta particles. These emitted light pulses were recorded in a photomultiplier unit over a time period of 2 minutes and the counts per minute (CPM) were calculated. Since the exact composition of the scintillation cocktail differs from company to company and is kept secret, commonly used scintillators are shown in figure 3.9.

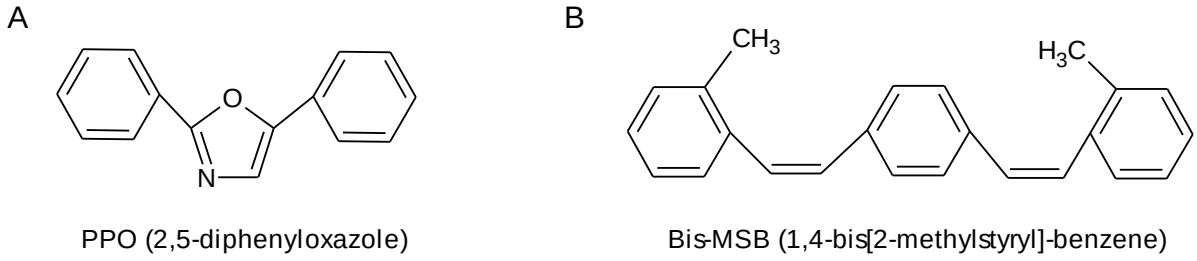

Figure 3.9 | Commonly used scintillators. Molecules are drawn by Chemsketch.

PPO (see figure 3.9 A) is a primary scintillator, e.g. is capable of converting beta particles into emitted light. Since this emitted wavelength is quite narrow and with high energy (357 nm) the secondary scintillator bis-MSB (see figure 3.9 B) is used as a wavelength-shifter. In this process the first emitted fluorescence is converted into light with lower energy (420 nm) which is much better permeable through the plastic sample tubes and therefore gives a higher efficiency of counting.

After overnight incubation in selective medium yeasts were harvested in the exponential phase with an OD_{600} of about 0.8. They were collected by centrifugation at 4000 *g* and thereafter washed with sterile water and resuspended in a buffer containing 50 mM HEPES/TRIS at pH 6.8 (or the indicated pH and buffer). The OD_{600} was set to 50 (± 10%) and the cells were kept on ice. In 1.5 ml reaction tubes, aliquots of yeast suspension were prepared and incubated for 2 minutes at 18° C immediate before each measurement. All experiments were performed at room temperature with at least three replicates.

3.4.2.1 Substrate import

To start the uptake assay, 80 µl of cell suspension (final OD_{600} 40) were mixed with 20 µl 0.02 µCi radiolabeled L-[1-14C]-lactate with a final concentration of 1 mM (or the indicated concentration) and 50 mM HEPES/TRIS buffer (for pH 6.8 or 7.8) or as indicated 50 mM citric acid/TRIS (for pH 2.8 to 4.8) or 50 mM MES/TRIS (for pH 5.8). The reaction was stopped at various time points by diluting with 1 ml ice cold water. The suspension was pipetted onto a GF/C filter membrane (Whatman™) and washed with 7 ml ice cold water by vacuum filtration (figure 3.10). The process of dilution, washing and filtration was accomplished within 10 seconds. The filter was transferred to a scintillation vial containing 5 ml scintillation fluid (Quicksafe A, Zinsser Analytic GmbH, Frankfurt, Germany) and measured in a Packard Tri Carb liquid scintillation photometer (PerkinElmer Inc.). Always at least triplicates were measured. The L-lactate that was lost during the washing and filtering procedure was about 15 % (compared to an experiment with 1 mM L-lactate solution used for dilution and washing) which was within the typical error margin of the method itself.

Figure 3.10 | Drawing of the measuring system. 100 ml Erlenmeyer flasks are equipped with Hirsch funnels and connected to an underpressure distribution device. Each flask has its own adjustable valve.

3.4.2.2 Substrate export

The 80 µl yeast suspension aliquots (final OD_{600} = 40) were preloaded with 20 µl 1 mM L-lactate containing 0.02 µCi radiolabeled L-[1-14C]-lactate (or the indicated substrate). After 4 minutes incubation the substrate uptake was stopped by centrifugation at 13500 *g*. Directly afterwards 90 µl supernatant was removed and the cells were resuspended in 1 ml suspension buffer (50 mM HEPES/TRIS, pH 6.8) to initiate the export measurement. At various time points the export was terminated by filtering the cell suspension through a GF/C filter membrane and washed with 7 ml ice cold water by vacuum filtration. The filter was transferred into a scintillation vial containing 5 ml scintillation liquid and counted in a liquid scintillation photometer. The exported lactate was calculated from the values of the intaken lactate after four minutes and the remaining lactate in the yeasts after stopping the export. All experiments were repeated for at least three times. There had to be made some adaptions for the export of D-lactate due its high metabolic rates in yeast. Therefore the temperature had to be lowered to 4 °C and 0.5% deoxyglucose was added to the assay buffer. Furthermore the preloading time of D-lactate was increased to eight minutes due to its slower transport rates.

3.4.2.3 Use of protonophors

An essential question was if the substrate uptake into yeast was dependent on the proton gradient over the plasma membrane. To elucidate this, chemicals with the property to abolish the proton gradient were used, called “proton decouplers” or “protonophors” (mechanism of action see figure 3.11).

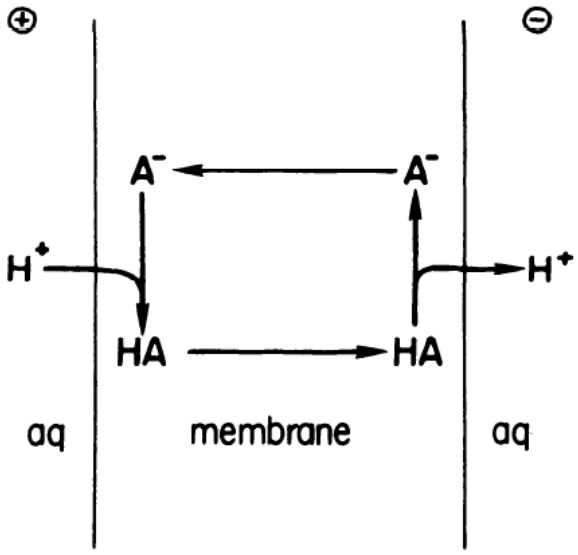

Figure 3.11 | Hypothetical mechanism of action of protonophors. Weak organic acids are thought of being cycled through the membrane. In this process they are able to carry protons along a concentration gradient (membrane potential) at a pH which is close to their own pKa. aq = aqueous phase; HA = protonated acid; A^- = corresponding acid anion [McLaughlin and Dilger, *Physiol rev.* 1980].

Since the efficiency of the protonophor depends on its pKa two different chemicals had to be used in order to cover the whole pH scale of interest. CCCP (carbonyl cyanide *m*-chlorophenylhydrazone) was used for the pH range between 5.8 and 8.8 (figure 3.12) and DNP (2, 4-dinitrophenol) between 2.8 and 4.8 (figure 3.13). For the assay a 5 mM CCCP stock solution in 70% ethanol and a 100 mM DNP stock solution in 70% ethanol were prepared. Cells were incubated prior to the uptake experiment for 5 to 10 min with a final concentration of 50 µM CCCP or 1 mM DNP at room temperature. The lactate uptake measurement itself was performed as previously described in 3.4.2.1.

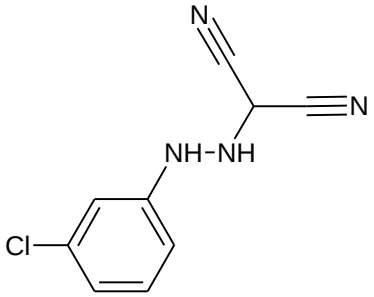

Figure 3.12 | CCCP (carbonyl cyanide *m*-chlorophenylhydrazone) molecule. Drawn with ChemSketch.

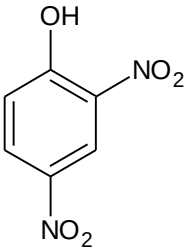

Figure 3.13 | DNP (2,4-dinitrophenol) molecule. Drawn with ChemSketch.

3.4.2.4 Use of DEPC

In order to elucidate the role of histidine residues for the L-lactate transport in the PfFNT protein the effect of the histidine modifying agent DEPC (diethylpyrocarbonate) (figures 3.14 and 3.15) on the import rates was investigated. Since DEPC is rapidly hydrolyzed in an aqueous environment a fresh solution in anhydrous ethanol was prepared right before each experiment. The stock solution was diluted in the yeast suspension to a final concentration of 1 mM with an incubation time of 10 to 15 minutes at room temperature prior to the uptake assay. The lactate uptake assay was done as described in 3.4.2.1.

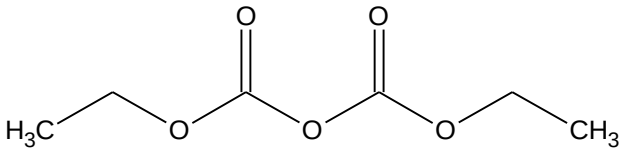

Figure 3.14 | DEPC (diethylpyrocarbonate) molecule. Drawn with ChemSketch.

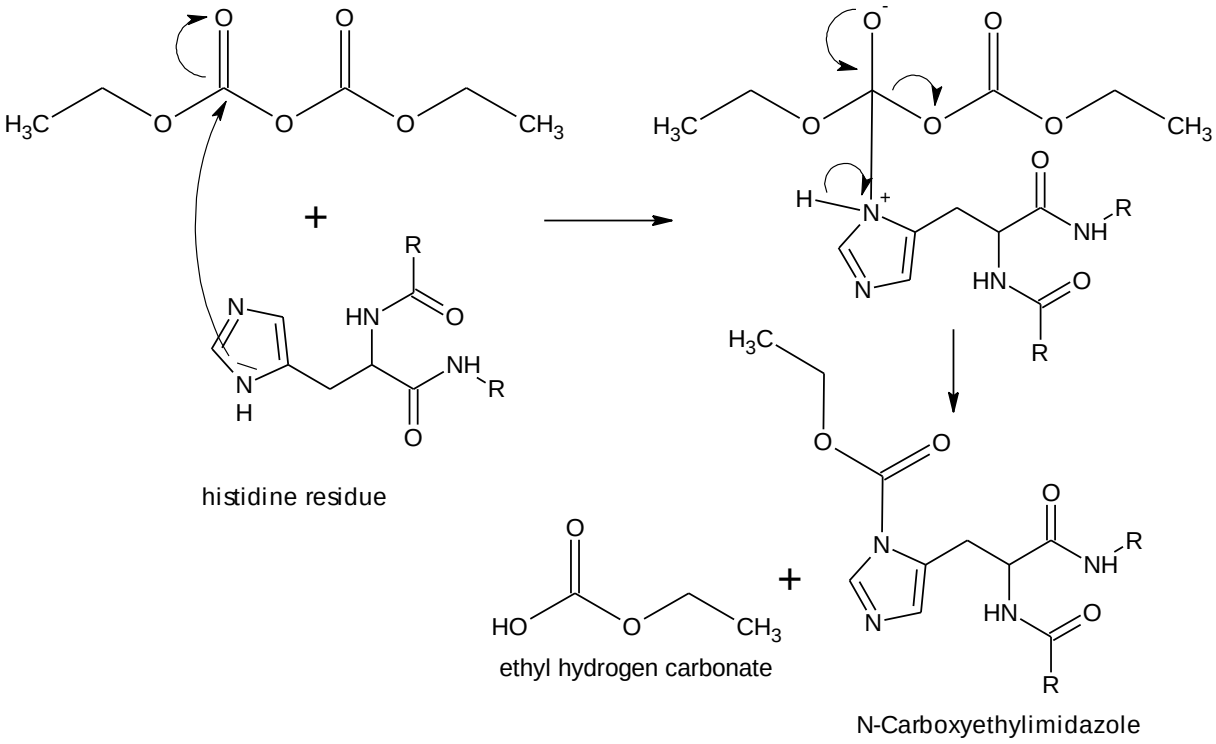

Figure 3.15 | Reaction of DEPC with histidine residues in a peptide. The π-electrons of the nitrogen atom in the pyrazole ring of histidine residues are attacking the carbon atom of the acid anhydride group. In the following reaction ethyl hydrogen carbonate is separated and a stable carbamate group is formed.

3.4.2.5 Inhibitors

To test the inhibitory potential of various compounds on the L-lactate uptake via PfFNT stock solutions were made. Depending on the solubility of the chemical they were dissolved in suspension buffer (pH 6.8 50 mM HEPES/TRIS), 70% ethanol or DMSO (dimethyl sulfoxide). The maximum concentration of DMSO in the assay never exceeded 3% and the ethanol concentration never 0.7%. The inhibitor stock solutions were diluted in yeast suspension to their final concentrations and incubated at room temperature for 10 to 15 minutes (except the incubation time for p-chloromercuribenzene sulfonate (pCMBS), which was 20 minutes). The lactate uptake assay was exerted as described previously.

3.4.2.6 Glycerol uptake

To ascertain if an uncharged molecule similar in size with lactate and a comparable topological polar surface area can pass PfFNT another yeast knock out strain was used. This strain (By4742 Δfps1) lacks its endogenous aquaglyceroporin and is therefore unable to conduct glycerol. The measurements were carried out with the same determining factors as in the substrate import assay (see 3.4.2.1), e.g. OD of the yeasts, buffers, incubation time etc. The glycerol concentration was 1 mM with pH 6.8 and the uptake was stopped after 20 and 180 seconds.

4 Results

4.1 Development of a yeast strain devoid of lactate transporters

Since the aim of this work was to elucidate a lactate transporter in the genome of *Plasmodium falciparum* a suitable test organism was inevitable. To reach this goal a *Saccharomyces cerevisiae* strain which had no endogenous lactate transporters and was therefore unable to grow on medium with lactate as the sole carbon source was generated. Although this objective was accomplished by generating BY4742Δjen1Δady2Δcyb2 LDH we used a different yeast strain W303-1A Δjen1 Δady2, a kind gift from M. Casal, which showed faster growth and was more applicable on this account. In the beginning of this work a different intention was pursued: to develop a yeast strain that would produce L-lactate but at the same time was unable to export it. This would ultimately lead to cell death or at least a much slower growth rate compared to those cells that expressed a functional lactate transporter. The L-lactate production was controlled through a repressible MET25 promoter which regulated the transcription of the L-lactate-dehydrogenase gene (LDH). LDH converts pyruvate to L-lactate in the following reaction:

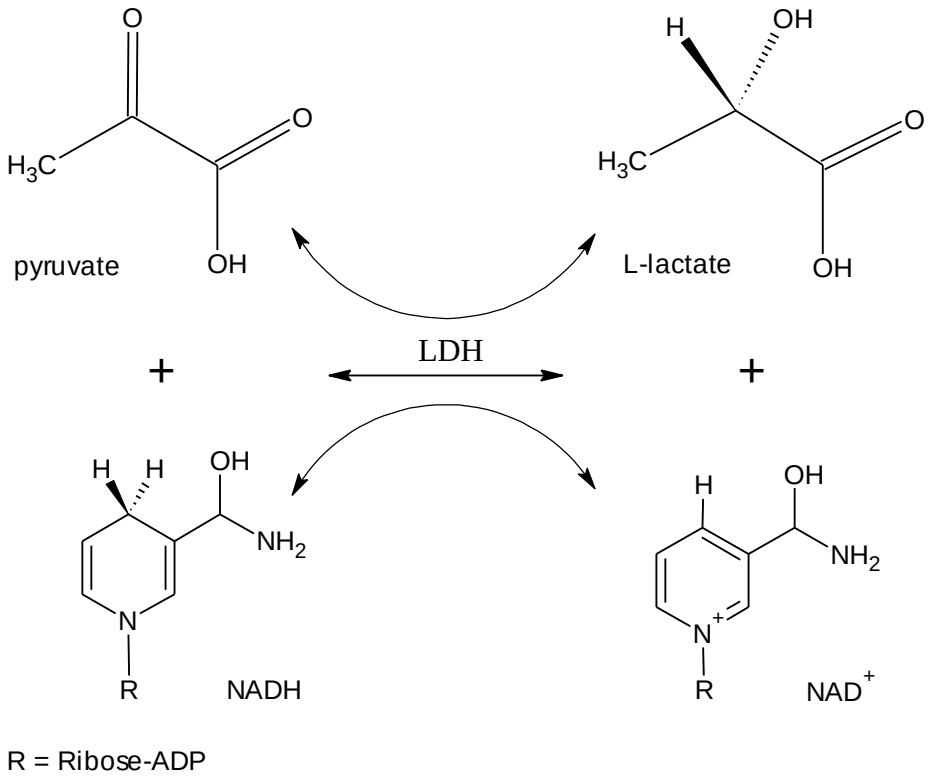

Figure 4.1 | Conversion of pyruvate to L-lactate via LDH. Pyruvate is reduced to L-lactate in a redox reaction while NADH is oxidized to NAD^+.

The reason for this intention is found in the physiological situation of the parasite. *Plasmodium* generates vast amounts of lactate during its developmental phase in the human red blood cells which have to be exported in order to keep the parasites viable. This metabolic situation was tried to copy and transfer to our test organism (figure 4.2).

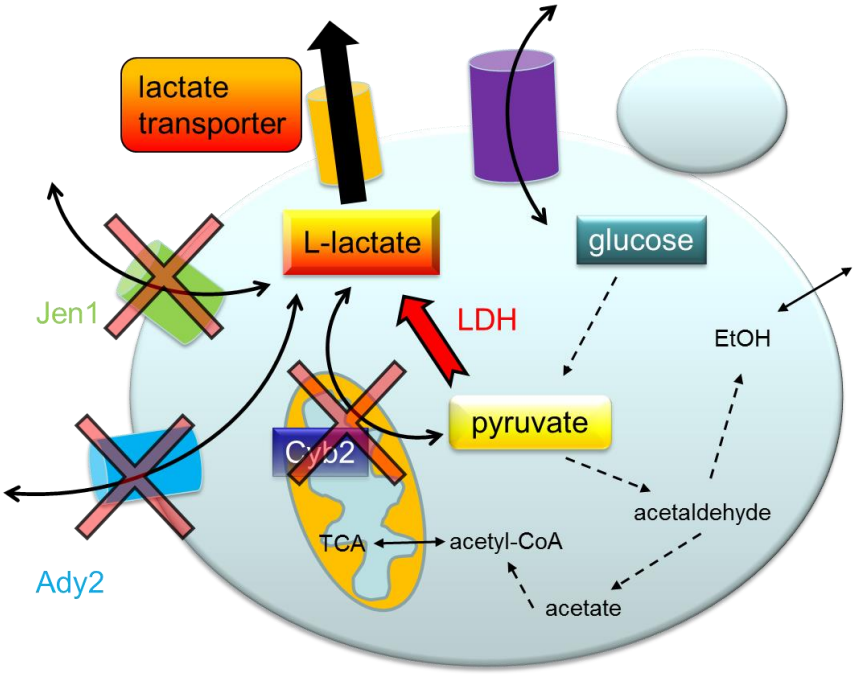

Figure 4.2 | Scheme of genetic engineered yeast strain. This triple knock-out yeast is devoid of its endogenous lactate transporters and L-lactate-dehydrogenase (as shown by red crosses). Additionally it converts pyruvate to L-lactate at a high rate by introduction of a plasmodial L-lactate-dehydrogenase into its genome (red arrow). Hypothetically lactate could only leave the cells via a lactate transporter.

This goal was not achieved. One possible explanation is that yeasts can cope with higher intracellular L-lactate concentrations by pumping them into their vacuole. This hypothesis was never checked.

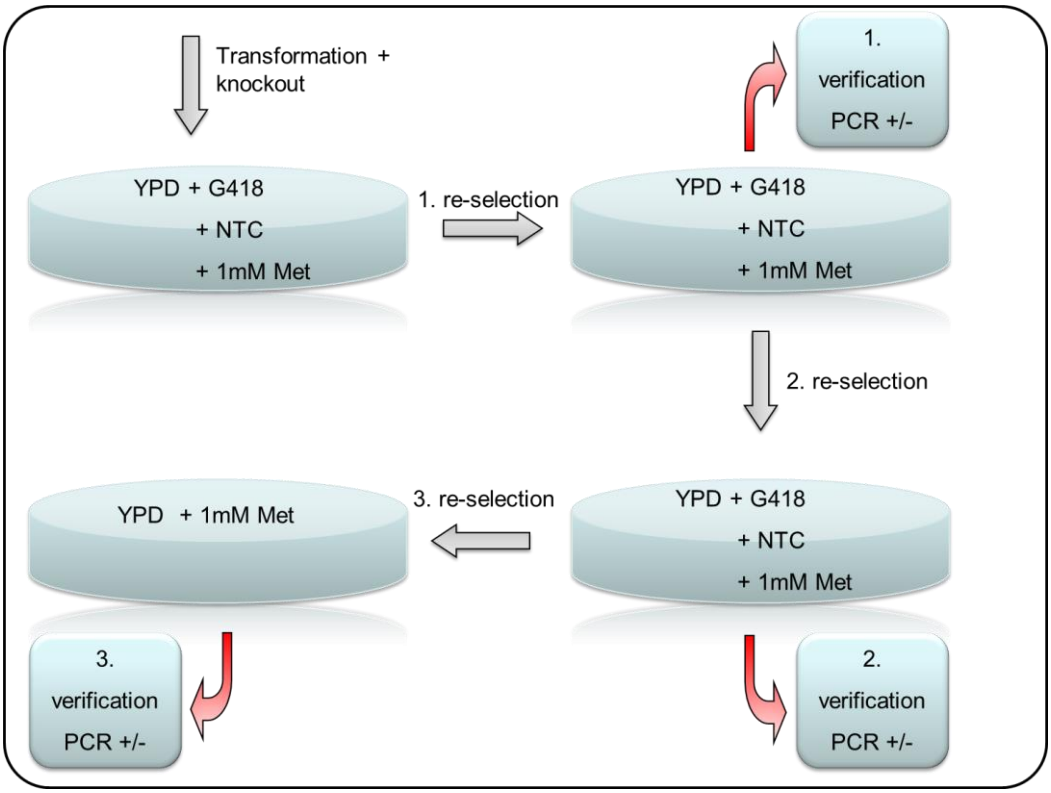

Figure 4.3 | Workflow of yeast knockout. Fresh cells derived from the procedure of gene knockout by homologous recombination are plated onto selection agar. At least three selection steps are necessary to ensure that the derived clone is pure. The verification is done by colony PCR's. Methionine suppresses L-lactate generation by the plasmodial L-LDH. G418 and NTC are selection marker for out knocked genes.

The yeast double knock out strain BY4742 Δjen1Δcyb2 LDH had already been established by Dr. Binghua Wu in this group. In this strain the lactate transporter Jen1 and the L-lactate-dehydrogenase cyb2 were knocked out while the plasmodial L-lactate-dehydrogenase was knocked in. It was the starting point to generate the triple knockout BY4742 Δjen1Δady2Δcyb2 LDH in which additionally the second lactate transporter, Ady2, was knocked out. The method used was adopted from Baudin et al. (1993) and is described in 3.1.14 using multiple selection steps with PCR verification in between (figure 4.3). One clone was isolated by this method and a permanent culture was generated.

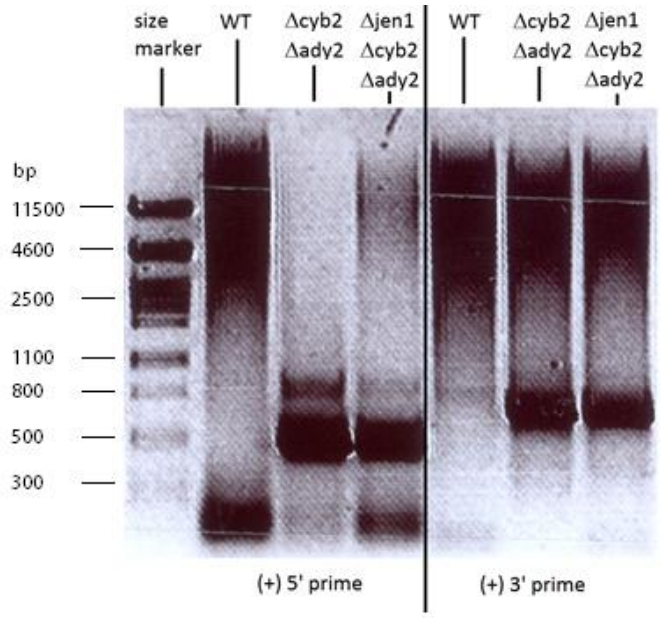

Figure 4.4 | Colony PCR of triple knockout By 4742. The double and triple knockout strains show a band for the PCR-product of the selection marker gene. This band is absent for the wild type yeast. This indicates a successful knockout. WT = wild type, Δcyb2 = deleted cytochrome b2 gene, Δady2 = deleted acetate transporter gene, Δjen1 = deleted lactate transporter gene.

The correct knockout of the desired genes in this clone was confirmed by colony PCR (figure 4.4). For this, primer pairs were applied which generated positive and negative PCR products. The 5' prime primer pair generated with a successful knockout a PCR product of 450 bp by amplification of a part of the natamycin cassette. The 3' prime primer pair did the same by amplification of a 700 bp long PCR product. All other visible bands are derived by unspecific primer binding (bands < 2500 bp) or template DNA (smear > 2500 bp).

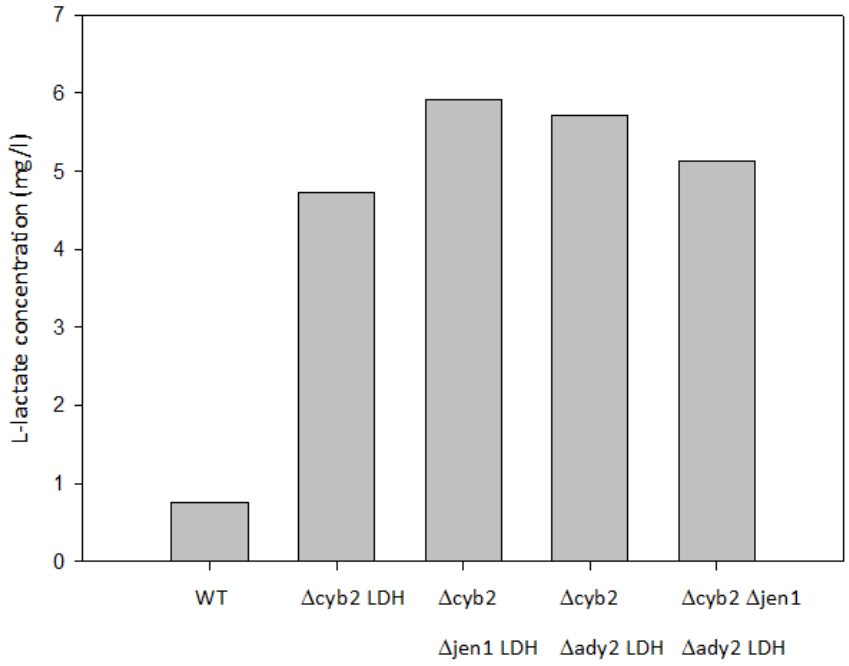

Figure 4.5 | L-lactate production of By 4742 knock-out strains. After overnight growth of these constructs the L-lactate concentration and the pH in the medium were determined. Lactate values are normalized to OD_{600}= 1 to enable a direct comparison. WT = wild type, Δcyb2 = deleted cytochrome b2 gene, Δady2 = deleted acetate transporter gene, Δjen1 = deleted lactate transporter gene, LDH = L-lactate dehydrogenase.

To check if the engineered yeast were able to produce lactic acid medium samples were taken after overnight incubation. L-lactate was detected with a commercial kit, Enzytec(TM) L-Milchsäure Test. In the buffered medium the pH was stable, without buffer it was lowered to pH 4. All strains with a cyb2 knockout and a LDH knock-in produced L-lactate to a certain amount (figure 4.5). Wild type yeast served as control and displayed no L-lactate production. Nevertheless there was no difference in the L-lactate concentration in the medium with yeast expressing lactate transporters compared to those without, e.g. strain Δcyb2 LDH compared to strain Δcyb2Δjen1Δady2 LDH, in which the yeast endogenous lactate transporter Jen1 and the yeast acetate transporter Ady2 had been knocked out. This indicated a different transport mechanism over the plasma membrane than via the known yeast lactate transporters.

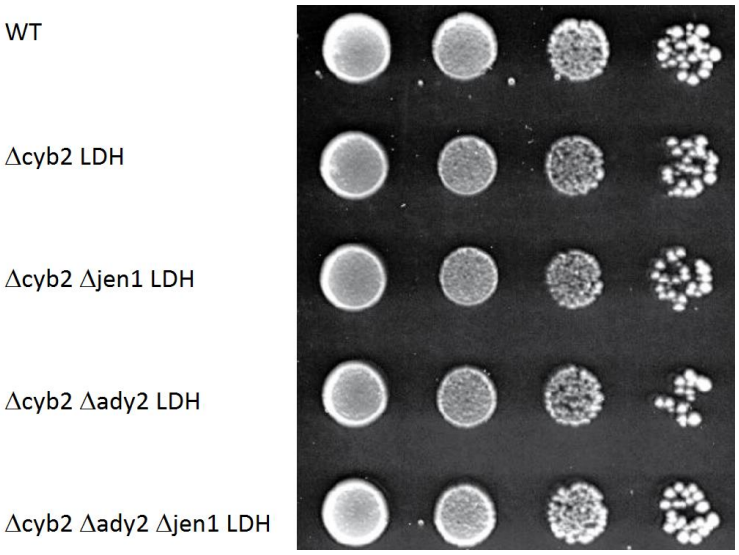

Figure 4.6 | Phenotypic lactate export assay with By 4742 strain. Medium was SGlc (2%) KHLU 20 mM MES pH 6.0. Yeast producing L-lactate as metabolic end product should show a reduced growth compared to wild-type yeast. All genetically altered strains and the wild type showed normal growth.
WT = wild type, Δcyb2 = deleted cytochrome b2 gene, Δady2 = deleted acetate transporter gene, Δjen1 = deleted lactate transporter gene, LDH = L-lactate dehydrogenase.

To check for a reduced growth of the knockout strains a phenotypic lactate export assay was performed. All tested strains showed the same growth (figure 4.6). This indicated that yeasts are able to cope with high(er) intracellular L-lactate concentrations. It displayed that the modified triple knockout strain was not suitable for the intended lactate export assay.

4.2 PfFNT gene identification

Like stated previously one aim was to develop a high throughput screening assay to identify a lactate transporter in the genome of *P. falciparum*. Therefore a database was established by Claudia Ramisch in which putative lactate transporter encoding genes were collected for further investigation. The enclosure criteria were:

- At least 400 amino acids length
- At least 6 predicted transmembrane domains

The found candidates were further manually selected with the outcome of 143 putative lactate transporter genes which were downloaded from the PlasmoDB website (http://plasmodb.org/plasmo/). Two of these genes (PF3D7_0926400, previous ID PFI1295c, internal identification Pf70 and PF3D7_0210300, previous ID PFB0465c, internal identification Pf75) had already been annotated as putative lactate transporters due to a moderate similarity to the human monocarboxylate transporters (MCTs). The BLAST on the PlasmoDB site against human MCT1 generated for both genes an identity of 21%. Since unforeseen difficulties on the establishment of the screening assay occurred the decision was made to switch the aim of this thesis to the elucidation of the role of these two candidate genes. To accomplish this, the route of the substrate assay direction was changed from export to import of lactate. Although this type of assay was soon arranged no lactate transport could be detected via the two annotated lactate transporter genes Pf70 and Pf75. In parallel to our efforts a bacterial transporter called FNT (formate nitrite transporter) was shown to conduct lactate (Lü et al. PNAS 2012). A search of the plasmodial genome identified an FNT homologue, PF3D7_0316600. PfFNT has 69% sequence identity and 80% similarity to the formate nitrite transporter family (FNT). Although this gene product showed only a hint of lactate transport in our assay a second circumstance led to successful expression. To that time Dr. Sinja Bock was working on the expression of proteins in a cell free system. Yet, she failed to express PfFNT due to the typically high A and T content of *P. falciparum* genes [Gardner et al. *Nature* 2002]. Generation of a codon-optimized version of the gene enabled yeast expression of PfFNT (figure 4.7).

Figure 4.7 | Codon optimized PfFNT sequence. The original sequence is displayed in the top line, optimized bases towards the yeast codon usage are given in red below, and the resulting, unchanged protein sequence is shown in the blue bottom line. Generated with GeneArt® Gene Synthesis (Life Technologies) by Dr. Sinja Bock.

The expression profile of the PfFNT gene matches quite closely the ones of the plasmodial hexose transporter, lactate dehydrogenase and glycolytic genes (figure 4.8).

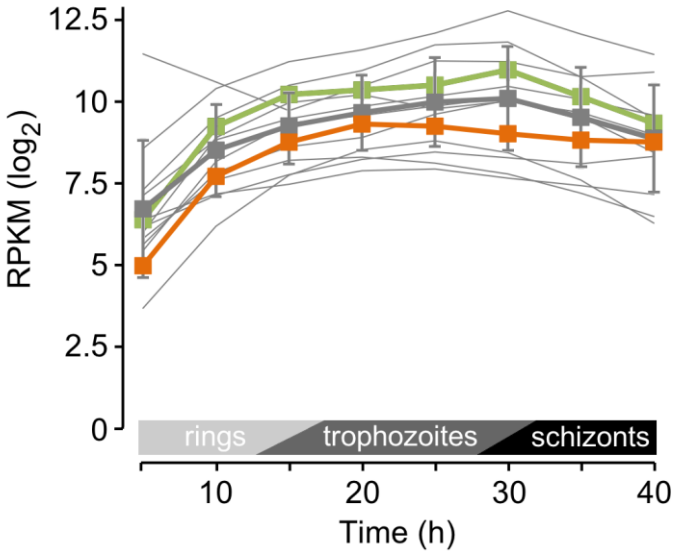

Figure 4.8 | Expression profile of PfFNT (orange), plasmodial lactate dehydrogenase (PF13_0141, green) and metabolically connected enzymes during blood-stage development of *P. falciparum*. Shown are as grey thin lines the following gene transcripts of *P. falciparum*: hexokinase (gene id: PFF1155w), glucose-6- phosphate isomerase (PF14_0341), phosphofructokinase (PFI0755c), fructose-1,6- bisphosphate aldolase (PF14_0425), triosephosphate isomerase (PF14_0378), glyceraldehyde- 6-phosphate dehydrogenase (PF14_0598), phosphoglycerate kinase (PFI1105w), phosphoglycerate mutase (PF11_0208), enolase (PF10_0195), and pyruvate kinase (PFF1300w). The gray squares show the average of the traces ± SD. Data were received from PlasmoDB and transcript levels are given as reads per kilobase of exon model per million mapped reads (RPKM).

4.3 PfFNT expression in yeast

Like stated above the codon optimized gene sequence of PfFNT was well expressed in *S. cerevisiae* (figure 4.9).

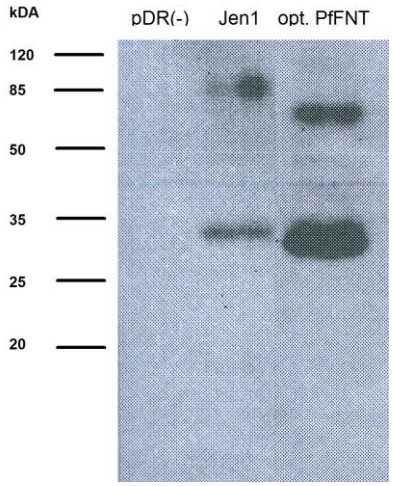

Figure 4.9 | Western blot of PfFNT. Detected with anti-HA antibody and an illumination time of 10 minutes. Calculated size of the PfFNT protein is 34 kDa. The other visible band at about 85 kDa is likely a peptide trimer.

The Western blot displayed as expected no band for the empty pDR vector. Jen1 was expressed and showed two bands. The calculated size is about 70 kDa, which is most probably the upper band. The lower one might be a fragment. There was no expression for non-optimized PfFNT, PFI1295c and PFB0465c. The optimized sequence of PfFNT lead to a strong protein expression with two bands, one being the monomer and the other one most probably the trimer.

The optimized sequences of PfFNT, PFI1295c and PFB0465c were expressed in yeast and targeted to the plasma membrane. This was shown in a biotinylation assay done by Julia Holm-Bertelsen.

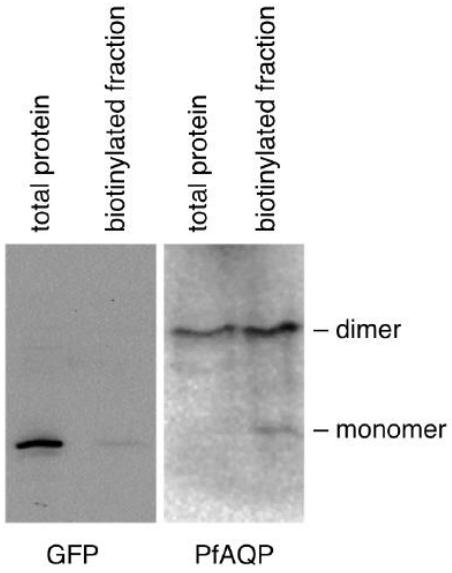

Figure 4.10 | Control experiment for biotinylation assay in yeast. Yeast protoplasts were generated which heterologously expressed a soluble GFP protein or a plasma membrane residing protein, PfAQP. They were lysed with (membrane proteins are detected) or without prior biotinylation (total protein detection). The biotinylation assay detects about 1% of intracellular, non-biotinylated proteins. This accounts for the weak GFP signal in the biotinylated fraction. Moreover proteins of the plasma membrane are easily detected which can be seen for PfAQP in the biotinylated fraction. Assay was performed by Julia Holm-Bertelsen.

Figure 4.10 illustrates that the biotinylation assay is suitable to detect membrane proteins in yeasts. In this method activated biotin is incubated with yeast protoplasts, e.g. cells whose cell wall was removed by digestion with zymolyase. Then, the activated biotin molecules bind to proteins that protrude from the cell membrane. Afterwards these biotinylated proteins are purified by binding them to streptavidin and later detected via Western blot. Two well characterized proteins were chosen as controls, one that is soluble and therefore accounts for the intracellular fraction of proteins and the other one a membrane peptide. The protein band of the soluble GFP was not visible in the biotinylated fraction whereas the band of the membrane peptide PfAQP was. The next picture illustrates that PfFNT, PFI1295c and PFB0465c proteins are targeted to the plasma membrane in yeast:

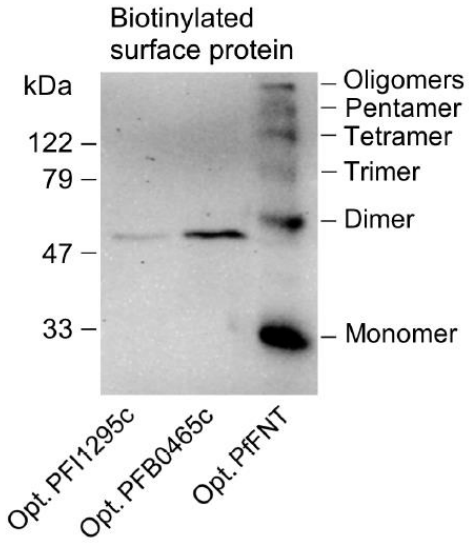

Figure 4.11 | Plasma membrane localization by biotinylation of codon-optimized PfFNT, PFI1295c and PFB0465c in yeast. Strain W303-1A Δjen1 Δady2 was transformed with the displayed constructs. Biotinylation was carried out before detection via Western blot. Assay was performed by Julia Holm-Bertelsen.

Figure 4.11 shows a weak expression profile for PFI1295c. The calculated size is about 60 kDa. PFB0465c was expressed a bit better. The estimated size is 51 kDa. Regardless the band ran slightly higher that the larger PFI1295c peptide. PfFNT was well expressed as already seen in other Western blots. This might be a hint to the oligomerization state of the protein when it functionally resides in the plasma membrane. Additionally the calculated size of 34 kDa matched the height of the band on the blot.

4.4 PfFNT restores growth of deficient yeast strain on L-lactate medium

This method, although originally intended as a screening assay, showed the first functional transport properties of PfFNT. There are two different test conditions with one in liquid medium and the other on solid agar plates. The yeast strain used for these assays was W303-1A Δjen1 Δady2 which is devoid of its endogenous lactate transporters. Jen1p is a member of the major facilitator superfamily (MFS) and is categorized into the Sialate:H^+ symporter (SHS) family. It is a lactate transporter with 12 transmembrane domains and is known to conduct

lactate, pyruvate, acetate and propionate [Soares-Silva et al. *Molecular Membrane Biology* 2007]. Ady2p is a membrane protein with 6 predicted transmembrane helices which facilitates the transport of acetate, propionate, formate and lactate [Paiva et al. *Yeast* 2004]. The double knockout mutant strain is therefore unable to grow on medium with lactate as the sole carbon source [de Kok et al. *FEMS Yeast Res.* 2012].

4.4.1 Phenotypic agar plate assay

First, a simple test was performed in which the lactate facilitator lacking yeast strain was transformed with putative lactate transporter genes and controls. Transformed yeasts were plated on agar with 0.25% L-lactate as the only carbon source. Result was either growth or not due to L-lactate uptake from the medium. The difference in growth between non- and codon-optimized PfFNT was obvious (figure 4.12).

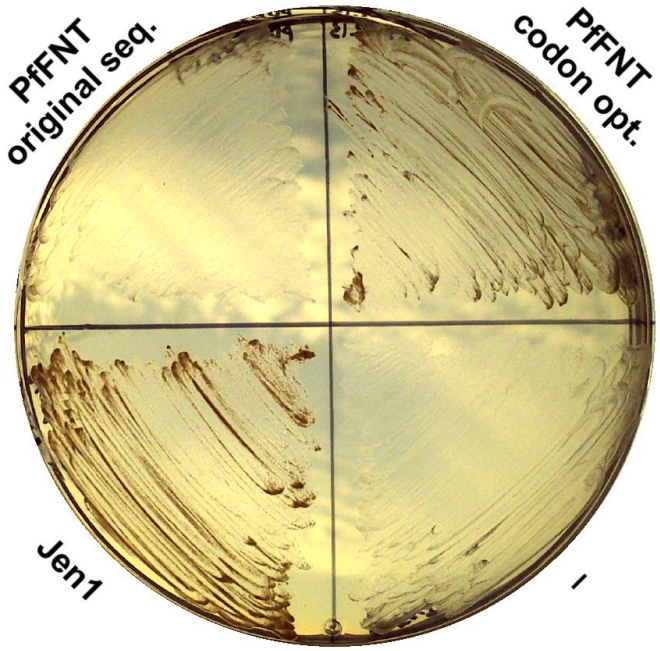

Figure 4.12 | Growth restoration of a lactate uptake insufficient yeast strain. Strain W303-1A Δjen1Δady2 was transformed with the indicated constructs and plated on agar plates with synthetic defined medium containing L-lactate (0.25%) pH 5.6 20 mM MES. Plates were incubated for 1 week at 29 °C. Growth indicates L-lactate transport.

Strain W303-1A Δjen1Δady2 was not able to grow due to inefficient L-lactate uptake as seen with the negative control, which was transformed with an empty pDR vector. Jen1 restored growth due to lactate facilitation as did the codon optimized PfFNT. Native PfFNT showed nearly no growth.

Next, plates with three factor ten dilutions were made which allowed a first semi-quantitative estimation of lactate transport. Additionally plates with glucose as carbon source served as control for detecting abnormal growth of the transformed deficient mutant strains. Yeast transformed with Jen1 were the positive control as they restored lactate uptake and with this, growth (figure 4.13).

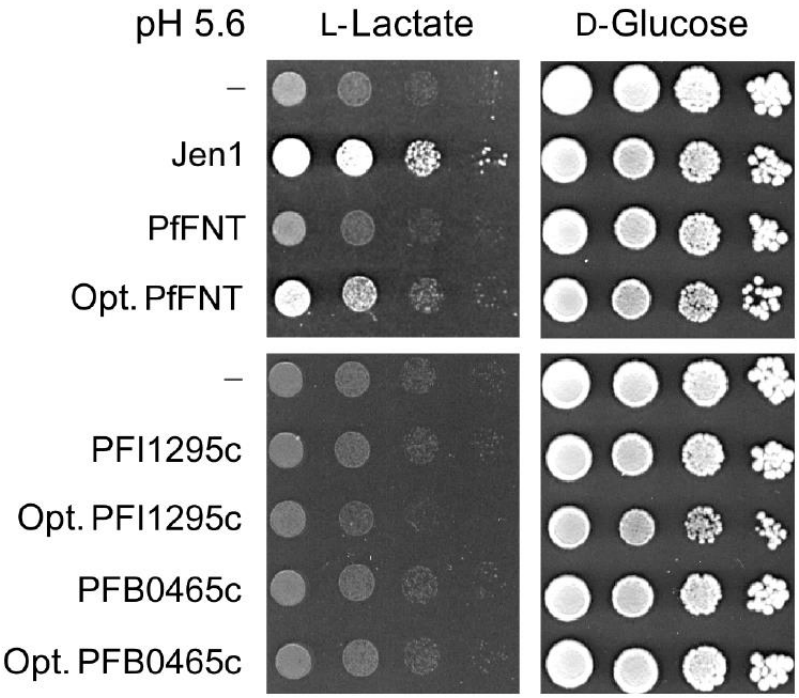

Figure 4.13 | Phenotypic L-lactate uptake assay. W303-1A Δjen1 Δady2 transformed with the indicated genes were incubated for 5 days at 29 °C. Agar growth medium was SDAHLW 20 mM MES with D-glucose 2% (right side) or L-lactate 0.25% (left side) as the sole carbon source. (–) = empty vector as negative control; Opt. = codon optimized sequence of the indicated gene

The strain with codon optimized PfFNT showed growth about ten time less than the Jen1 strain. Both native and codon optimized genes of annotated plasmodial MCTs presented no

better growth than the negative control. All yeast strains displayed normal growth on glucose medium (figure 4.13).

4.4.2 Semi-quantitative liquid culture assay

The principles of this assay are the same as for the agar plate assay but a liquid medium was used instead of solid medium allowing for more quantitative growth evaluation. Growth was monitored with a Bioprofile machine which detected the OD_{600} of the cultures at various time intervals (mostly every 30 minutes) in 200 well plates. Moreover it was much easier to test for different pH conditions. From the monitored growth curves the area under the curve (AUC) was calculated.

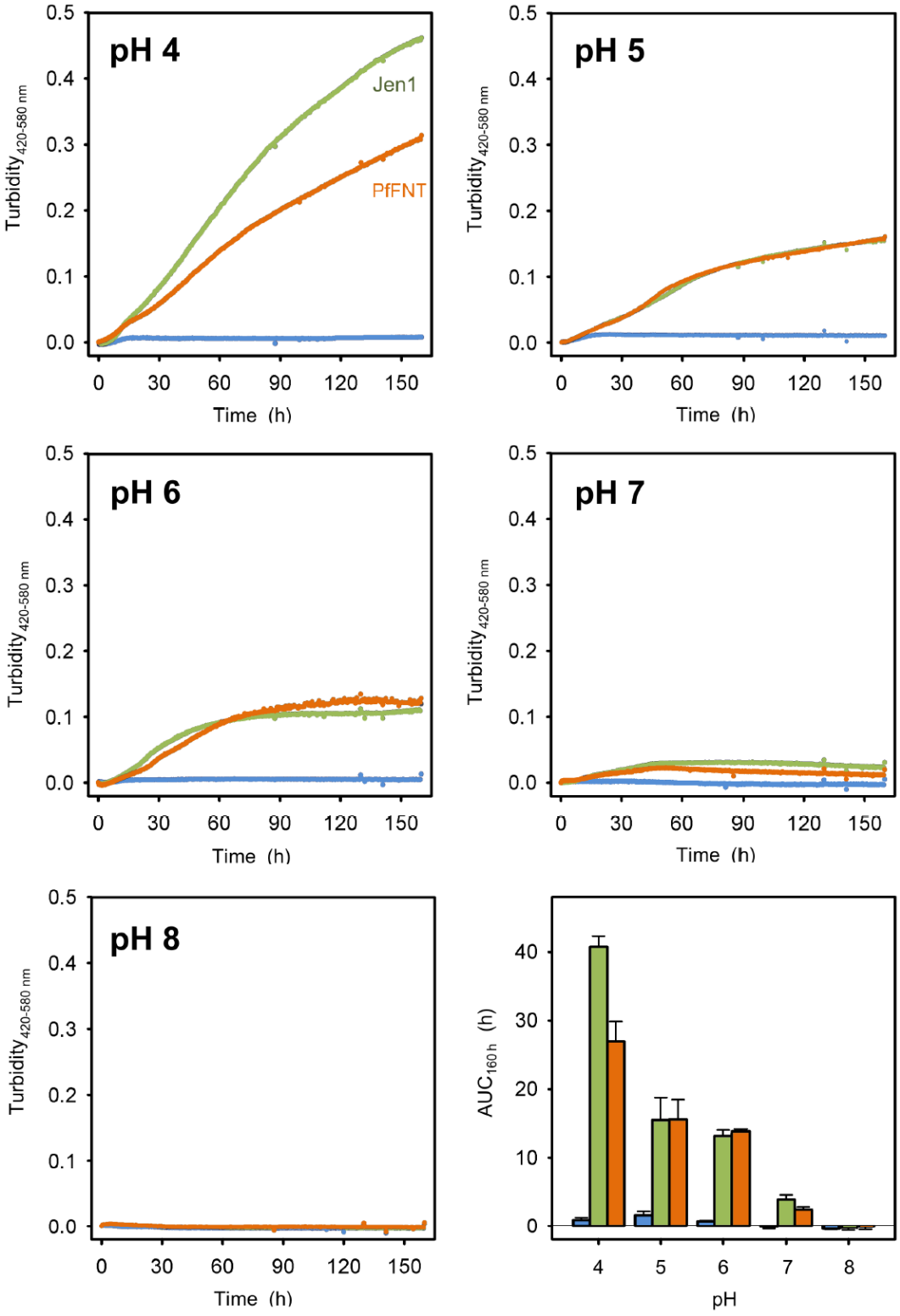

Figure 4.13 | Liquid phenotypic lactate uptake assay. Growth curves of W303-1a ΔjΔa strain at pH values from 4 to 8. Cells were incubated for one week with buffer containing L-lactate as the sole carbon source at 30 °C. The turbidity was recorded in a BioScreen C Analyzer®. For better comparison the AUC for 160 hours was calculated. Colors: blue = no protein, green = Jen1, orange = PfFNT

Growth of yeasts expressing PfFNT as the only lactate transporter is pH dependent as shown in figure 4.13. Since L-lactate was the sole carbon source in this experiment growth of cells implicated lactate transport. Cells without expression of a lactate transporter (blue) showed no growth at any pH. At pH 4 the highest ODs were measured and the curves of Jen1 (green) and PfFNT (orange) showed staedy growth over the whole timescale. This is reflected in high AUC values for pH 4. Growth of the strains with a functional lactate transporter is very similar at pH 5 and 6. Here a plateau phases is reached after about 90 hours. At pH 7 and 8 there was no growth detectable.

4.5 PfFNT radiolabeled substrate transport characterization in yeast

For direct transport characterization of PfFNT various ^{14}C-radiolabled substrate transport assays were established.

4.5.1 Setting the assay parameters

Since the assay had to be established first its basic parameters were set.

4.5.1.1 Optimal yeast OD_{600} determination

L-lactate uptake was tested with yeast suspensions resulting in final OD_{600} of 20, 40 and 80. Surprisingly there was no difference in the amount of radiolabel taken up between the different OD_{600} besides a higher error of the OD_{600} 80 samples (figure 4.14). Furthermore it was more difficult to accurately pipette a yeast suspension with OD_{600} 80 since it was more viscous. Therefore the decision was made to use an OD_{600} of 40 for the assay.

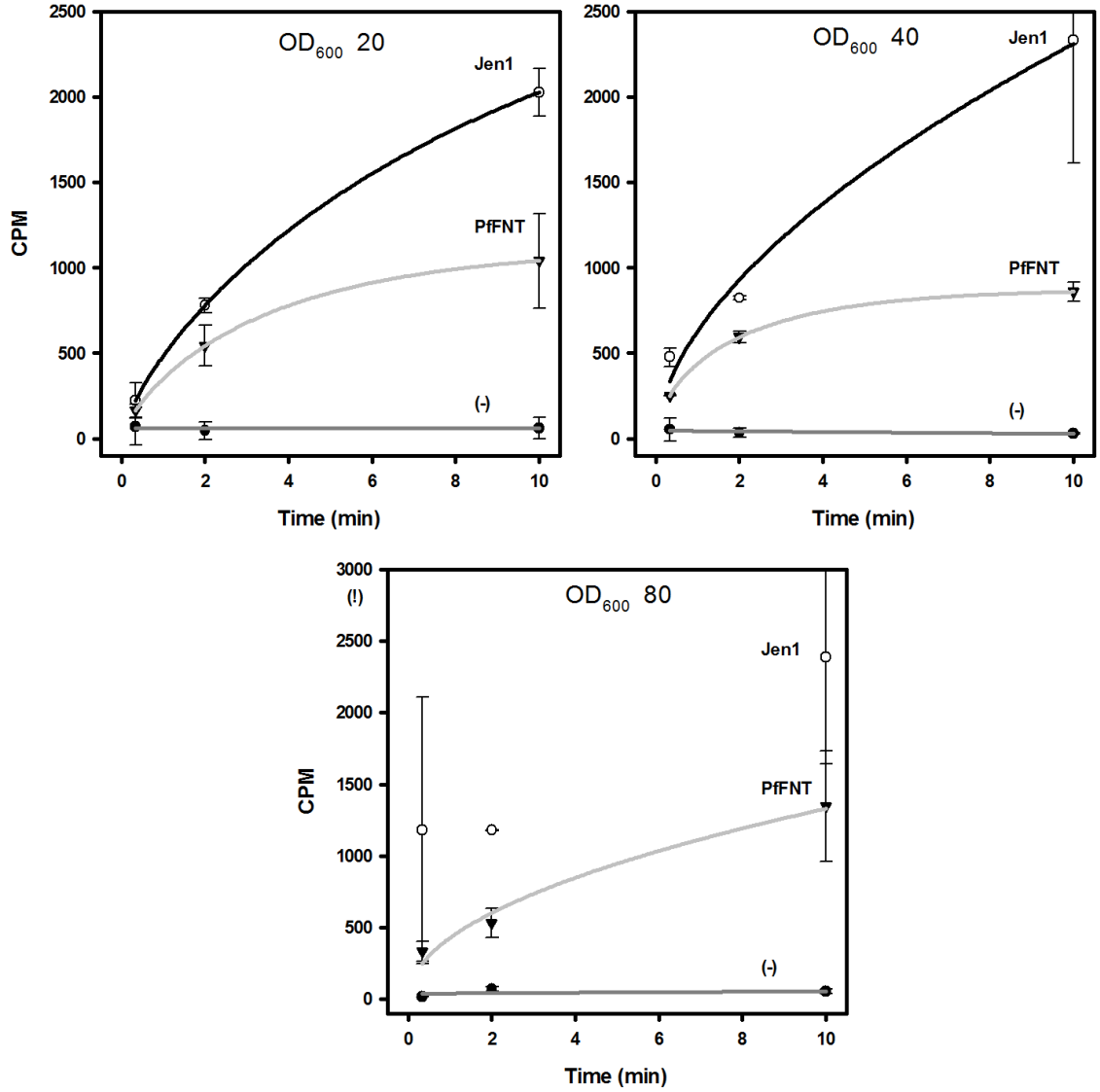

Figure 4.14 | Influence of OD_{600} on radiolabel uptake in yeast. Strain W303-1A Δjen1 Δady2 was incubated at OD_{600} 20, 40 and 80 at room temperature with 1 mM L-lactate buffer pH 6.8 for up to ten minutes. Jen1 was the positive control since it is the endogenous yeast lactate transporter and the empty pDR vector (-) served as the negative control. 1 time point includes 2 samples and error bars indicate the difference between the 2 values. Note that the ordinate scale of OD_{600} 80 is altered as indicated by an exclamation point.

4.5.1.2 Determination of yeast suspension and buffer mixing ratio

Four different mixing ratios and their implication on repeatability were tested. The optimum ratio was found to be 1:5 which was a compromise between complete and fast mixing and viscosity of the suspension before mixing the two liquids (figure 4.15).

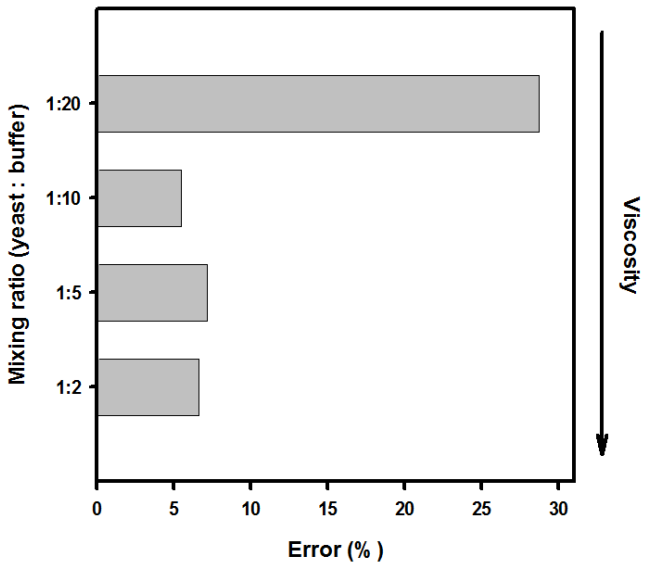

Figure 4.15 | Influence of yeast suspension to buffer ratio for mixing. Strain W303-1A Δjen1 Δady2 PfFNT was incubated at OD_{600} 40 at room temperature with 1 mM L-lactate buffer pH 6.8 for ten minutes. The bars show the difference between two values as percentage. The arrow indicates rising viscosity of the yeast suspension before mixing.

4.5.1.3 Radioactive ^{14}C quantity per sample

The influence of the amount of radiolabel per sample was tested. For this radioactivity was doubled from 0.02 to 0.04 µCi. This resulted in a about twice better resolution (figure 4.16). Nevertheless, a major point in the use of radioactive chemicals is to keep the environmental pollution at a minimum. Therefore the aim was to use as less radioactivity per sample as possible while keeping the signal to noise ratio at a satisfactory level, i.e. about 5:1. This was achieved with 0.02 µCi (740 Bq) per sample for a substrate concentration of 1 mM.

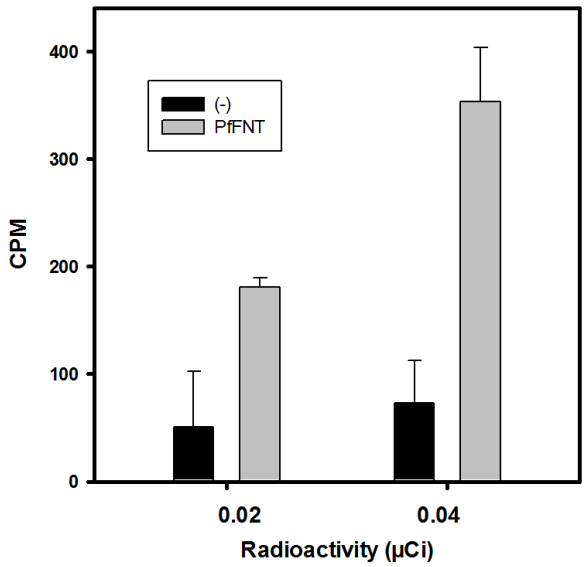

Figure 4.16 | Amount of radioactivity per sample and its impact on the signal to noise ratio. Strain W303-1A Δjen1 Δady2 was incubated at OD_{600} 40 at room temperature with 1 mM L-lactate buffer pH 6.8 containing either 0.02 or 0.04 ^{14}C per sample. Measuring time was 20 seconds. The empty vector served as negative control (-). One time point includes 3 samples and error bars indicate standard deviation.

4.5.2 Substrate import kinetics

Although faster and more convenient to handle, the import of radiolabeled substrates does not reflect the physiological situation of the parasite while it resides in the host erythrocytes. Nevertheless, it was a valuable tool to get insight into transport kinetics and characteristics, e.g. the profile of facilitated substrates.

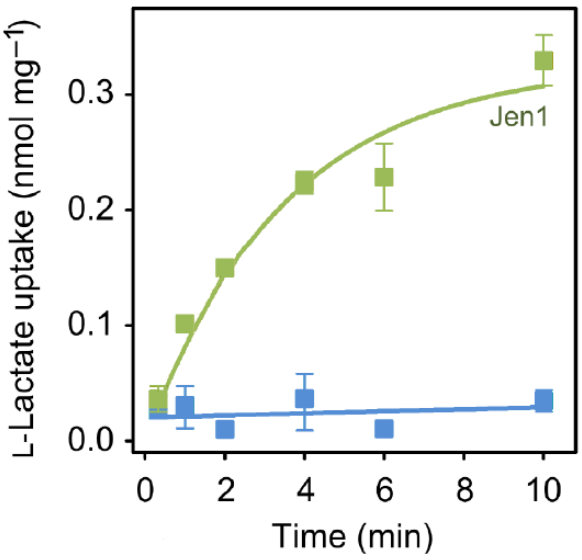

Figure 4.17 | Control for L-lactate import kinetic characterization in yeast. Strain W303-1A Δjen1 Δady2 was incubated at room temperature with 1 mM L-lactate buffer at pH 6.8 for up to 10 minutes. Jen1 was the positive control since it is the endogenous yeast lactate transporter and the empty pDR vector (blue) served as the negative control. One time point includes 3 to 6 samples and error bars indicate SEM. Uptake rates were normalized to 1 mg dry yeast.

Yeast were transformed with several constructs and tested on their L-lactate transport kinetics. The empty vector as negative control exhibited a very low background and therefore proofed this test system as very suitable (figures 4.17 and 4.18).

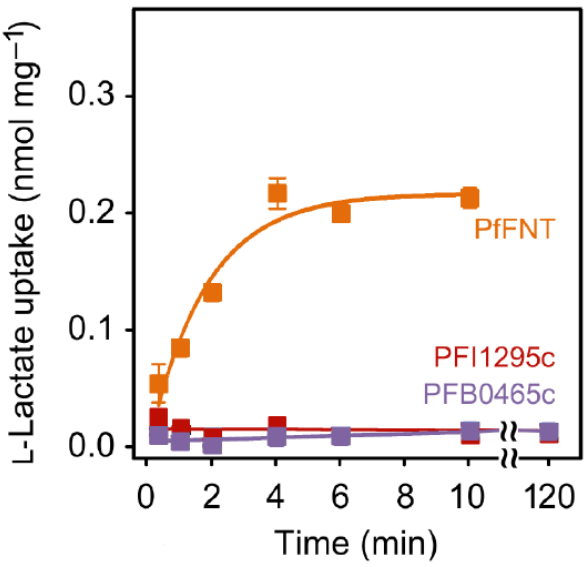

Figure 4.18 | Kinetic characterization of L-lactate transport of PfFNT, PFI1295c and PFB0465c. Strain W303-1A Δjen1 Δady2 was incubated at room temperature with 1 mM L-lactate buffer at pH 6.8 for 10 minutes, respectively for up to 2 hours in the case of PFI1295c and PFB0465c. 6 measurements contributed to 1 sample and error bars indicate SEM.

Unsurprisingly Jen1 displayed the highest lactate facilitation rates (see figure 4.17) since it is the native lactate transporter in yeast. The codon optimized PfFNT construct showed with 0.25 nmol • mg^{-1} • min^{-1} similar initial lactate import rates to Jen1. After 4 minutes lactate uptake was saturated (the same was observed for *E. coli* FocA (figure 4.31)). Transport increased linearly with the L-lactate concentration throughout the physiological, low-millimolar range and saturated above 50 mM. An apparent L-lactate affinity of 87 mM for PfFNT was found. This value strongly depends on the prevailing pH. When the external pH was shifted from 6.8 to 4.8, the affinity of PfFNT for lactate increased 5-fold to 17 mM whereas the maximal transport rate remained unchanged at 14 nmol • mg^{-1} • min^{-1} (figure 4.19).

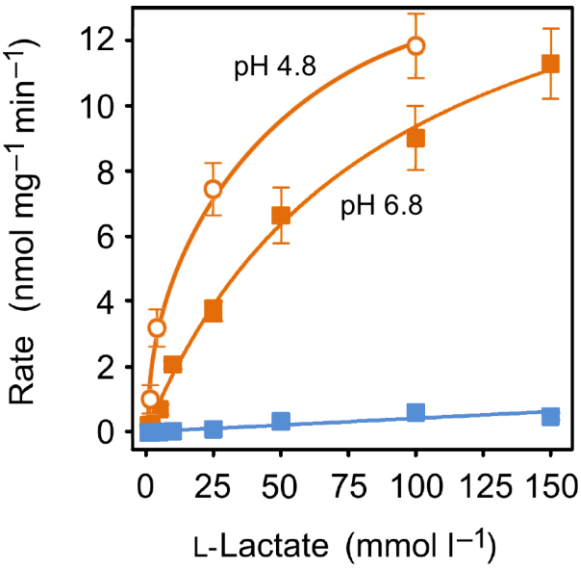

Figure 4.19 | Concentration dependency of PfFNT lactate transport. Strain W303-1A Δjen1 Δady2 was incubated at room temperature with 1 to maximum 150 mM L-lactate buffer for 20 seconds at pH 6.8 and pH 4.8, respectively. Error bars denote SEM of 3 measurements.

Since the two annotated MCT-like plasmodial lactate transporters (PFI1295c and PFB0465c) showed less expression than PfFNT in Western blots (figure 4.11) the time for lactate uptake was increased up to 2 hours. The idea was to compensate the lower expression levels of the two proteins by a higher exposure time. This was possible since the test system showed nearly no background lactate uptake. But even under prolonged incubation in lactate buffer there was no radiolabeled lactate uptake detectable for the codon-optimized sequences of PFI1295c and PFB0465c (figure 4.19). This was also the case for PfAQP. It exhibited after 1 hour an L-lactate uptake of 0.03 ± 0.007 nmol • mg^{-1} which equates the average background uptake of the negative control (data not shown).

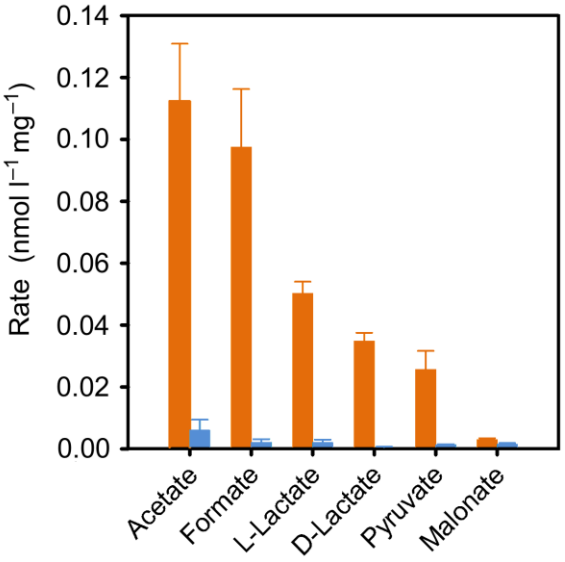

Figure 4.20 | Substrate selectivity profile of PfFNT. Strain W303-1A Δjen1 Δady2 was incubated at room temperature with 1 mM buffer of the respective substrate at pH 6.8 for 20 seconds to ensure true initial transport rates. 3 measurements contributed to one sample and error bars indicate SEM. Orange = PfFNT; blue = empty vector

The substrate selectivity of PfFNT is displayed in figure 4.20. Highest rates were obtained with acetate followed by formate. The affinity for lactate was about half of these values while there was little difference between the two enantiomers, reflecting the physiological situation of the parasite. Pyruvate is transported at about half of the rate of L-lactate while the dicarboxylate malonate is not facilitated via PfFNT.

For testing glycerol uptake *S. cerevisiae* strain BY4742 Δfps1 was used which lacks its endogenous glycerol transporter.

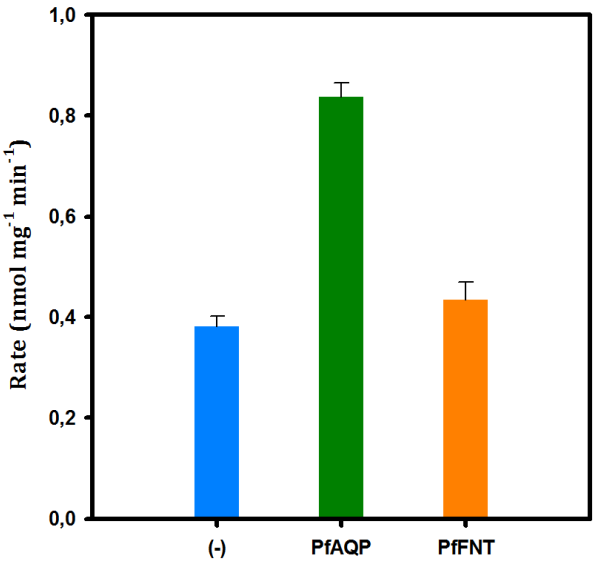

Figure 4.21 | Glycerol uptake into yeast. Strain BY4742 Δfps1 lacks its endogenous glycerol facilitator. Uptake was recorded over 180 seconds at room temperature with 20 mM glycerol buffer at pH 6.8. Error bars represent SEM resulting from 3 samples.

Glycerol is not a substrate of PfFNT. This was proved by radiolabeled glycerol uptake into yeast deficient of their endogenous glycerol facilitator. There was no difference between cells expressing PfFNT and the negative control (empty vector). A known glycerol channel, PfAQP, showed a twice-higher uptake of glycerol than the other two constructs (figure 4.21).

4.5.3 Substrate export kinetics

The substrate export is compared to the natural situation of the blood stage parasites the more valuable test condition. *Plasmodia* need to get rid of vast amounts of lactic acid while they reside inside the red blood cells of their hosts. For this they export lactic acid derived from glycolysis out of their cells via the host cell ultimately into the blood serum. This situation is mimicked in this method. Nevertheless it was not used as the standard method due to a much longer sample preparation and overall assay time compared to the import assay.

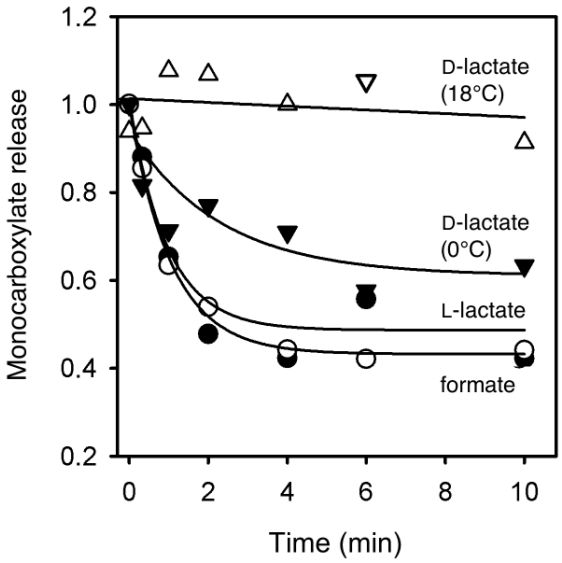

Figure 4.22 | Monocarboxylate export via PfFNT. Strain W303-1A Δjen1 Δady2 was incubated at room temperature with 1 mM monocarboxylate buffer at pH 6.8. To begin efflux the external solution was diluted 100fold by addition of monocarboxylate-free buffer. In order to compensate for variations in cell loading the amount of intracellular monocarboxylate was normalized. If not indicated, substrate efflux was measured at room temperature.

PfFNT L-lactate export followed the same time dependence as the import with saturation of efflux after 4 minutes (figures 4.18 and 4.22) at room temperature. D-lactate displayed no efflux due to rapid metabolism by three D-lactate dehydrogenases in *S. cerevisiae* (DLD 1-3). Therefore it was furthermore analyzed at 0°C to lower the metabolic activity of the dehydrogenases to a minimum. This was not necessary for the L-enantiomer since the endogenous yeast L-lactate dehydrogenase was mostly down regulated by reason of the culture conditions in high glucose. Formate is not a metabolic precursor in yeast and could be measured at room temperature as well. It was facilitated with similar properties to L-lactate (figure 4.22). The amount of remaining monocarboxylates in the cells after the assay was probably because of trapping by metabolic conversion and compartmentalization.

4.5.4 pH dependency

To get more insight into the mode of PfFNT transport, specifically whether it would be proton linked or not, pH dependence of substrate facilitation was investigated.

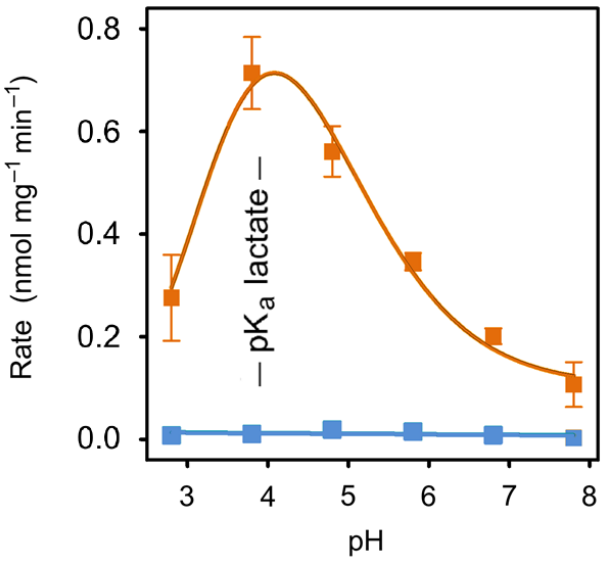

Figure 4.23 | pH-dependency of L-lactate transport via PfFNT. Strain W303-1A Δjen1 Δady2 was incubated at room temperature with 1 mM L-lactate buffer at the given pH's. Error bars donate SEM of 3 measurements. Orange = PfFNT; blue = empty vector

The transport rate of lactate increased with lowering the pH (figure 4.23) until the pKa of lactic acid was reached ($pKa_{\text{lactic acid}} = 3.9$). At this pH lactate and lactic acid are equimolar. At a pH below 3.9 transport rates dropped indicating that the anionic species is needed for transport rather than the protonated lactic acid.

$$\text{pH} = \text{p}K_a + log_{10}\left(\frac{[A^-]}{[HA]}\right)$$

Formula 4.24 | Henderson-Hasselbalch equation. [HA] is the molar concentration of the undissociated acid and [A$^-$] is the concentration of the deprotonated conjugated base. pK_a is $-\log_{10}(K_a)$ with K_a being the acid dissociation constant.

The Henderson-Hasselbalch equation can be transposed to the following formula:

$$A^- = HA \cdot 10^{pH-pK_a}$$

This allows calculating the ratio of the protonated acid to anion at a defined pH. If the ratio is considered and integrated into the pH dependency curve the following graph results:

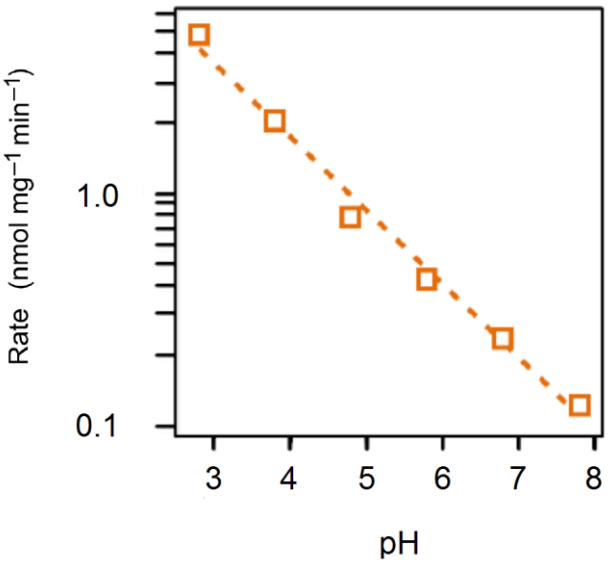

Figure 4.25 | L-lactate transport after correction for the pH-dependent lactate/lactic acid ratio. The Henderson-Hasselbalch equation was applied and the percentage of the lactate anion at the displayed pH was calculated. The pH curve (figure 4.23) was then corrected for these values.

The corrected values showed a linear correlation between the proton concentration, e. g. pH, and the transport rate of L-lactate (figure 4.25). This finding hints towards a proton/lactate symport.

4.5.5 Use of protonophors

To test the assumption made above, protonophors were employed. Protonophors are weak organic acids that are able to abolish the proton gradient over the plasma membrane. As

described in the methods section (see 3.4.2.3) two different protonophors were used, CCCP and DNP, with different pKa values.

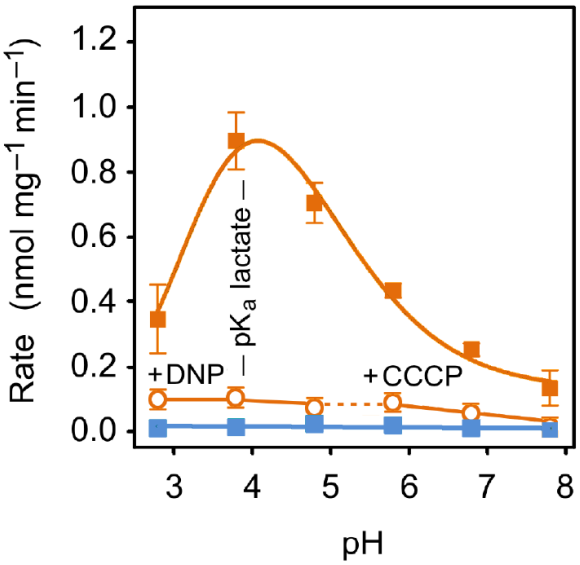

Figure 4.26 | Proton gradient decoupling by protonophors. W303-1A Δjen1 Δady2 yeast were used. Shown is the effect of CCCP and DNP at the respecting pH's. Errors bars denote SEM of triple determinations. Orange = PfFNT; blue = negative control

The transport of PfFNT dropped to rates close to the empty vector negative control when DNP (pH 2.8 to 4.8) or CCCP (pH 5.8 to 7.8) were employed (figure 4.26). This indicates a proton motive force in the lactate facilitation via PfFNT.

4.5.6 Medium alkalization during L-lactate uptake via PfFNT

Uptake of L-lactate into yeast cells coincided with alkalization of the weakly buffered external medium. This happened in a concentration dependent manner directly showing lactate/proton co-transport (figure 4.27).

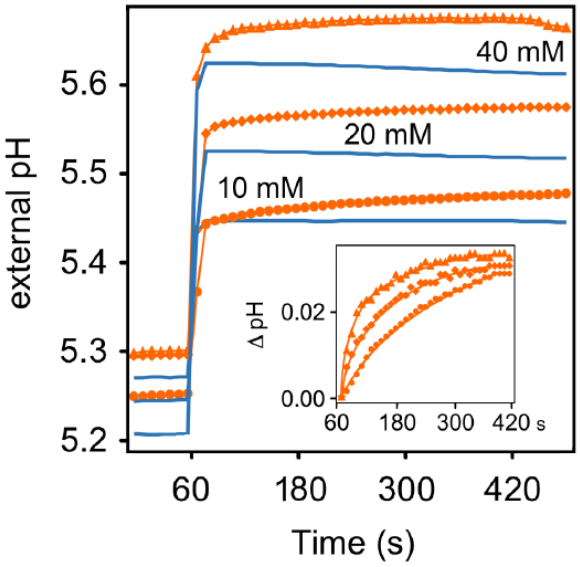

Figure 4.27 | pH change during substrate transport via PfFNT. The external buffer was alkalized due to lactate/proton symport in PfFNT expressing yeast (W303-1A Δjen1 Δady2) at different inward directed L-lactate gradients. The inset depicts the initial, concentration-dependent proton uptake kinetics. Blue = non-expressing control, orange = PfFNT, L-lactate concentration: circles = 10 mM, diamonds = 20 mM and triangles = 40 mM; performed by Dr. Binghua Wu

When the L-lactate concentration was doubled from 10 to 20 mM or 20 to 40 mM respectively, the alkalization rate was doubled also (figure 4.27, small insert). With the empty vector control there was no change in pH detectable.

4.5.7 Blocking the yeast potassium/proton antiporter

S. cerevisiae is capable of maintaining its cytosolic pH via various mechanisms. One of these are proton-potassium-antiporters (figure 4.28). To exclude the possibility that protons took the alternate route in exchange to potassium ions into the cells through proton-potassium-antiporter the potassium concentration in the test buffer was raised.

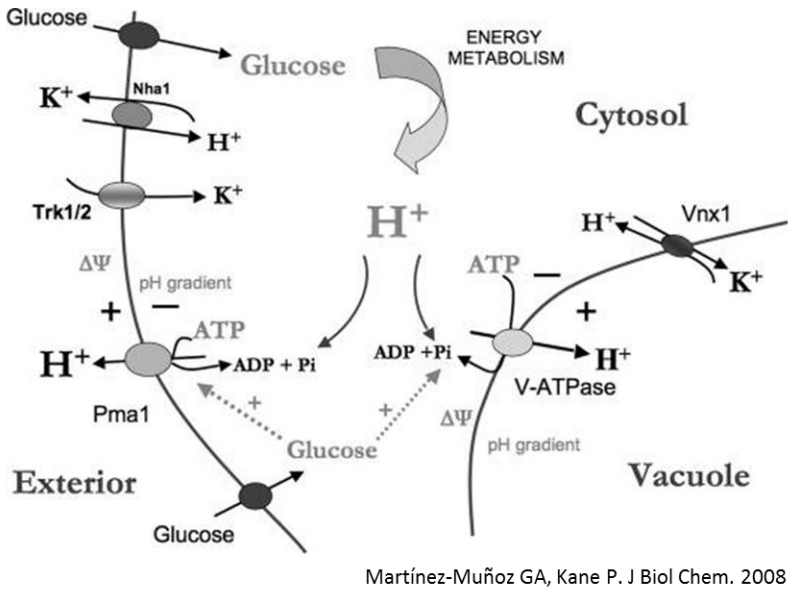

Figure 4.28 | Model for pH homeostasis in yeast. *S. cerevisiae* has numerous different mechanisms to sustain a stable intracellular pH. One of these is the Nha1 potassium / proton antiporter which resides in the plasma membrane. It exchanges protons for potassium ions. [Martínez-Muñoz et al. *JBC* 2008]

An increased external potassium concentration did not affect the L-lactate transport rate. This was tested by the use of 40, 80 and 120 mM potassium in the test buffer. L-lactate concentration was 1 mM and the pH 6.8 (figure 4.29).

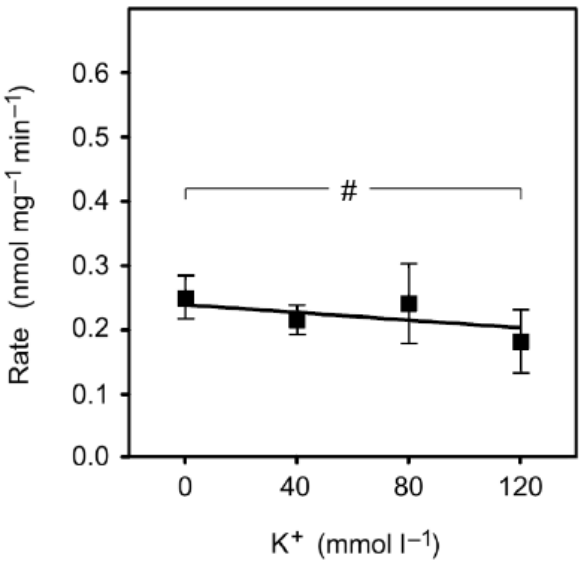

Figure 4.29 | Blocking the proton/potassium antiporter has no effect on L-lactate uptake in yeast. Strain W303-1A Δjen1 Δady2 was incubated at room temperature with 1 mM L-lactate buffer at pH 6.8 containing the shown potassium concentrations. The alternative proton uptake pathway via Nha1 is inhibited by high external potassium concentrations. Nevertheless the rate of L-lactate uptake remains stable (#: no significant difference according to Student's t-test). Errors bars denote SEM of triple determinations.

4.5.8 Inhibitors that reduce lactate transport via PfFNT

To get an idea of the physiological relevance of PfFNT in living plasmodia inhibitors with known antimalarial activity were tested. The compounds used were furosemide, phloretin, pCMBS and derivatives of cinnamic acid which is a known inhibitor of lactate transporters (figure 4.30).

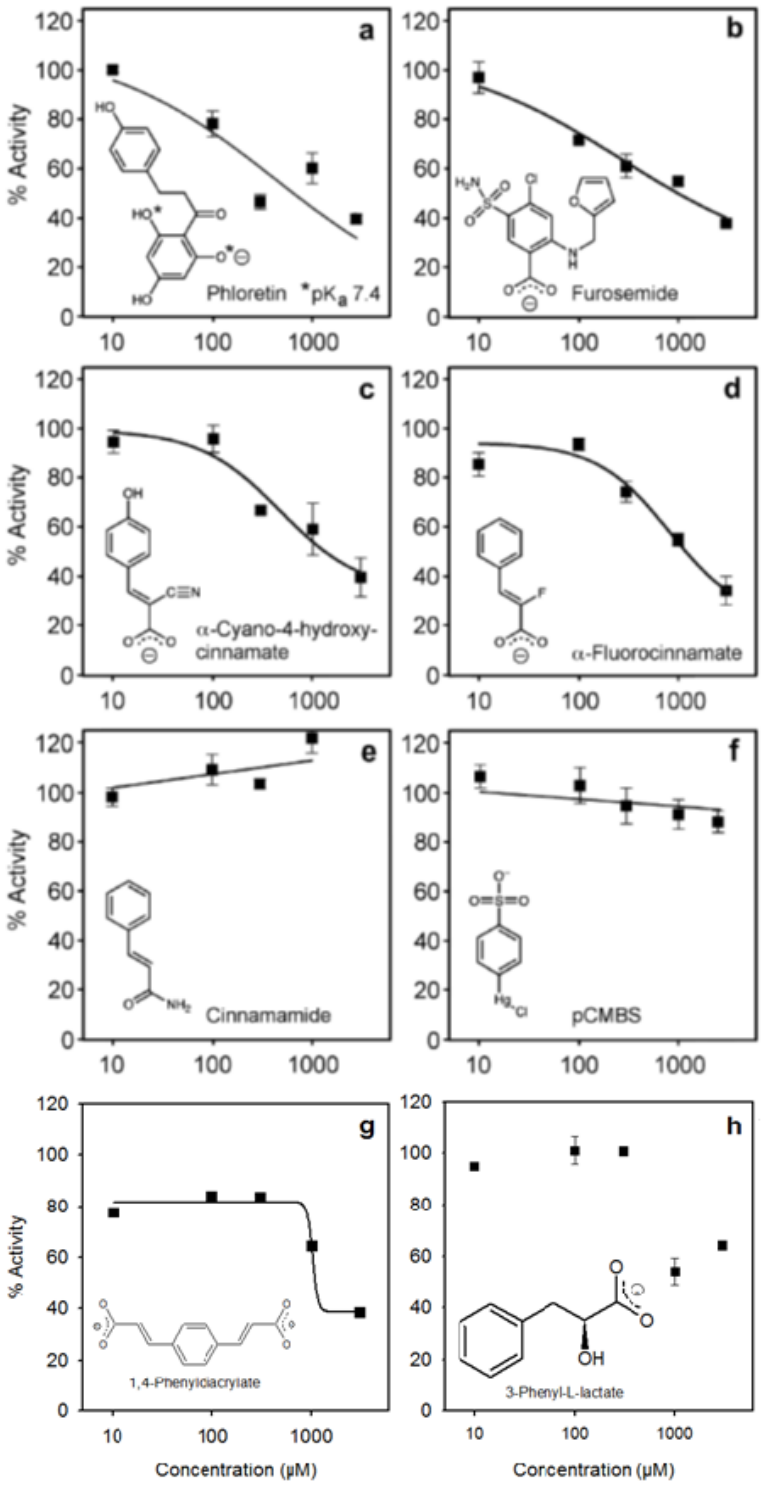

Figure 4.30 | Inhibition of PfFNT L-lactate transport. Strain W303-1A Δjen1 Δady2 was incubated at room temperature for 10 to 15 minutes in storage buffer at pH 6.8 containing the respective inhibitor in its final concentration. Directly afterwards transport rates with 1 mM L-lactate were recorded. Phloretin (a), furosemide (b), cinnamic acid derivatives (c, d, and g) and L-lactate derivative

inhibit PfFNT, neutral cinnamamide (e) and pCMBS do not (f). Errors bars denote SEM of triple determinations.

For all compounds with an inhibitory effect the activity-curves looked very similar with slight differences in the maximum effect, being around 40% remaining activity. These compounds, except 3-phenyl-L-lactate, had an IC_{50}-value of about 1 mM. Since the substrate, L-lactate, was applied in a concentration of 1 mM it is likely that all substrates inhibited transport in a competitive mode. 3-phenyl-L-lactate had a maximum inhibitory effect of about 65% remaining activity at 3 mM. The tested concentrations reached from 10 µM to 3 mM. Phloretin and pCMBS had to be, due to poor solubility, dissolved in DMSO. This had an inhibitory effect of about 10% on its own. This value was subtracted from the obtained data. Cinnamamide and pCMBS had no effect on the L-lactate transport rates via PfFNT. The highest inhibitory effect was reached with α-fluorocinnamic acid and was 35% activity at 3 mM.

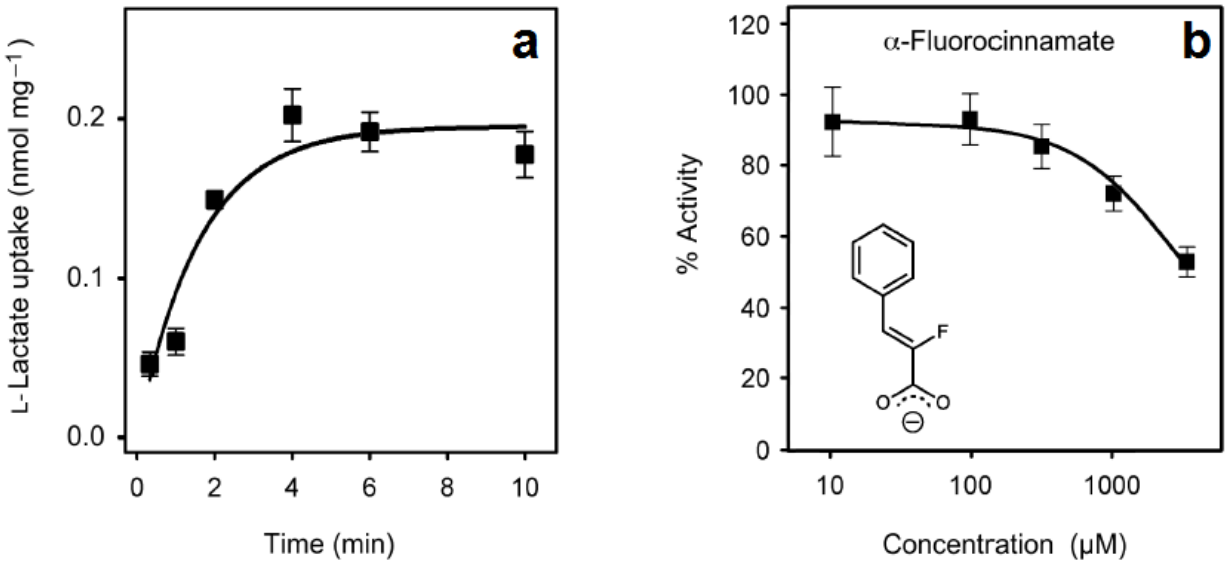

Figure 4.31 | Lactate transport via *E. coli* FocA is inhibited by α-fluorocinnamate. Strain W303-1A Δjen1 Δady2 was employed and FocA tested exactly as previously PfFNT. 1 mM L-lactate at pH 6.8 was used for the uptake curve (a) and inhibition by α-fluorocinnamate (b). Error bars indicate SEM for 3 measurements.

Figure 4.31 displays kinetics of L-lactate transport through EcFocA. The uptake rate is similar to PfFNT while α-fluorocinnamate is less effective on FocA (55% activity versus 35% activity in PfFNT). Nevertheless this experiment might point to an antibiotic potential of cinnamic acid derivatives.

4.6 Altering the crucial pore lining amino acids of PfFNT

First attempts to elucidate the exact mechanism of transport of lactate through the pore of PfFNT were made. For this, mutations of expected crucial pore lining amino acids were made to see whether alterations in size or polarity would have an effect on the transport.
Three constructs were derived:

- Threonine 106 to serine
- Threonine 106 to valine
- Histidine 230 to phenylalanine

All constructs were successfully mutated, sequenced and cloned. Nevertheless only the T106V and T106S mutants were tested in the radiolabeled L-lactate transport assay due to time limitations (figure 4.32).

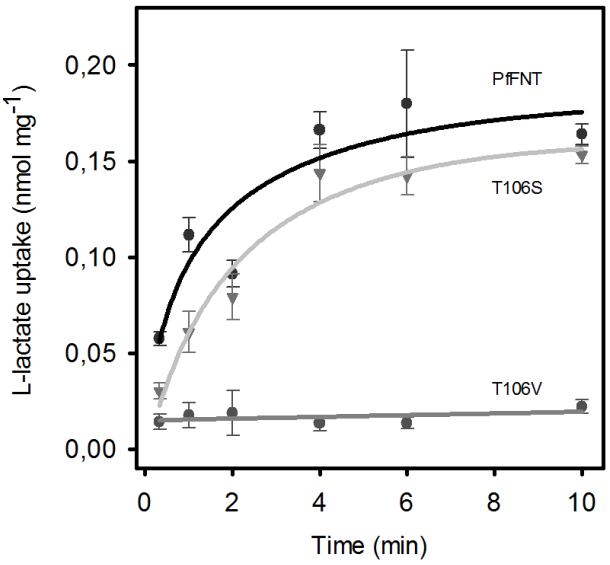

Figure 4.32 | Kinetic characterization of L-lactate transport via T106S and T106V. Strain W303-1A Δjen1 Δady2 was incubated at room temperature with 1 mM L-lactate buffer at pH 6.8 for up to 10 minutes. 3 measurements contributed to 1 sample and error bars indicate SEM.

The threonine to serine mutant showed an about 50% reduced L-lactate transport rate compared to the wild type PfFNT. But there was no lactate transport detectable with the threonine to valine mutant. This gives an impression of the importance of a hydrogen bond interaction partner at the position 108 in the protein.

4.7 The PfFNT-GFP fusion protein is targeted to the parasite plasma membrane

The idea was in order to gain insight into the relevance of PfFNT for living parasites to perform direct radiolabeled L-lactate uptake measurements on permeabilized infected RBCs. For this the PfFNT gene was cloned into a plasmodial vector. *P. falciparum* 3D7 were transfected to overexpress the protein. This was confirmed by confocal fluorescence microscopy since the construct contained a GFP at the C-terminus. Alexandra Blancke-Soares in the group of Tobias Spielmann took pictures (figure 4.33) which clearly show expression and targeting of PfFNT into the plasma membrane of the parasites.

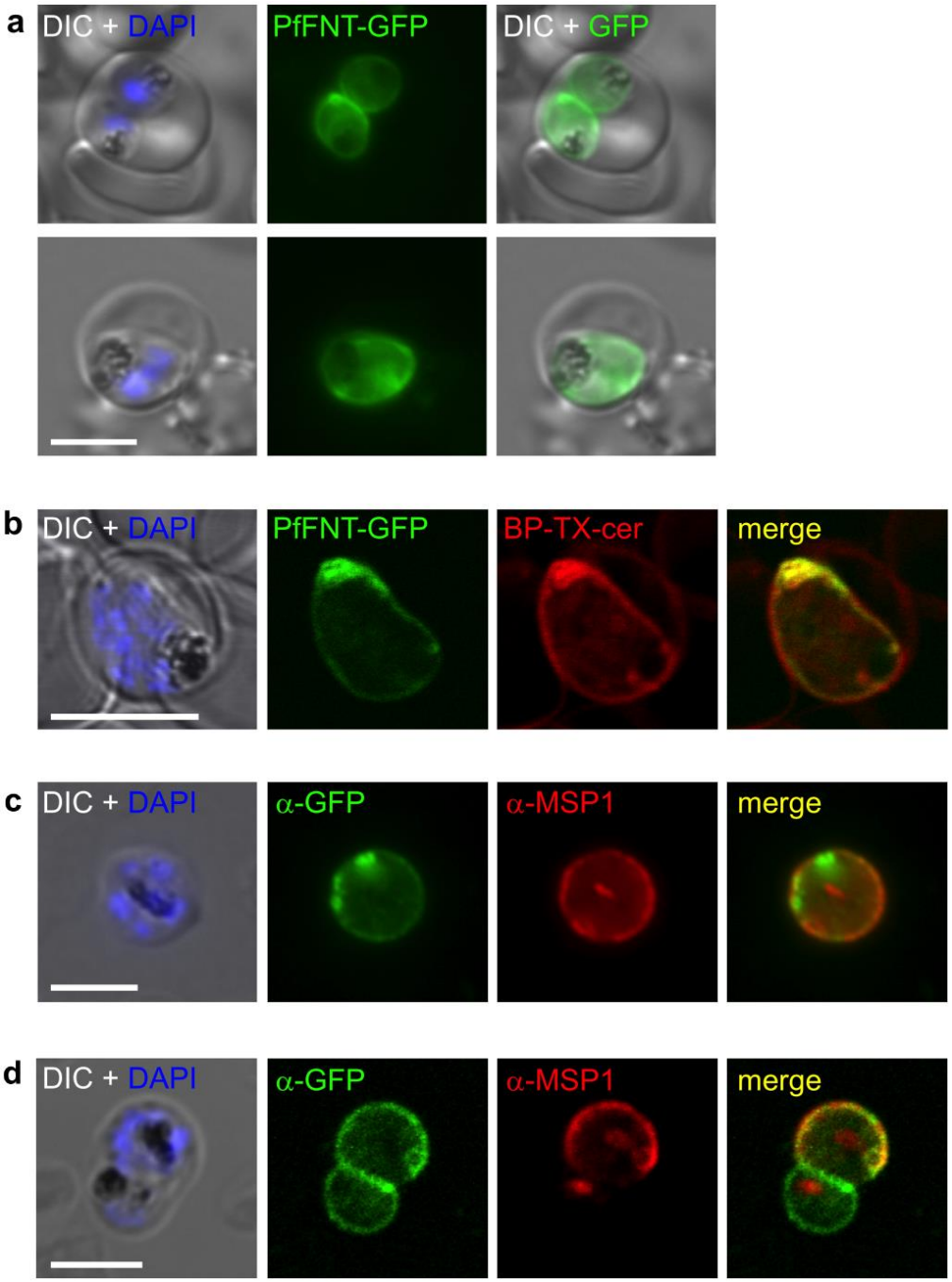

Figure 4.33 | Visualization of PfFNT in infected erythrocytes. a. Fluorescence emission of living, PfFNT-GFP expressing early (top panel) and late trophozoites (bottom panel) within erythrocytes. DIC, differential interference contrast; DAPI (blue), nuclear stain; GFP (green). **b.** A single confocal section through an infected RBC. Bodipy-TX-ceramide (red), lipid membrane stain. **c, d.** Co-localization of PfFNT-GFP with merozoite surface protein 1 (MSP1) in the plasma membrane by fluorescence microscopy (c) or a single confocal section (d) using anti-GFP and anti-MSP1 antibodies. Scale bars indicate 5 μm.

The PfFNT-GFP fusion construct showed a clear staining of the plasma membrane of plasmodium. Nuclei were marked with DAPI which resulted in a blue staining. For lipid membrane staining the dye Bodypi-TR-C_5-ceramide was used which is illustrated in red color. As controls, antibodies were used which were directed against the membrane residing peptide MSP1 and GFP. A merge of these markers with PfFNT resulted in a yellow color when both proteins co-localized.

Although first radiolabeled substrate measurements in *P. falciparum* seemed to be quite promising the obtained data could not be repeated and are therefore not shown.

5 Discussion

The aim of this thesis was to elucidate and characterize the protein that is responsible for lactate transport out of the malaria causing parasite *Plasmodium falciparum*. This is of special importance because this target has escaped elucidation since the first reports on lactate production in plasmodia emerged over 60 years ago [McKee et al. *J Exp Med.* 1946]. Furthermore, the last publication on this topic was published 13 years ago [Elliott et al. *Biochem J.* 2001] and until then no new knowledge on that topic was released. This fact is surprising since lactate is known to be the metabolic end product of plasmodium while it resides in the red blood cells of its host [McKee et al. *J Exp Med.* 1946]. Moreover there is evidence that blockage of this pathway would highly stress or even kill the parasite [Cranmer et al. *J Biol Chem.* 1995]. The lactate permease might therefore be a valuable drug target [Elliott et al. *Biochem J.* 2001].

At the beginning the aim was to mimic the physiological situation of the parasite while it resides inside the host erythrocytes. During this phase there are two striking characteristics that reflect the situation of the parasite inside the RBC (figures 5.1 and 5.2):

- Generation of vast amounts of lactate (18 mmol $\cdot$ l^{-1} $\cdot$ min^{-1}) [Ginsburg *Trends Parasitol.* 2002]
- Need for export of lactate and protons, generated by glycolysis [Ginsburg *Trends Parasitol.* 2002]

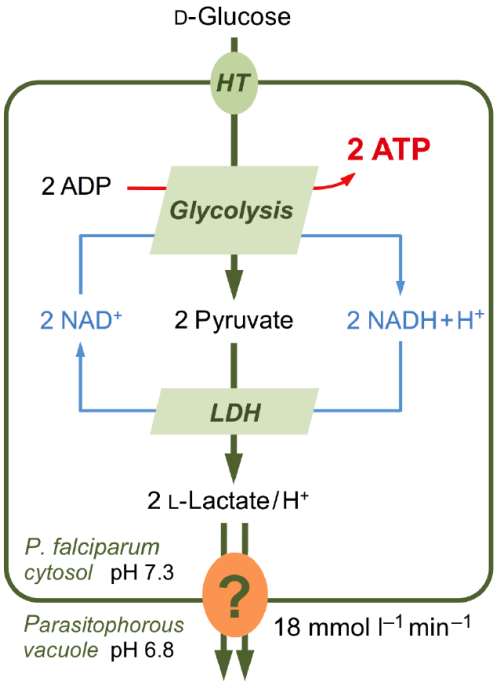

Figure 5.1 | Glucose degradation of *P. falciparum* inside the red blood cell. D-glucose is anaerobically metabolized by glycolysis to pyruvate. In order to restore two redox equivalents pyruvate is further reduced to L-lactate. This metabolic end product is exported through an until then unknown transporter. HT = hexose transporter; LDH = L-lactate dehydrogenase

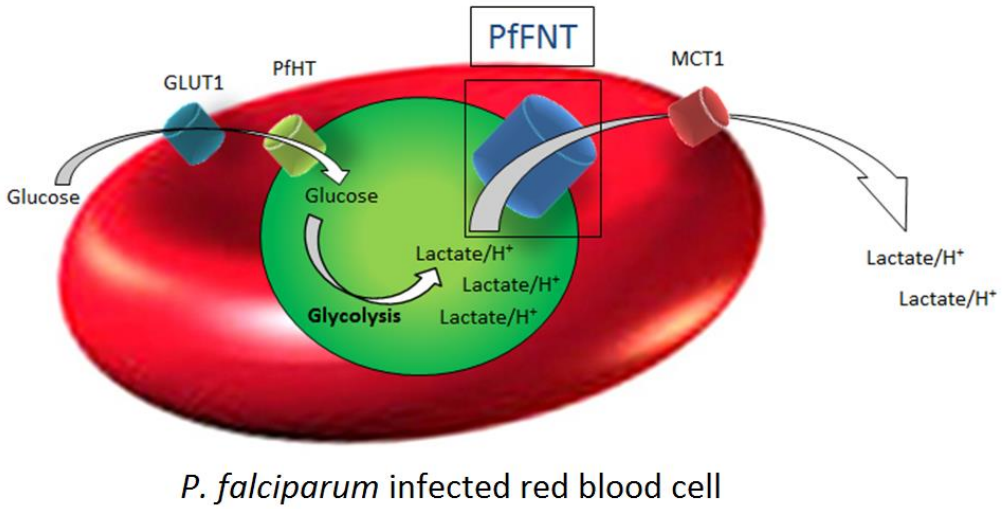

Figure 5.2 | Simplified scheme of carbon transport- and metabolic-processes of the infected erythrocyte. Abundant glucose is taken up from the host serum via the human glucose transporter (GLUT1) and the plasmodial hexose transporter (PfHT). Once inside the parasite it is converted via anaerobic glycolysis to lactate. Lactate as the metabolic end product is exported together with protons in a 1:1 stoichiometric manner via PfFNT and the human monocarboxylate transporter (MCT1).

In order to reflect this situation a yeast strain BY4742 Δjen1Δady2Δcyb2Δadh1 LDH was engineered, producing L-lactate with no export pathway apparent. The strain produced high amounts of L-lactate. Nevertheless there was no difference between yeasts expressing lactate transporters and those without (figure 4.5). Most likely the yeasts shuffle the produced lactate into their vacuoles and accordingly are able to cope with the, compared to wild type yeast, abnormal high concentrations.

Therefore the assay direction was changed from export to import. Lactate permeases from different species are known to show bidirectional facilitation of substrates, e.g. the monocarboxylate transporters 1 to 4 of mammals [Halestrap et al. *IUBMB Life* 2012], formate nitrite transporters of bacteria [Lü et al. *Biol. Chem.* 2013] and the pyruvate transporter in *Trypanosoma brucei* [Sanchez *J Biol Chem.* 2013]. The yeast based test system (strain W3031A Δjen1Δady2) had the advantage of a nearly absent background substrate transport compared to control cells. Moreover the sequence optimized PfFNT led to a strong protein expression in yeast. Western blots performed by Marie Wiechert and Julia Holm-Bertelsen showed multiple bands, ranging from monomers and trimers up to pentamers (Identity of a Plasmodium lactate/H+ symporter structurally unrelated to human transporters, Rambow et al. currently

under revision). All tested proteins were well expressed in the yeast system and integrated into the plasma membrane. This was confirmed by a biotinylation assay performed by Julia Holm-Bertelsen (figures 4.10 and 4.11).

5.1 Putative plasmodial MCT's

At the beginning it was investigated whether two plasmodial monocarboxylate transporter candidates would conduct lactate. These putative lactate permeases had been annotated reasoned by a certain degree of sequence similarity (about 30%, figure 5.3) and analogous predicted membrane topology to MCT's (figures 5.4 and 5.5).

	hMCT1	hMCT2	hMCT3	hMCT4	hMCT5	hMCT6	hMCT7	hMCT8	hMCT9	hMCT10	hMCT11	hMCT12	hMCT13	PfB0465c	Pfl1295c
hMCT1	—	75.7	56.7	59.7	44.6	48.9	45.2	44.7	43.6	42.1	46.5	47.2	48.2	30.6	25.0
hMCT2	61.0	—	61.0	64.8	45.8	54.1	48.7	46.3	43.9	44.5	51.3	49.6	51.6	32.9	29.7
hMCT3	39.5	43.1	—	73.1	44.0	53.0	46.7	42.4	44.8	45.5	51.8	45.8	52.1	32.3	27.0
hMCT4	43.7	46.5	58.3	—	47.0	55.4	51.1	45.4	46.6	45.5	50.1	51.2	52.8	35.8	27.5
hMCT5	23.0	25.5	24.0	25.6	—	43.0	43.5	43.2	42.3	44.4	48.5	49.7	50.1	29.7	29.2
hMCT6	27.6	31.3	36.4	35.9	23.5	—	45.6	42.4	42.6	43.2	45.8	45.0	47.2	33.4	28.2
hMCT7	26.5	31.1	28.8	31.4	25.6	28.2	—	42.0	43.4	41.8	48.3	45.4	53.7	33.2	29.3
hMCT8	23.7	24.1	25.8	25.9	22.0	24.1	21.6	—	41.3	67.3	41.0	39.6	45.2	31.2	27.4
hMCT9	25.0	26.0	27.2	28.0	24.0	23.3	24.5	24.4	—	43.9	44.3	43.7	47.9	32.4	29.2
hMCT10	24.2	25.2	26.5	25.8	24.2	23.1	20.0	53.0	26.9	—	44.9	41.7	47.6	32.0	29.0
hMCT11	27.5	32.4	36.0	32.1	27.0	29.4	24.0	25.2	26.2	26.4	—	46.8	65.0	32.0	29.6
hMCT12	27.7	29.7	32.5	34.1	30.1	27.3	25.7	20.9	26.2	21.9	28.8	—	51.4	34.9	28.6
hMCT13	31.2	32.8	35.3	31.6	28.9	27.7	33.1	23.6	29.0	24.6	47.8	31.1	—	34.9	33.0
PfB0465c	12.6	14.5	14.7	15.6	14.2	15.1	12.4	18.4	15.8	15.0	14.6	15.8	15.8	—	31.5
Pfl1295c	11.0	12.3	10.4	12.4	12.5	10.4	10.4	13.1	13.6	12.1	12.3	11.6	14.0	18.2	—

% identity

% similarity

Figure 5.3 | Identity and similarity between the proteins of MCT's, PFI1295c and PFB0465c. TeXshade [Beitz *Bioinformatics* 2000] was used to visualize the data generated from the sequence alignment (figure 5.6).

To date only MCT1-4 have been shown to carry monocarboxylates. They transport important metabolic compounds such as lactate, pyruvate and ketone bodies in a proton-coupled fashion [Halestrap *Mol Aspects Med.* 2013]. They share characteristic sequence motifs, which were confirmed by labeling studies and proteolytic digestion [Halestrap *Mol Aspects Med.* 2013].

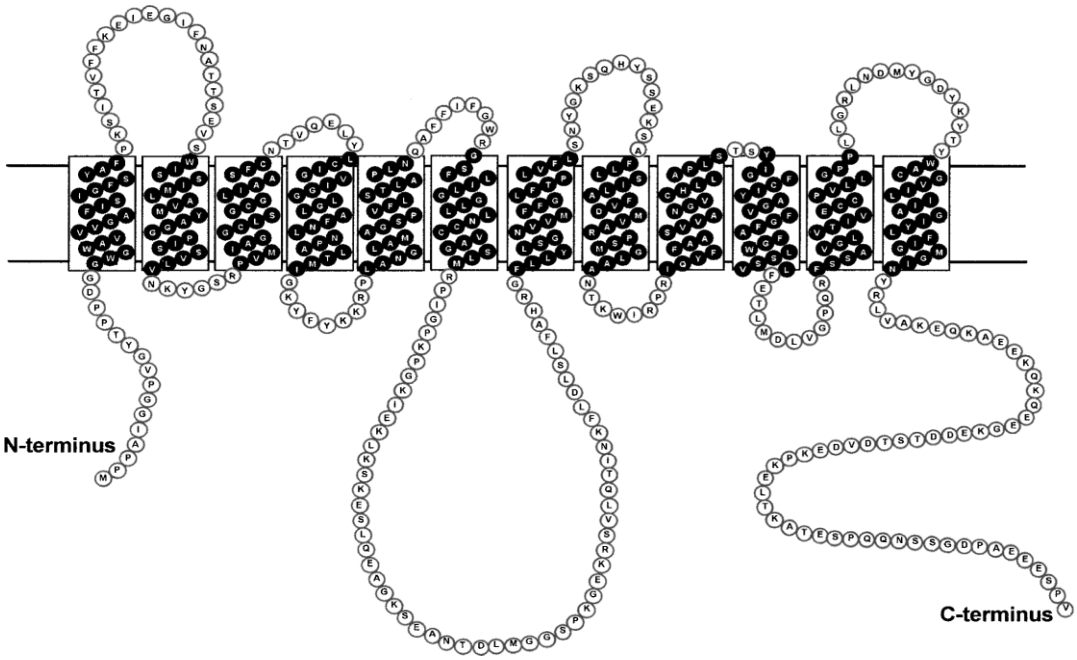

Figure 5.4 | Predicted membrane topology of human MCT1. It is built of 12 transmembrane helices with intracellular C- and N-termini and a large intracellular loop between helices 6 and 7 (Halestrap et al. *Biochem. J.* 1999).

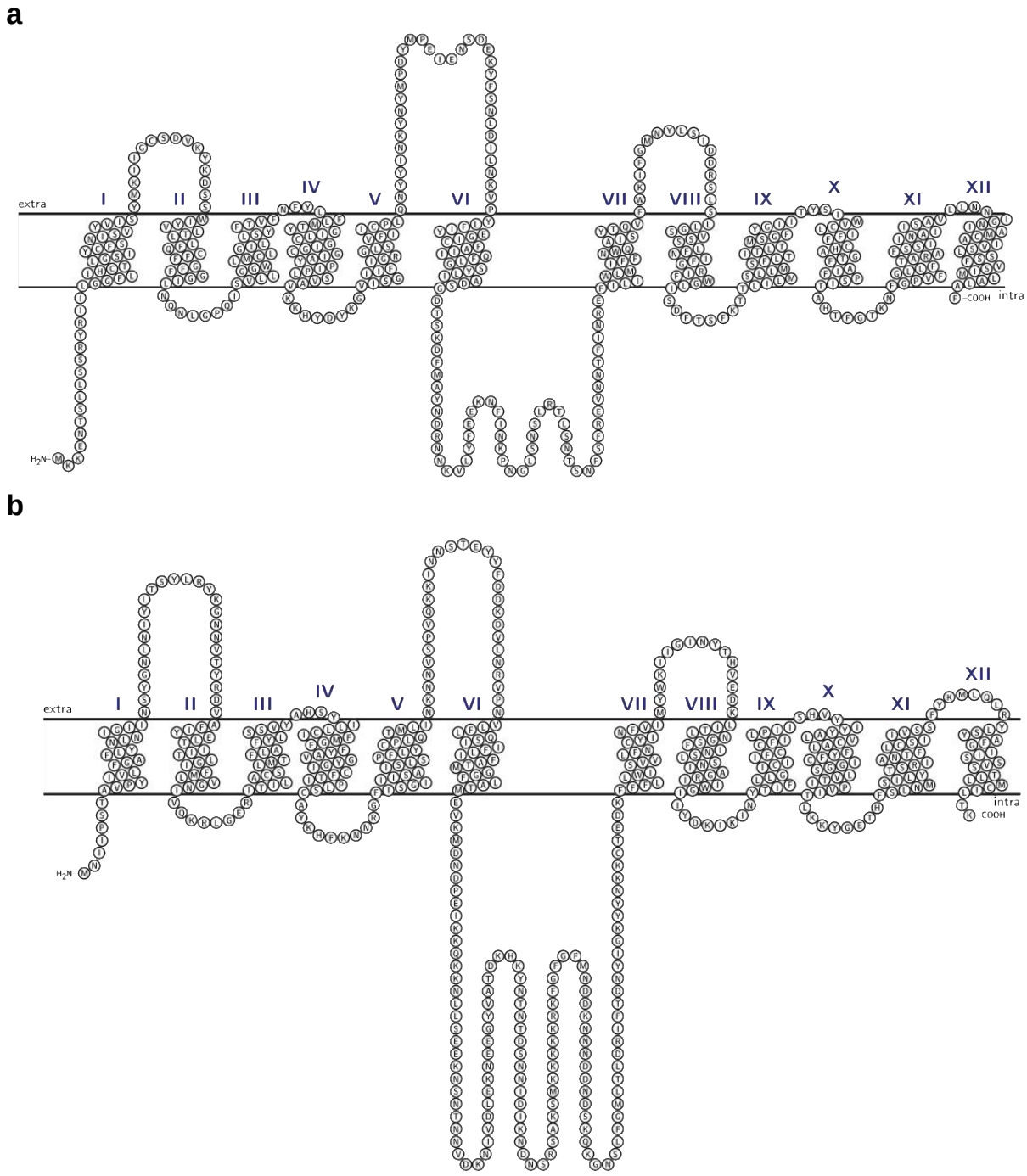

Figure 5.5 | Predicted topology of PFI1295c (b) and PFB0465c (a). The topology plots are based on the sequence alignment shown in figure 5.6 and were set using TeXtopo [Beitz *Bioinformatics* 2000].

Although there is a certain degree of apparent resemblance in the predicted topology of PFI1295c, PFB0465c and MCT1 the alignment of the candidates with the SLC16 members shows absence of crucial residues for transport. These amino acids are conserved throughout MCT1 – 4. They reside in transmembrane span 1 (lysine) and in span 8 (aspartate and arginine) (figure 5.6).

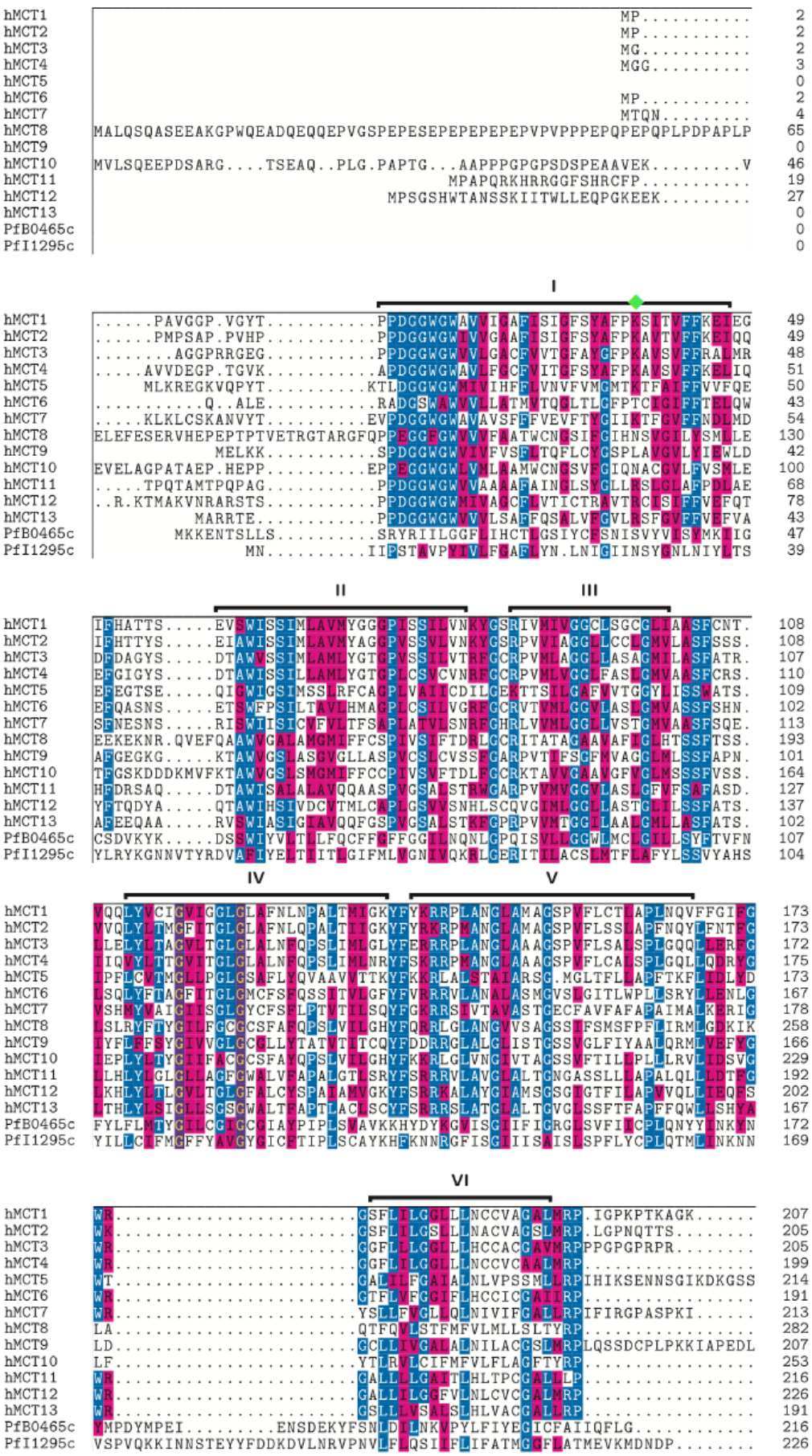
I
II
III
IV
V
VI

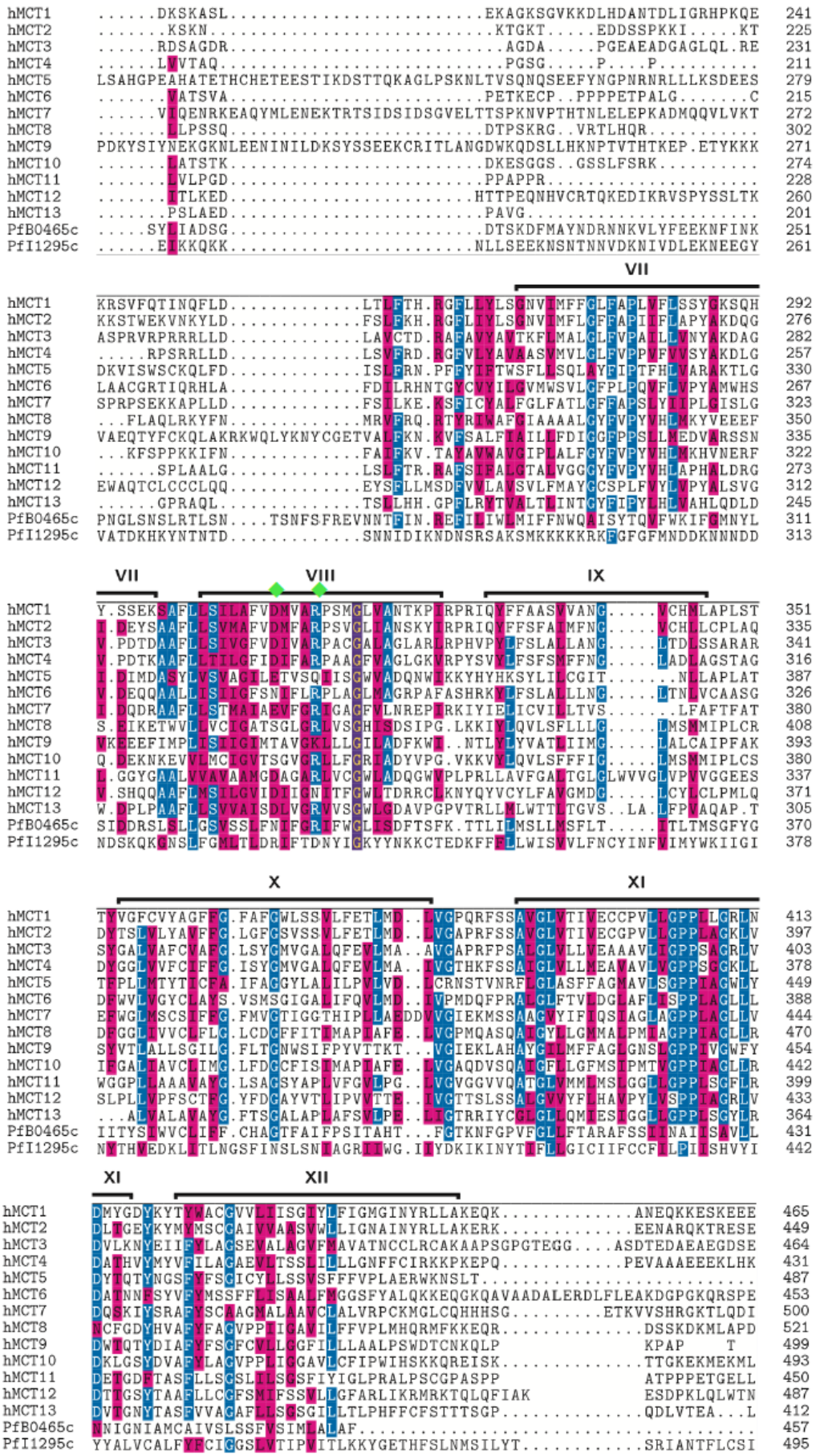
VII
VII
VIII
IX
X
XI
XI
XII

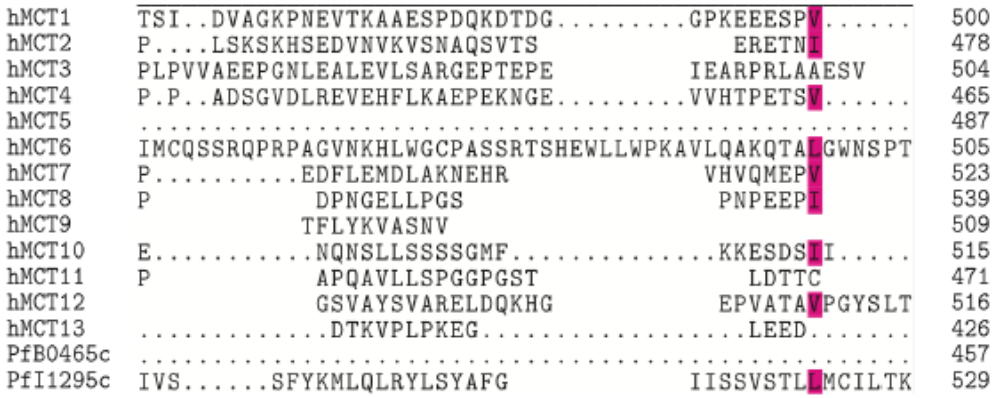

Figure 5.6 | Alignment of human MCT 1 to 13 with PFI1295c and PFB0465c. The alignment was created using the clustalw algorithm and envisioned using TeXshade [Beitz *Bioinformatics* 2000]. Positions with conserved residues throughout are colored yellow on purple and respectively identical and similar residues are shaded in blue and magenta. The roman letters and bars symbolize the regions of the proposed MCT1 transmembrane spans. The green diamonds in transmembrane spans 1 and 8 mark the positions of a conserved lysine, an aspartate, and an arginine, which have been shown to be required for hMCT1 functionality; none of these are present in the plasmodial peptides.

But there are more arguments against a role in lactate facilitation of the putative plasmodial MCTs. For instance when the expression levels of these peptides are considered (figure 5.7).

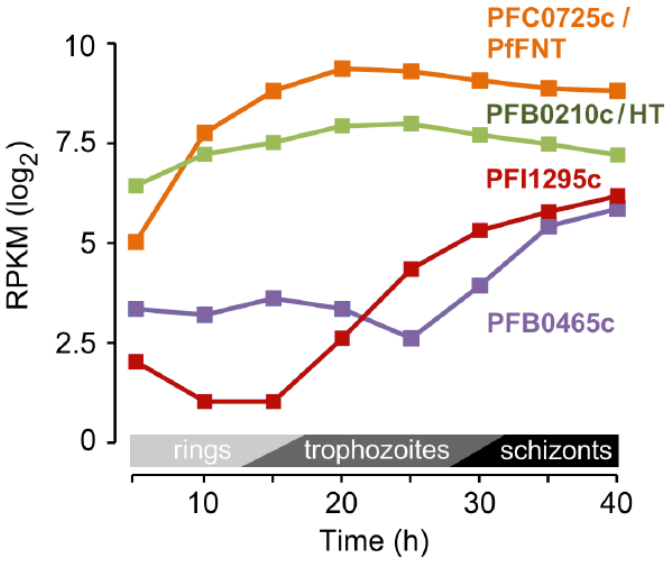

Figure 5.7 | Expression profile of the putative plasmodial MCT's during development inside the RBC. Green = plasmodial hexose transporter; purple = PFB0465c; red = PFI1295c; orange = PfFNT. Data were from PlasmoDB and transcript level is set as reads per kilobase of exon model per million mapped reads (RPKM) [Bártfai et al. *PLoS Pathog.* 2010].

In the early trophozoite-phase (about 20 hours past invasion) the parasites exhibit a strong metabolic activity due to their rapid growth [Roth *Blood Cells* 1990; Olszewski et al. *Mol. Biochem. Parasitol.* 2011]. This is reflected by high expression levels of glycolytic enzymes, such as glucose-6-phosphate isomerase (PF14_0341), and the hexose transporter (PFB0210c) (figure 5.7). At that stage PfFNT is expressed at levels comparable to the hexose transporter whereas PFI1295c and PFB0465c levels are low (about 4 times less) with maximum expression at the late schizont stage (40 hours post invasion). This indicates a different role of these two proteins other than lactate export, which would give an explanation why there was no lactate facilitation for PFI1295c and PFB0465c detectable. It was shown that the peptides were expressed in our test organism *S. cerevisiae* and integrated into the plasma membrane (figure 4.11). Anyway growth was not restored in the yeast phenotypic L-lactate uptake assay by the two candidates and there was also no radiolabeled substrate facilitation detectable, even under a prolonged uptake time (figure 4.18). In the end this fact is not surprising since a) the expression profile of these peptides misfits the plasmodial development inside the red blood cells (figure 5.7) and b) the deficiency of functionality may be credited to the absence of three conserved residues in transmembrane spans 1 and 8, which have been shown to be

essential for lactate transport by MCT1 (figure 5.6) [Halestrap *Mol. Aspects Med.* 2013]. Together with the fact that until now functional MCTs are found exclusively in mammals allows the assumption that the role as lactate transporters of this family was established later in evolution. For example the yeast *S. cerevisiae* encodes for five MCT like proteins, yet for none of these lactate facilitation could be demonstrated [Makuc et al. *Yeast* 2001]. The exact function of PFI1295c and PFB0465c remains to be elucidated.

Furthermore, data on aquaporins that are able to channel lactate were published [Tsukaguchi et al. *J Biol Chem.* 1998; Choi et al. *J Biol Chem.* 2007; Bienert et al. *Biochem J* 2013; Faghiri *PLoS One* 2010; reviewed in Rambow et al. *Front. Pharmacol.* 2014]. Therefore the plasmodial aquaporin PfAQP was checked for lactate conductance. The assay parameters were the same as for the PFI1295c and PFB0465c radiolabeled L-lactate uptake measurements with a prolonged time. There was no lactate facilitation via PfAQP detectable underlying the important role of PfFNT for lactate detoxification due to virtually absent further candidates that could be supportive regarding this matter.

5.2 Origin and classification of PfFNT

In the genome of *P. falciparum* is a single putative formate nitrite transporter sequence found. Its expression profile matches the plasmodial glycolytic enzymes as well as the glucose transporter (figure 5.7). A BLAST search yielded throughout the *Plasmodium ssp.* one FNT gene each, with high identity (about 70%) between the sub species and a high similarity to the bacterial FNTs (>40%) (figures 5.8 and 5.9).

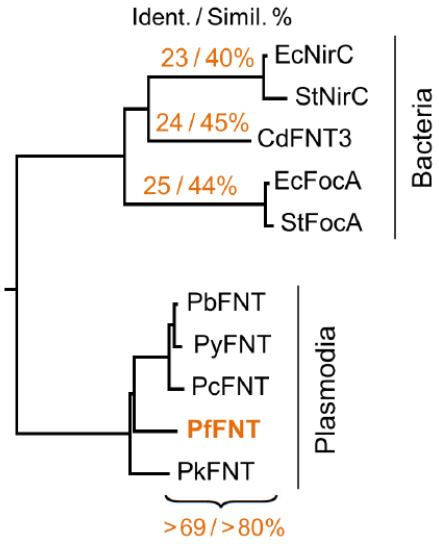

Figure 5.8 | Phylogenetic classification of PfFNT. Within the *Plasmodium ssp.* (Pb = *P. berghei*; Py = *P. yoelii*; Pc = *P. chabaudi*; Pk = *P. knowlesi*) persists a high degree of similarity and identity. To the bacterial FNTs (Ec = *Escherichia coli*; St = *Salmonella typhimurium*, Cd = *Clostridium difficile*) exists a minor relationship of PfFNT, nevertheless with about 40% of similarity.

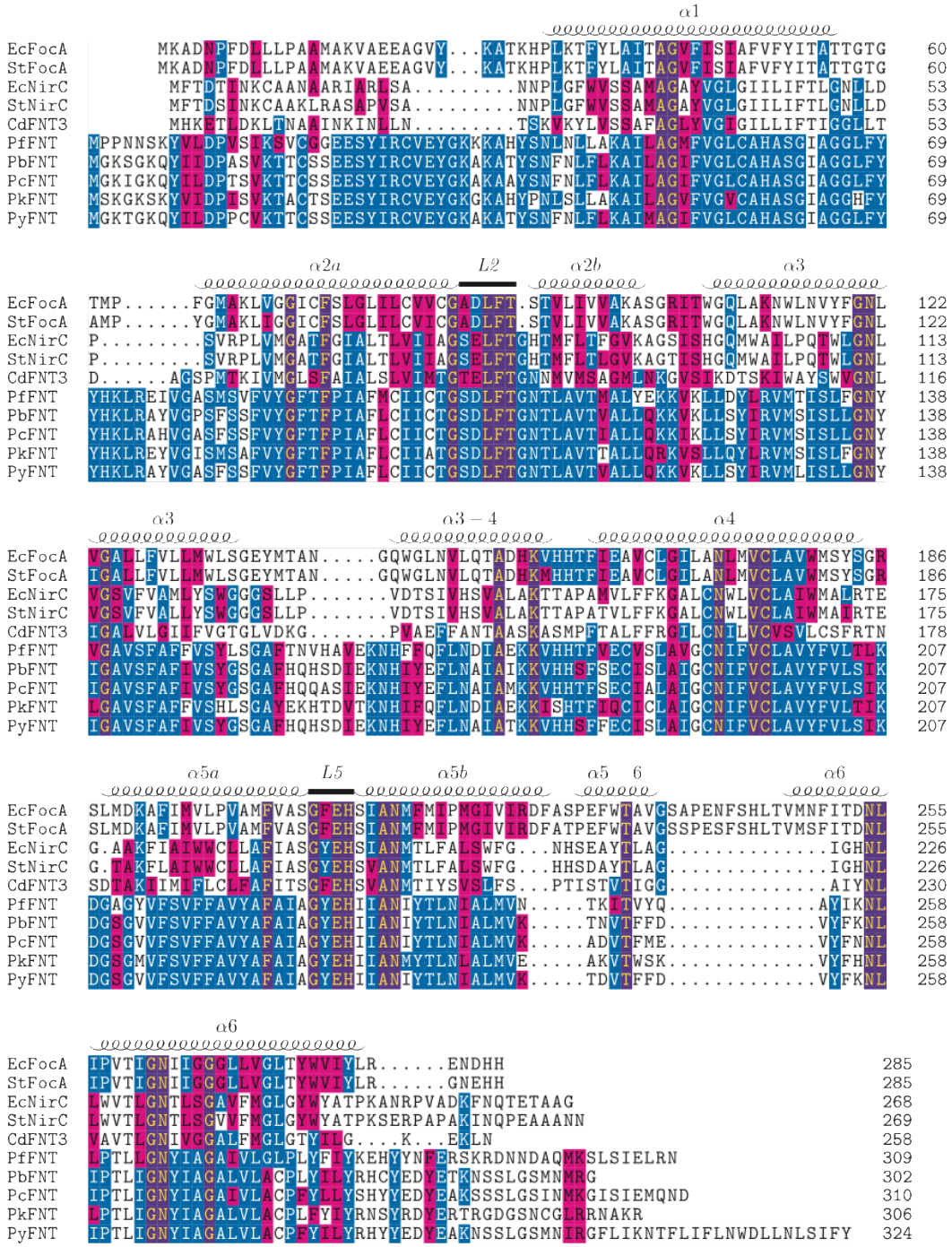

Figure 5.9 | Sequence alignment of FNT peptides in plasmodia and bacteria. The alignment was created using the clustalw algorithm and visualized using TeXshade [Beitz *Bioinformatics* 2000]. Positions with conserved residues in all sequences are highlighted yellow on purple; identical and similar residues are colored in blue and magenta, respectively. Helical domains according to the *E. coli* FocA crystal data [Wang et al. *Nature* 2009] are numbered consecutively. The positions of the helix-interrupting loops L2 and L5 (figure 5.10) are indicated by bars. The plasmodial FNT proteins lack apparent cell export signals [Heiber et al. *PLoS Pathog.* 2013].

An indication that PfFNT plays a crucial role in the parasitic carbon metabolism is the high expression level during maturation of the parasites (figure 5.7). Furthermore it is most probably the only protein (non functional MCT like peptides and non conductive PfAQP for lactate) that is capable of coping with export of metabolic end products, i.e. lactate.

Generally FNTs, which are found exclusively in lower organisms, such as bacteria, archaea, fungi, algae, and unicellular parasites [Saier et al. *Biochim. Biophys. Acta* 1999] operate as pentamers [Waight et al. *Curr Opin Struct Biol* 2013]. Each peptide complex is built by five identical protomers that reside in the plasma membrane [Lü et al *Biol. Chem.* 2013]. FNTs exhibit an aquaporin like architecture, referred to as molecular mimicry [Wang et al. *Nature* 2009]. Each protomer is composed of six transmembrane segments and a seventh pseudo helix which is formed by two half helices (figure 5.10). The inner core, which can be superimposed on aquaglyceroporins with r.m.s.ds of 3.3 Å, contains two constriction sites. These filter regions narrow the channel on the periplasmatic and on the cytoplasmatic end [Wang et al. 2009; Waight et al. *Nat Struct Mol Biol* 2010; Lü et al. 2011, 2012; Czyzewski et al. 2012] and are built by lipophilic amino acids being mainly leucine and phenylalanine. Within the central hydrophobic cavity lies a highly conserved histidine residue. It is thought of playing an essential role in substrate translocation since it is the only charged residue that is sited inside the inner channel [Waight et al. *Curr Opin Struct Biol* 2013]. The actual hypothesis is that the electrostatic potential surrounding the entrances of the channel attracts the anion. Once inside, there are two transport processes currently under discussion [Lü et al. *Biol Chem.* 2013] (figure 5.14): the polar negatively charged ion gets transiently protonated by the histidine residue which passes a proton to it. Now being much more lipophilic the molecule is able to pass the two hydrophobic barriers. After passing the second constriction the neutral acid is deprotonated again. At this situation there are two possibilities for the fate of the proton. First, it is cycled back via a fixed water molecule, which is coordinated by a conserved threonine (helix-interrupting loop L2) to the histidine residue (helix-interrupting loop L5). Its basic side chain would be now ready to protonate another substrate molecule again. Or second, the anion leaves the channel together with the proton. The latter would imply that protons are transported together with the substrate in a 1:1 symport action. In fact there are arguments for both ways of transport [Lü et al. *Proc Natl Acad Sci USA* 2012; Lü et al. *Biol Chem.* 2013] while the prevailing pH must be considered as well. This is the case when the pH gradient over the membrane rises, e.g. during anaerobic energy metabolism. In this situation a drop of the cytosolic pH occurs due to fermentation of various weak monoacids, such as lactate. This is known as a physiological condition from not only *Lactobacillus* and *Schistosoma* spp., [Faghiri et al. *PLoS One* 2010] but also for *Plasmodium* [McKee et al. *J. Exp. Med.* 1946].

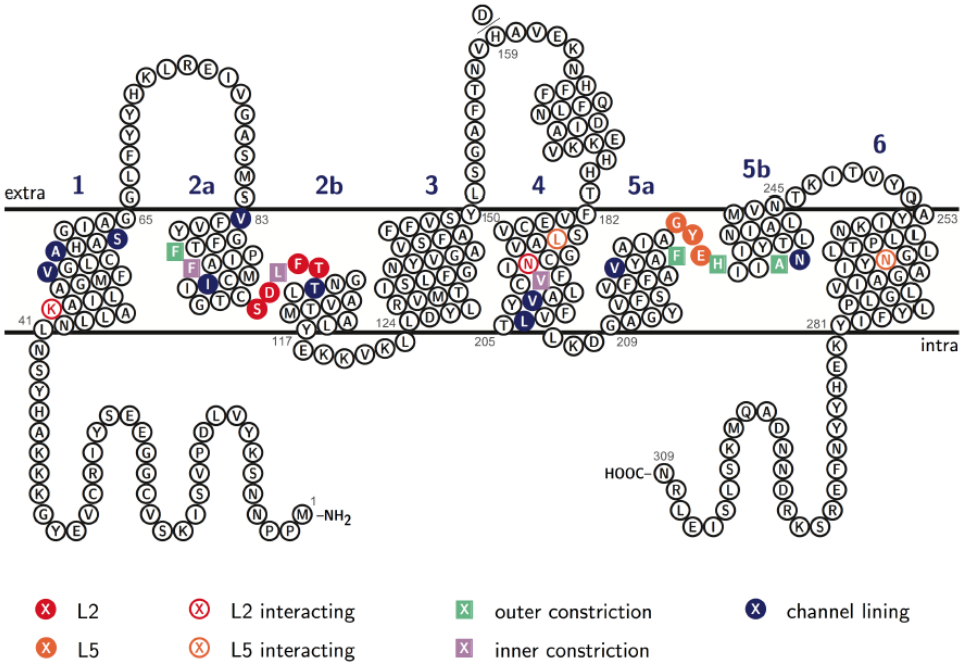

Figure 5.10 | Topology plot of PfFNT. This predicted model is based on the CdFNT3 crystal structure [Czyzewski et al. *Nature* 2012] and was generated using TeXtopo [Beitz *Bioinformatics* 2000]. Amino acids of particular interest are highlighted. L2 and L5 denote to the intra-membrane loops disrupting transmembrane spans 2 and 5, respectively. One nonsynonymous single nucleotide polymorphism has been identified [Aurrecoechea et al. *Nucleic Acids Res.* 2009] changing His159 to Asp.

The facilitated substrates are monovalent anions, which can be either organic or inorganic (figure 5.13). It seems to be a common feature of anion channels to show univalent polyspecificity of the transported moiety [Hille *Ionic Channels of Excitable Membranes* 1992; Yasui et al. *Nature* 1999; Rychkov et al. *J Gen Physiol* 1998]. This is contrary to what can be observed on for example cation channels, which display a high specificity over the channeled substrate [Payandeh *Biochim Biophys Acta* 2013; Liu et al. *Nat Commun* 2013; DeCoursey et al. *J R Soc Interface* 2013]. FNTs transport formate [Wang et al. *Nature* 2010; Lü et al. *Science* 2011; Whaigt et al. *Nat. Struct. Mol. Biol* 2010], nitrite [Lü et al. *Proc. Natl. Acad. Sci. USA* 2012] hydrosulfite [Czyzewski et al. *Nature* 2012] and monocarboxylates such as lactate [Lü et al. *Proc. Natl. Acad. Sci. USA* 2012].

We generated a model of PfFNT using the plentiful existing crystal data of the bacterial FNTs [Wang *Nature* 2009; Waight *Nat. Struct. Mol. Biol* 2010; Lü *Proc. Natl. Acad. Sci. USA* 2012; Czyzewski *Nature* 2012] (figure 5.11).

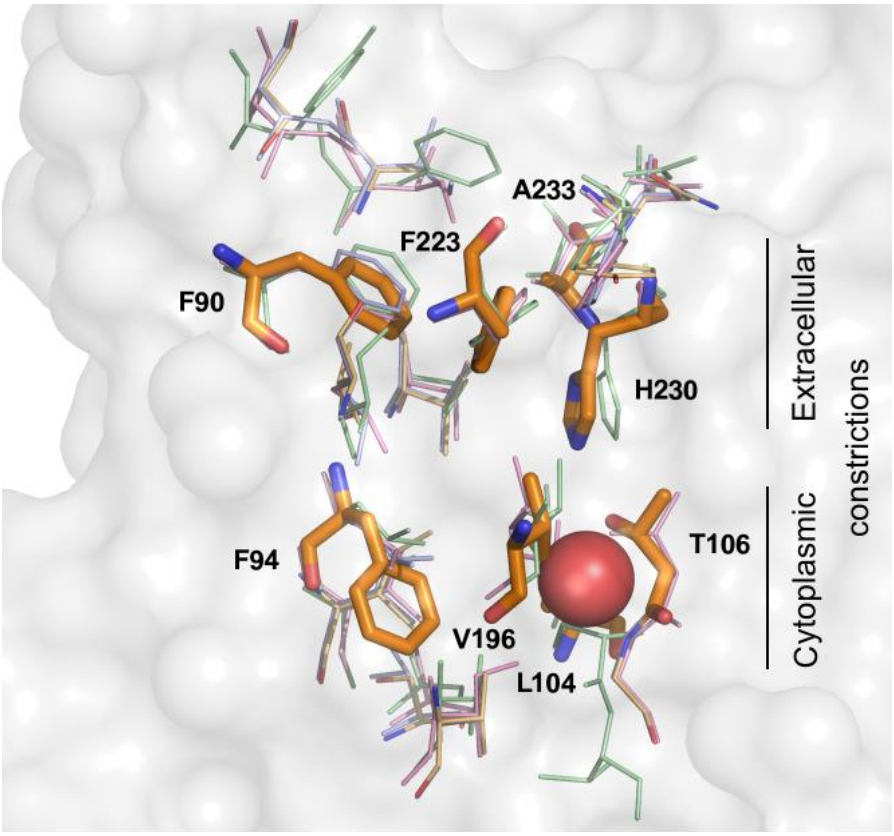

Figure 5.11 | 3 dimensional model of PfFNT. Green = EcFocA [Wang *Nature* 2012; Waight *Nat. Struct. Mol. Biol* 2010]; pink = StNirC [Lü et al. *Proc. Natl. Acad. Sci. USA* 2012]; blue = CdFNT3 [Czyzewski *Nature* 2012]; orange = PfFNT. Illustrated are residues of the transport channel with the constriction sites as sticks and a fixed water molecule (red sphere).

The PfFNT model aligns with sub-Ångstrom deviations at two conserved constriction sites of the bacterial FNTs. Furthermore it exhibits identical residues in seven of these crucial positions (F90, L104, T106, V196, F223, H230 and A233); the final, eighth position holds a phenylalanine (Phe94) instead of leucine. As already mentioned the constrictions together with a proton relay [Lü et al. *Proc. Natl. Acad. Sci. USA* 2012] consisting of a histidine (His230 in PfFNT), a fixed water molecule, and a threonine (Thr106) are thought to define selectivity by transient protonation of permeating weak monoacids [Lü et al. *Proc. Natl. Acad. Sci. USA* 2012]. Since the pore structures of plasmodial and bacterial FNTs resemble closely lets one assume similar transport properties of these peptides. The same applies for the molecular substrate channeling mechanism.

Whether FNTs should be termed as channels or as transporters is still under debate. I propose an intermediate definition called “chansporters” [Csanády et al. *EMBO Rep.* 2008] due to the fact that their architecture resembles channels (mimicry to AQPs) but they are able to make use of a secondary substrate (protons) a feature exclusive for transporters (figure 5.12).

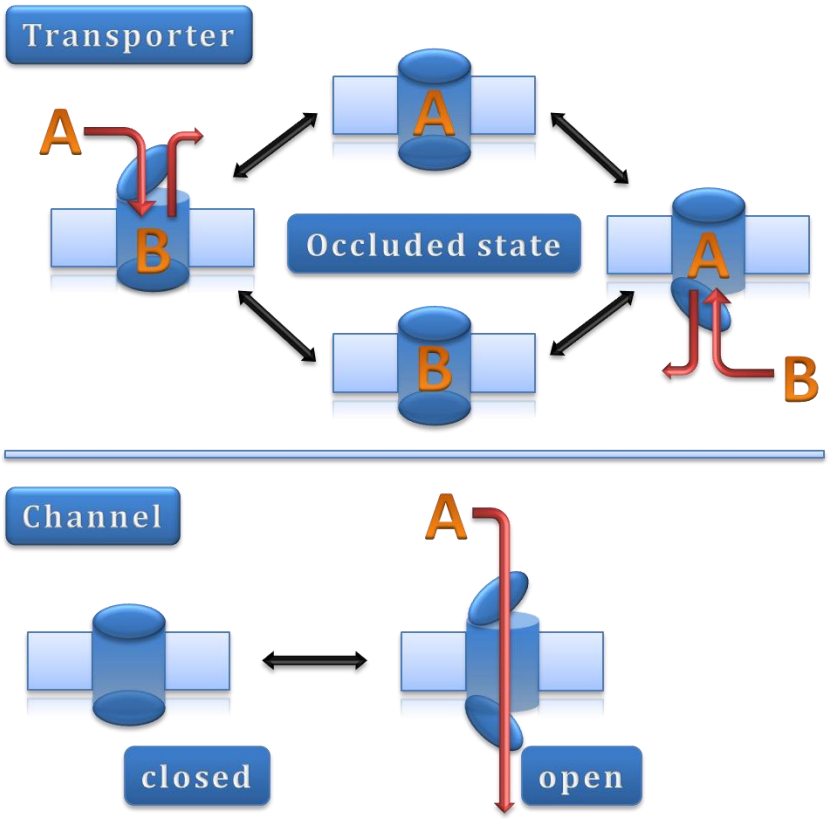

Figure 5.12 | Schematic transporter and channel mechanisms. While transporters keep only one access gate open at a time and have an occluded state, channels open both sides and rapidly facilitate substrates over the cell membrane. In between lies the mechanism for “chansporters” [Csanády et al. *EMBO Rep.* 2008].

5.3 PfFNT transport characteristics

As already mentioned FNTs are known to transport univalent anions ranging from inorganic nitrite and hydrosulfide to small monocarboxylates [Lü et al *Biol. Chem.* 2013] (figure 5.13).

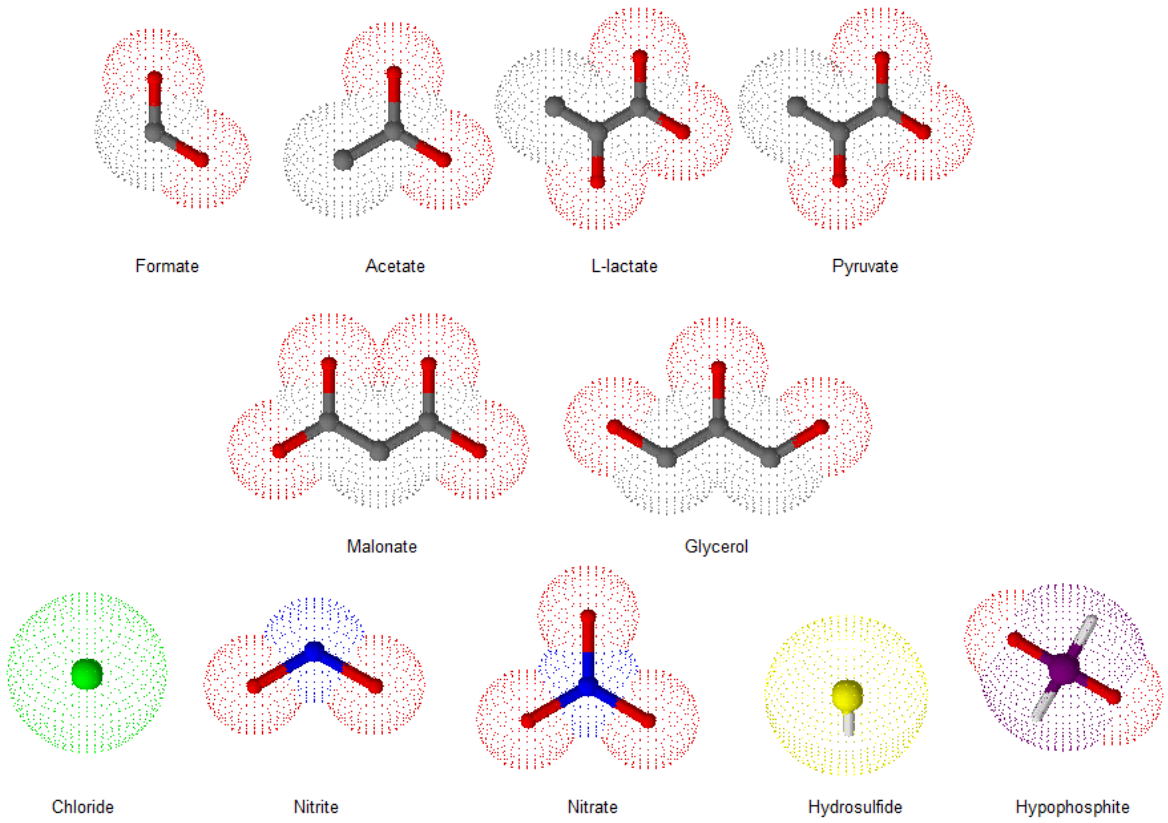

Figure 5.13 | Substrate transport pattern of FNTs. Small univalent anions are channeled while the dicarboxylate malonate and the non-charged glycerol are excluded. Molecules are drawn as sticks with dots for the atomic radius. Generated with ChemSketch.

Moreover FocA was shown to switch to monocarboxylate/proton symport below pH 5.7 [Lü et al. *Science* 2011]. This observation led to the following proposed actions of transport: Since the architecture of the conductive pore is highly conserved (figure 5.14 A) the central histidine is assumed to play an integral role in both states. First, it is involved in a three-step proton relay together with a threonine hydroxyl group, and a coordinated water molecule. This allows transient protonation of a monovalent anion that is able to overcome the central vestibule as an uncharged species (figure 5.14 B). Second, at low external pH reprotonation of

the conserved histidine may happen before the channeled acid is deprotonated. Dissociation will happen in the cytoplasm, leading to a net movement of the anion with a proton in a 1:1 stoichiometry. This exhibits secondary active import fueled by the proton motive force (figure 5.14 C).

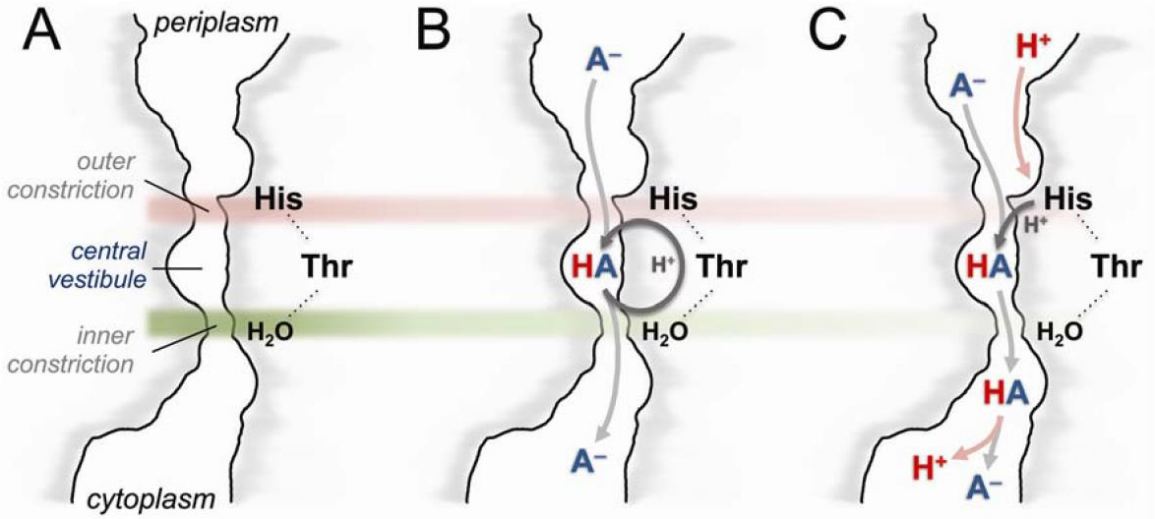

Figure 5.14 | Proposed transport mechanism of the FNT family. Side view on the conductive pore of FNTs. A) Substrates have to cross 2 barriers on their way through FNT, an outer constriction with a histidine and an inner constriction with a fixed water molecule. B) Monovalent anions are transiently protonated and can transcend the central vestibule as an uncharged species by a three-step proton relay. This involves a conserved histidine in the central vestibule region, a threonine hydroxyl group, and a coordinated water molecule. In this mode, FNT proteins act as bidirectional channels. C) When the external pH drops FNTs exhibit secondary active import fueled by the proton motive force. With a high external concentration of protons, reprotonation of the conserved histidine happens before the transported acid is deprotonated. In this case dissociation will happen in the cytoplasm, leading to a 1:1 translocation of the anion together with a proton. [Lü et al. *Biol Chem.* 2013]

Using direct radiolabeled substrate assays the transport characteristics of the plasmodial FNT protein were elucidated. L-lactate was facilitated likewise to EcFocA with an initial rate of

transport (0.25 nm • mg^{-1} • min^{-1}). The affinity to lactate (87 mM) was analog to the data exhibited by the homologous *Salmonella typhimurium* FocA ($k_{lactate}$ 96 mM) [Lü et al. *Proc. Natl. Acad. Sci. USA* 2012]. Notably to say that the data on lactate affinity in living parasites underlies strong variations depending on the assay conditions ranging from 3.8 mM as obtained by pH-shift measurements with isolated parasites [Elliott et al. *Biochem. J.* 2001] to actually non-saturable when determined as uptake of radiolabeled lactate into permeabilised, infected erythrocytes [Kanaani et al. *Cell. Physiol.* 1991]. This remembers of affinity determinations of *E. coli* lactose permease varying 100-fold upon changing the membrane potential, the transmembrane proton gradient, or transiting from intact cells to vesicle preparations [Kaczorowski et al. *Biochemistry* 1979]. Interestingly, equal to FNTs, a histidine is protonated during transduction [Abramson et al. *Science* 2003]. Likewise, when the external pH was shifted from 6.8 to 4.8, affinity of PfFNT for lactate increased about 5-fold probably due to a higher level of protonation of His230. There is reliable evidence that *P. falciparum* transports lactate in a proton symport manner [Kanaani et al. *Cell. Physiol.* 1991; Cranmer et al. *J. Biol. Chem.* 1995; Elliott et al. *Biochem. J.* 2001]. According to that, lactate transport via PfFNT increased with acidity and was maximal at pH 3.9, i.e. the pKa of lactate (figure 5.15).

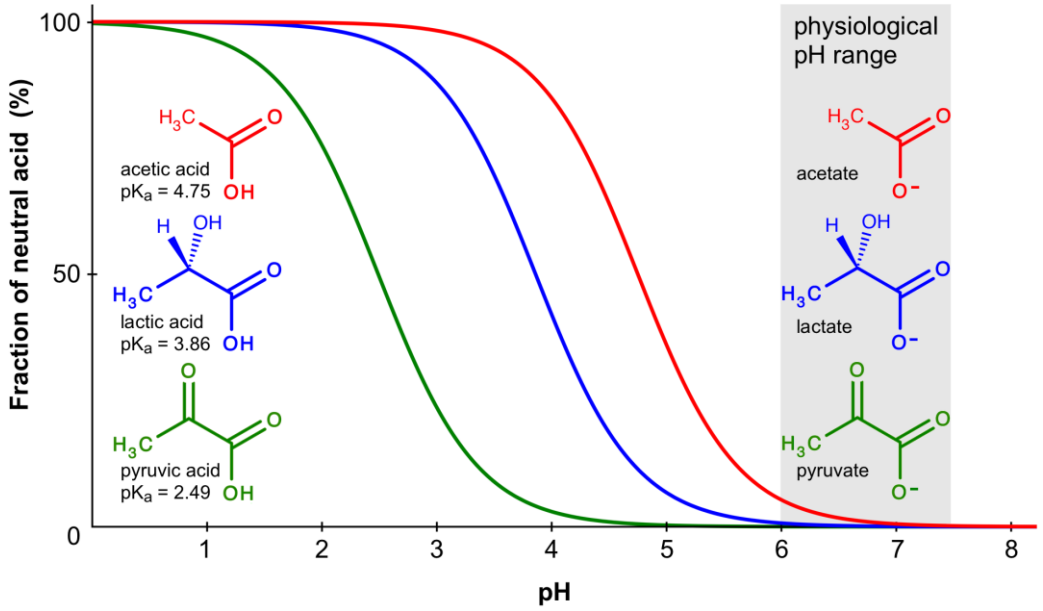

Figure 5.15 | pH dependent protonation states of monocarboxylates. Towards pH 6 there are negligible concentrations of the lactic acid apparent, while at pH 3.86 the anion to acid ratio is 1:1 (pH = pKa).

At this pH, protonated and deprotonated moieties are equimolar. Towards more acidic conditions, the proportion of lactate anions decreases as did the transport rate. When the curve is corrected for the lactate/lactic acid ratio using the Henderson-Hasselbalch equation a direct correlation of pH and lactate transport is visible. This implies lactate/proton symport at all tested pH conditions (figure 4.25). This hypothesis can be strengthened since transport ceased when proton decouplers such as CCCP and DNP were applied (figure 4.26) indicating that the transmembrane proton gradient fuels PfFNT lactate facilitation. Additionally Dr. Binghua Wu was able to show that uptake of L-lactate into yeast cells coincided with alkalization of the weakly buffered external medium. This happened in a concentration dependent manner directly showing lactate/proton co-transport (figure 4.27). Besides the possibility of an alternate proton uptake route could be excluded by blocking Nha1. This peptide is the yeasts potassium / proton antiporter which was disabled by using a high extracellular potassium concentration (figure 4.29). Finally PfFNT was able to transport lactate bidirectional. This is of certain importance when the physiological situation of the parasite inside the RBC is considered. Still, the exact transport mechanism trough PfFNT remains to be elucidated. First progress was achieved by confirming proton involvement and requirement of a hydrogen bond interaction partner at position 106 in the channel core. For this T106 has been mutated to valine and serine. Giving the hydroxyl group more room resulted in a 50% reduced transport rate while removal of the polar hydroxyl group (T106V) completely ceased transport (figure 4.32). This endorsed the hypothesized triad of the proton relay (figure 5.14). In this situation the hydrogen bond partner of the fixed water molecule was exchanged by a lipophilic side chain. Therefore the water molecule was no longer kept in place and the proton relay was interrupted. Furthermore a first hint for the relevance of the central histidine was caught by using the histidine modifying agent diethylpyrocarbonate (DEPC). When applied there was no measurable radiolabeled lactate permeation via PfFNT apparent. To found this conclusion a mutation of the charged residue to phenylalanine is necessary. This should abolish monocarboxylate facilitation like already shown for EcFocA [Lü et al. *Proc. Natl. Acad. Sci. USA* 2012]. These experiments could contribute to ascertain the prevailing transport theory for FNTs. Marie Wiechert continues further research on this topic.

Our experiments revealed two characteristics of PfFNT lactate transport. First, PfFNT accepts lactate in the anion form, which is protonated during transport most likely via the His230-water-Thr106 proton relay. Second, unlike FocA, PfFNT acts as a lactate/proton co-transporter throughout the measured pH range. Both properties are conforming to plasmodial physiology. The parasite resides inside the acidic parasitophorous vacuole (figure 1.3) [Ginsburg *Parasitol.* 2002], which by protonation reduces the quantity of local vacuolar lactate anions. Moreover, the retention time of lactate in the parasitophorous vacuole is kept low by

rapid release into the host's blood stream [Kanaani et al. *Cell. Physiol.* 1991; Ginsburg *Parasitol.* 2002]. Summarized, the outward gradient of lactate together with the anion selectivity of PfFNT drives transport in the export direction while the symport with protons prevents acidification of the parasite's cytosol.

The selectivity pattern of PfFNT is a little bit different to the one displayed by FocA [Lü et al. *Proc. Natl. Acad. Sci. USA* 2012]. Reasons for this must be found elsewhere than in the arrangement of the channel core since the two proteins are so close in structure in this region (figure 5.11). It is unlikely that this altered selectivity scheme is based on the only variation of the crucial pore lining amino acid composition, being phenylalanine (Phe94) instead of leucine. PfFNT transports besides other monovalent ion cargo molecules D-lactate comparable to the L enantiomer. This is consistent with the prevailing physiological state of *P. falciparum* in which as a non-enzymatic byproduct of glycolysis certain amounts of D-lactate (6-7% of total lactate) are produced in order to detoxify methylglyoxal [Vander et al. *Mol. Biochem. Parasitol.* 1990] (figure 5.16). The finding that dicarboxylates (malonate) and uncharged glycerol were not transducted fit into the affinity properties of FNTs.

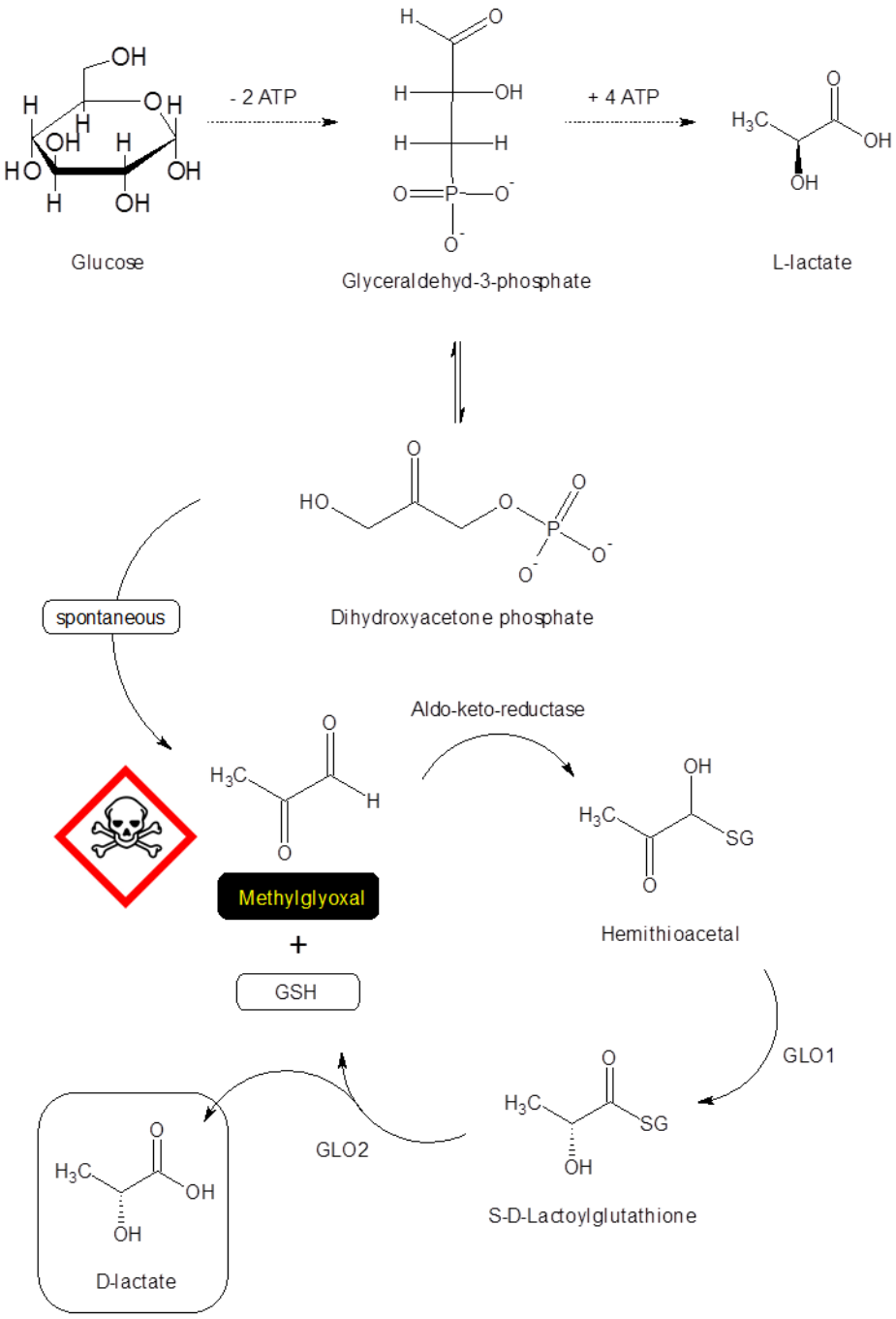

Figure 5.16 | D-lactate formation pathway in *Plasmodium falciparum*. During glycolysis glyceraldehyde-3-phosphate and in further steps dihydroxyacetone phosphate are generated. This can be converted via non-enzymatic phosphate elimination to the cytotoxic and mutagenic methylglyoxal. This is further detoxified via two glyoxalases and an aldo-keto reductase to D-lactate [Silva et al. *Int J Med Microbiol.*2012]. GSH = glutathione; GLO1 = glyoxalase 1; GLO2 = glyoxalase 2

5.4 PfFNT inhibition profile

The inhibition profile found matches earlier studies in living *P. falciparum* parasites. There was shown that certain compounds, such as phloretin, furosemide, and cinnamic acid derivatives, inhibit plasmodial lactate transport [Cranmer et al. *J. Biol. Chem.* 1995; Elliott et al. *Biochem. J.* 2001] and may lead to parasite death [Kanaani et al. *Antimicrob. Agents Chemother.* 1992]. Notably, the organomercurial pCMBS, that inhibits human MCTs by convalently binding to their essential ancillary proteins, basigin or embigin [Wilson et al. *J. Biol. Chem.* 2009], does not block *Plasmodium* lactate transport [Cranmer et al. *J. Biol. Chem.* 1995]. This is not surprising since FNTs operate without ancillary peptides as does PfFNT, respectively. Confirm with the *in vivo* data PfFNT was not inhibited by pCMBS. In our experiments, phloretin, furosemide, α-cyano-4-hydroxy-cinnamate, and α-fluorocinnamate inhibited PfFNT with IC50 values around 1 mM (figure 4.30). The inhibitory effect of the compounds reflects the data that were obtained from parasite (or infected RBC) experiments. For example α-flourocinnamate inhibited L-lactate uptake in a range of 47% to 69% while the biflavonoid phloretin had an effect of about 77%, both depending on the test system and the assay conditions [Kanaani et al. *Antimicrob. Agents Chemother.* 1992; Cranmer et al. *J. Biol. Chem.* 1995; Elliott et al. *Biochem. J.* 2001]. This thesis data fit to that with 65% inhibition effectivity of α-flourocinnamate and 73% for phloretin. Inhibition required a negatively charged moiety because the neutral cinnamamide was non-functional (figure 4.30).

There are several things that can be learned especially from the inhibition profile of PFNT. First and most important the inhibitor pattern of the plasmodial FNT in our heterologous expression system *S. cerevisiae* reflects the one found in living parasites. This finding, together with the fact that PfFNT-GFP fusion proteins were integrated into the plasmodial plasma membrane (figure 4.33), implies not only a physiological but also a chemotherapeutic addressable function of PfFNT in malaria therapy. Second, the curves obtained show a competitive inhibition of the transporter. This is most likely due to the fact that all chemicals (except phloretin and furosemide) have the functional group α-hydroxy-carboxylic acid as structural element mimicking lactate. The theory is that the bulkier aromatic elements of these molecules prohibit a transduction by getting stuck in the pore entrance of PfFNT. Even though these compounds offer no alternative for medical treatment of clinical malaria in humans since their affinity to the permease is too low, one could think of an alternate use. They could serve as a lead structure for an inhibitor which would have been chemically optimized to perfectly fit to the pore and with this have a much higher affinity than lactate. Prerequisite for this is a high resolution crystal structure of PfFNT. Experiments towards this goal are currently performed in this group. Third, FNT inhibitors could have the

potential to act as a novel class of antibiotics. We were able to inhibit EcFocA with α-flourocinnamate (figure 4.31). Although there won't be applicability for medical treatment of infections caused by *E. coli* (normal growth of a FocA knock out strain) [Tran et al. *Appl Microbiol Biotechnol* 2014] it might be for *Salmonella*. NirC is believed to be an important virulence factor and blockage of it could proof as a possible new drug target [Das et al. *Microbiology* 2009].

5.5 Outlook

In the future when the crystal structure of PfFNT will be revealed *in silico* designed and chemically synthetized inhibitors may ascertain whether the transporter is a valuable drug target in the fight against malaria or not. Nevertheless first inhibitor experiments targeting anion transporters revealed the potential to kill parasites *in vitro*. The basic requirements as a drug target are prevailing though. There is no sequence for a structural related protein apparent in the human genome which dramatically reduces the possibility of drug related side effects.

6 Literature

Aikawa M. The fine structure of the erythrocytic stages of three avian malarial parasites, *Plasmodium fallax, P. lophurae*, and *P. cathemerium. Am J Trop Med Hyg*. 1966; 15(4):449-71.

Abramson J, Smirnova I, Kasho V, Verner G, Kaback HR, Iwata S. Structure and mechanism of the lactose permease of *Escherichia coli. Science*. 2003; 301(5633):610-5.

Aurrecoechea C, Brestelli J, Brunk BP, Dommer J, Fischer S, Gajria B, Gao X, Gingle A, Grant G, Harb OS, Heiges M, Innamorato F, Iodice J, Kissinger JC, Kraemer E, Li W, Miller JA, Nayak V, Pennington C, Pinney DF, Roos DS, Ross C, Stoeckert CJ Jr, Treatman C, Wang H. PlasmoDB: a functional genomic database for malaria parasites*. Nucleic Acids Res*. 2009; 37(Database issue):D539-43.

Bártfai R, Hoeijmakers WA, Salcedo-Amaya AM, Smits AH, Janssen-Megens E, Kaan A, Treeck M, Gilberger TW, Françoijs KJ, Stunnenberg HG. H2A.Z demarcates intergenic regions of the *plasmodium falciparum* epigenome that are dynamically marked by H3K9ac and H3K4me3. *PLoS Pathog*. 2010; 6(12):e1001223.

Baudin A, Ozier-Kalogeropoulos O, Denouel A, Lacroute F, Cullin C. A simple and efficient method for direct gene deletion in *Saccharomyces cerevisiae*. *Nucleic Acids Res*. 1993; 21(14):3329-30.

Beitz E. T(E)Xtopo: shaded membrane protein topology plots in LAT(E)X2epsilon. *Bioinformatics*. 2000; 16(11):1050-1.

Beitz E. TEXshade: shading and labeling of multiple sequence alignments using LATEX2 epsilon. *Bioinformatics*. 2000; 16(2):135-9.

Bienert GP, Desguin B, Chaumont F, Hols P. Channel-mediated lactic acid transport: a novel function for aquaglyceroporins in bacteria. *Biochem J.* 2013; 454(3):559-70.

Bröer S, Schneider HP, Bröer A, Rahman B, Hamprecht B, Deitmer JW. Characterization of the monocarboxylate transporter 1 expressed in *Xenopus laevis* oocytes by changes in cytosolic pH. *Biochem J.* 1998; 333 (Pt 1):167-74.

Brooks JT, Elvidge GP, Glenny L, Gleadle JM, Liu C, Ragoussis J, Smith TG, Talbot NP, Winchester L, Maxwell PH, Robbins PA. Variations within oxygen-regulated gene expression in humans*. J Appl Physiol* (1985). 2009; 106(1):212-20.

Choi WG, Roberts DM. *Arabidopsis* NIP2;1, a major intrinsic protein transporter of lactic acid induced by anoxic stress. *J Biol Chem*. 2007; 282(33):24209-18.

Clegg S, Yu F, Griffiths L, Cole JA. The roles of the polytopic membrane proteins NarK, NarU and NirC in *Escherichia coli* K-12: two nitrate and three nitrite transporters. *Mol Microbiol*. 2002; 44(1):143-55.

Cori CF, Cori GT. Carbohydrate metabolism. *Annu Rev Biochem*. 1946; 15:193-218

Crabb BS, Cooke BM, Reeder JC, Waller RF, Caruana SR, Davern KM, Wickham ME, Brown GV, Coppel RL, Cowman AF. Targeted gene disruption shows that knobs enable malaria-infected red cells to cytoadhere under physiological shear stress. *Cell*. 1997; 89(2):287-96

Cranmer SL, Conant AR, Gutteridge WE, Halestrap AP. Characterization of the enhanced transport of L- and D-lactate into human red blood cells infected with *Plasmodium falciparum* suggests the presence of a novel saturable lactate proton cotransporter. *J Biol Chem*. 1995; 270(25):15045-52.

Crosnier C, Bustamante LY, Bartholdson SJ, Bei AK, Theron M, Uchikawa M, Mboup S, Ndir O, Kwiatkowski DP, Duraisingh MT, Rayner JC, Wright GJ. Basigin is a receptor essential for erythrocyte invasion by *Plasmodium falciparum. Nature*. 2011; 480(7378):534-7.

Csanády L, Mindell JA. The twain shall meet: channels, transporters and things between. Meeting on Membrane Transport in Flux: the Ambiguous Interface Between Channels and Pumps. *EMBO Rep*. 2008; 9(10):960-5.

Czyzewski BK, Wang DN. Identification and characterization of a bacterial hydrosulphide ion channel. *Nature*. 2012; 483(7390):494-7.

Das P, Lahiri A, Lahiri A, Chakravortty D. Novel role of the nitrite transporter NirC in *Salmonella* pathogenesis: SPI2-dependent suppression of inducible nitric oxide synthase in activated macrophages. *Microbiology*. 2009; 155(Pt 8):2476-89.

de Kok S, Nijkamp JF, Oud B, Roque FC, de Ridder D, Daran JM, Pronk JT, van Maris AJ. Laboratory evolution of new lactate transporter genes in a jen1Δ mutant of *Saccharomyces cerevisiae* and their identification as ADY2 alleles by whole-genome resequencing and transcriptome analysis. *FEMS Yeast Res*. 2012.

DeCoursey TE, Hosler J. Philosophy of voltage-gated proton channels. *J R Soc Interface*. 2013; 11(92):20130799.

Desai SA, Krogstad DJ, McCleskey EW. A nutrient-permeable channel on the intraerythrocytic malaria parasite. *Nature.* 1993; 362(6421):643-6.

Dimmer KS, Friedrich B, Lang F, Deitmer JW, Bröer S. The low-affinity monocarboxylate transporter MCT4 is adapted to the export of lactate in highly glycolytic cells. *Biochem J*. 2000; 350 Pt 1:219-27.

Elliott JL, Saliba KJ, Kirk K. Transport of lactate and pyruvate in the intraerythrocytic malaria parasite, *Plasmodium falciparum*. *Biochem J*. 2001; 355(Pt 3):733-9.

Faghiri Z, Camargo SM, Huggel K, Forster IC, Ndegwa D, Verrey F, Skelly PJ. The tegument of the human parasitic worm *Schistosoma mansoni* as an excretory organ: the surface aquaporin SmAQP is a lactate transporter. *PLoS One*. 2010; 5(5):e10451.

Francia ME, Striepen B. Cell division in apicomplexan parasites. *Nat Rev Microbiol*. 2014; 12(2):125-36.

Gardner MJ, Hall N, Fung E, White O, Berriman M, Hyman RW, Carlton JM, Pain A, Nelson KE, Bowman S, Paulsen IT, James K, Eisen JA, Rutherford K, Salzberg SL, Craig A, Kyes S, Chan MS, Nene V, Shallom SJ, Suh B, Peterson J, Angiuoli S, Pertea M, Allen J, Selengut J, Haft D, Mather MW, Vaidya AB, Martin DM, Fairlamb AH, Fraunholz MJ, Roos DS, Ralph SA, McFadden GI, Cummings LM, Subramanian GM, Mungall C, Venter JC, Carucci DJ, Hoffman SL, Newbold C, Davis RW, Fraser CM, Barrell B. Genome sequence of the human malaria parasite *Plasmodium falciparum. Nature*. 2002; 419(6906):498-511.

Ginsburg H. Abundant proton pumping in *Plasmodium falciparum*, but why? *Trends Parasitol*. 2002; 18(11):483-6.

Halestrap AP. The monocarboxylate transporter family--Structure and functional characterization. *IUBMB Life*. 2012; 64(1):1-9.

Halestrap AP. The SLC16 gene family - structure, role and regulation in health and disease. *Mol Aspects Med*. 2013; 34(2-3):337-49.

Heiber A, Kruse F, Pick C, Grüring C, Flemming S, Oberli A, Schoeler H, Retzlaff S, Mesén-Ramírez P, Hiss JA, Kadekoppala M, Hecht L, Holder AA, Gilberger TW, Spielmann T. Identification of new PNEPs indicates a substantial non-PEXEL exportome and underpins common features in *Plasmodium falciparum* protein export. *PLoS Pathog*. 2013; 9(8):e1003546.

Hille B. Ionic channels in excitable membranes. Current problems and biophysical approaches. *Biophys J*. 1978; 22(2):283-94

Jia W, Tovell N, Clegg S, Trimmer M, Cole J. A single channel for nitrate uptake, nitrite export and nitrite uptake by *Escherichia coli* NarU and a role for NirC in nitrite export and uptake. *Biochem J.* 2009; 417(1):297-304.

Kabil O, Banerjee R. Redox biochemistry of hydrogen sulfide. *J Biol Chem*. 2010; 285(29):21903-7.

Kaczorowski GJ, Kaback HR. Mechanism of lactose translocation in membrane vesicles from *Escherichia coli*. 1. Effect of pH on efflux, exchange, and counterflow. *Biochemistry*. 1979; 18(17):3691-7.

Kanaani J, Ginsburg H. Effects of cinnamic acid derivatives on in vitro growth of *Plasmodium falciparum* and on the permeability of the membrane of malaria-infected erythrocytes. *Antimicrob Agents Chemother*. 1992; 36(5):1102-8.

Kanaani J, Ginsburg H. Transport of lactate in *Plasmodium falciparum*-infected human erythrocytes. *J Cell Physiol*. 1991; 149(3):469-76.

Kobayashi M, Otsuka Y, Itagaki S, Hirano T, Iseki K. Inhibitory effects of statins on human monocarboxylate transporter 4. *Int J Pharm*. 2006; 317(1):19-25.

Krungkrai J, Burat D, Kudan S, Krungkrai S, Prapunwattana P. Mitochondrial oxygen consumption in asexual and sexual blood stages of the human malarial parasite, *Plasmodium falciparum*. *Southeast Asian J Trop Med Public Health*. 1999; 30(4):636-42.

Kumar S, Bandyopadhyay U. Free heme toxicity and its detoxification systems in human. *Toxicol Lett.* 2005; 157(3):175-88.

Liu J, Istvan ES, Gluzman IY, Gross J, Goldberg DE. *Plasmodium falciparum* ensures its amino acid supply with multiple acquisition pathways and redundant proteolytic enzyme systems. *Proc Natl Acad Sci U S A*. 2006; 103(23):8840-5.

Liu S, Lockless SW. Equilibrium selectivity alone does not create K+-selective ion conduction in K+ channels. *Nat Commun*. 2013; 4:2746.

Lü W, Du J, Schwarzer NJ, Wacker T, Andrade SL, Einsle O. The formate/nitrite transporter family of anion channels. *Biol Chem*. 2013; 394(6):715-27.

Lü W, Du J, Wacker T, Gerbig-Smentek E, Andrade SL, Einsle O. pH-dependent gating in a FocA formate channel. *Science*. 2011; 332(6027):352-4.

Makuc J, Paiva S, Schauen M, Krämer R, André B, Casal M, Leão C, Boles E. The putative monocarboxylate permeases of the yeast *Saccharomyces cerevisiae* do not transport monocarboxylic acids across the plasma membrane. *Yeast*. 2001; 18(12):1131-43.

Manning Fox JE, Meredith D, Halestrap AP. Characterisation of human monocarboxylate transporter 4 substantiates its role in lactic acid efflux from skeletal muscle. *J Physiol*. 2000; 529 Pt 2:285-93.

Manoharan C, Wilson MC, Sessions RB, Halestrap AP. The role of charged residues in the transmembrane helices of monocarboxylate transporter 1 and its ancillary protein basigin in determining plasma membrane expression and catalytic activity. *Mol Membr Biol*. 2006; 23(6):486-98

Markus MB. The hypnozoite concept, with particular reference to malaria. *Parasitol Res*. 2011; 108(1):247-52.

Martínez-Muñoz GA, Kane P. Vacuolar and plasma membrane proton pumps collaborate to achieve cytosolic pH homeostasis in yeast. *J Biol Chem*. 2008; 283(29):20309-19.

McKee RW, Ormsbee RA, Anfinsen CB, Geiman QM, Ball EG. Studies on malarial parasites : VI. The chemistry and metabolism of normal and parasitized (*p. Knowlesi*) monkey blood. *J Exp Med*. 1946; 84(6):569-82.

McLaughlin SG, Dilger JP. Transport of protons across membranes by weak acids. *Physiol Rev*. 1980; 60(3):825-63.

Miller LH, Roberts T, Shahabuddin M, McCutchan TF. Analysis of sequence diversity in the *Plasmodium falciparum* merozoite surface protein-1 (MSP-1). *Mol Biochem Parasitol*. 1993; 59(1):1-14.

Morelli A, Benatti U, Gaetani GF, De Flora A. Biochemical mechanisms of glucose-6-phosphate dehydrogenase deficiency. *Proc Natl Acad Sci U S A*. 1978; 75(4):1979-83.

Nene V, Shallom SJ, Suh B, Peterson J, Angiuoli S, Pertea M, Allen J, Selengut J, Haft D, Mather MW, Vaidya AB, Martin DM, Fairlamb AH, Fraunholz MJ, Roos DS, Ralph SA, McFadden GI, Cummings LM, Subramanian GM, Mungall C, Venter JC, Carucci DJ, Hoffman SL, Newbold C, Davis RW, Fraser CM, Barrell B. Genome sequence of the human malaria parasite *Plasmodium falciparum. Nature*. 2002; 419(6906):498-511.

Olszewski KL, Llinás M. Central carbon metabolism of *Plasmodium* parasites. *Mol Biochem Parasitol*. 2011; 175(2):95-103.

Otto M, Rapoport TA, Heinrich R. An extended model of the glycolysis in erythrocytes. *Acta Biol Med Ger*. 1977; 36(3-4):461-8.

Paiva S, Devaux F, Barbosa S, Jacq C, Casal M. Ady2p is essential for the acetate permease activity in the yeast *Saccharomyces cerevisiae*. *Yeast*. 2004; 21(3):201-10.

Payandeh J, Pfoh R, Pai EF. The structure and regulation of magnesium selective ion channels. *Biochim Biophys Acta*. 2013; 1828(11):2778-92.

Poole RC, Halestrap AP. Transport of lactate and other monocarboxylates across mammalian plasma membranes. *Am J Physiol*. 1993; 264(4 Pt 1):C761-82.

Rambow J, Wu B, Rönfeldt D, Beitz E. Aquaporins with anion/monocarboxylate permeability: mechanisms, relevance for pathogen-host interactions. *Front Pharmacol*. 2014; 5:199.

Roigas H, Dietze F, Rapoport S, Sauer G. On the effect of glycolytic intermediary products on the 2,3-PGase activity of red blood cells. *Folia Haematol Int Mag Klin Morphol Blutforsch*. 1965; 83(4):383-8.

Roth E Jr. *Plasmodium falciparum* carbohydrate metabolism: a connection between host cell and parasite. *Blood Cells*. 1990; 16(2-3):453-60.

Rudzinska MA. The fine structure of malaria parasites. *Int Rev Cytol*. 1969; 25:161-99.

Rychkov GY, Pusch M, Roberts ML, Jentsch TJ, Bretag AH. Permeation and block of the skeletal muscle chloride channel, ClC-1, by foreign anions. *J Gen Physiol*. 1998; 111(5):653-65.

Saier MH Jr, Eng BH, Fard S, Garg J, Haggerty DA, Hutchinson WJ, Jack DL, Lai EC, Liu HJ, Nusinew DP, Omar AM, Pao SS, Paulsen IT, Quan JA, Sliwinski M, Tseng TT, Wachi S, Young GB. Phylogenetic characterization of novel transport protein families revealed by genome analyses. *Biochim Biophys Acta*. 1999; 1422(1):1-56.

Saliba KJ, Horner HA, Kirk K. Transport and metabolism of the essential vitamin pantothenic acid in human erythrocytes infected with the malaria parasite *Plasmodium falciparum*. *J Biol Chem*. 1998; 273(17):10190-5.

Sanchez MA. Molecular identification and characterization of an essential pyruvate transporter from *Trypanosoma brucei*. *J Biol Chem*. 2013; 288(20):14428-37.

Sawers G. The hydrogenases and formate dehydrogenases of *Escherichia coli*. *Antonie Van Leeuwenhoek*. 1994; 66(1-3):57-88.

Sawers RG. Differential turnover of the multiple processed transcripts of the *Escherichia coli* focA-pflB operon. *Microbiology*. 2006; 152(Pt 8):2197-205.

Scheibel LW, Ashton SH, Trager W. *Plasmodium falciparum*: microaerophilic requirements in human red blood cells. *Exp Parasitol*. 1979; 47(3):410-8.

Smith RC, Vega-Rodríguez J, Jacobs-Lorena M. The *Plasmodium* bottleneck: malaria parasite losses in the mosquito vector. *Mem Inst Oswaldo Cruz*. 2014; 109(5):644-61.

Soares-Silva I, Paiva S, Diallinas G, Casal M. The conserved sequence NXX[S/T]HX[S/T]QDXXXT of the lactate/pyruvate:H(+) symporter subfamily defines the function of the substrate translocation pathway. *Mol Membr Biol*. 2007; 24(5-6):464-74.

Sousa Silva M, Ferreira AE, Gomes R, Tomás AM, Ponces Freire A, Cordeiro C. The glyoxalase pathway in protozoan parasites. *Int J Med Microbiol*. 2012; 302(4-5):225-9.

Stephenson M, Stickland LH. Hydrogenlyases: Bacterial enzymes liberating molecular hydrogen. *Biochem J*. 1932; 26(3):712-24.

Stokes JL. Fermentation of glucose by suspensions of *Escherichia coli*. *J Bacteriol*. 1949; 57(2):147-58.

Sui H, Han BG, Lee JK, Walian P, Jap BK. Structural basis of water-specific transport through the AQP1 water channel. *Nature*. 2001; 414(6866):872-8.

Suppmann B, Sawers G. Isolation and characterization of hypophosphite--resistant mutants of *Escherichia coli*: identification of the FocA protein, encoded by the pfl operon, as a putative formate transporter. *Mol Microbiol*. 1994; 11(5):965-82.

Torrentino-Madamet M, Desplans J, Travaillé C, James Y, Parzy D. Microaerophilic respiratory metabolism of *Plasmodium falciparum* mitochondrion as a drug target. *Curr Mol Med.* 2010; 10(1):29-46.

Trager W, Jensen JB. Human malaria parasites in continuous culture. *Science*. 1976; 193(4254):673-5.

Tran KT, Maeda T, Wood TK. Metabolic engineering of *Escherichia coli* to enhance hydrogen production from glycerol. *Appl Microbiol Biotechnol*. 2014; 98(10):4757-70.

Tsukaguchi H, Shayakul C, Berger UV, Mackenzie B, Devidas S, Guggino WB, van Hoek AN, Hediger MA. Molecular characterization of a broad selectivity neutral solute channel. *J Biol Chem*. 1998; 273(38):24737-43.

Vander Jagt DL, Hunsaker LA, Campos NM, Baack BR. D-lactate production in erythrocytes infected with *Plasmodium falciparum*. *Mol Biochem Parasitol*. 1990; 42(2):277-84.

van Dooren GG, Stimmler LM, McFadden GI. Metabolic maps and functions of the *Plasmodium* mitochondrion. *FEMS Microbiol Rev*. 2006; 30(4):596-630.

Waight AB, Czyzewski BK, Wang DN. Ion selectivity and gating mechanisms of FNT channels. *Curr Opin Struct Biol*. 2013; 23(4):499-506.

Waight AB, Love J, Wang DN. Structure and mechanism of a pentameric formate channel. *Nat Struct Mol Biol*. 2010; 17(1):31-7.

Waller RF, McFadden GI. The apicoplast: a review of the derived plastid of apicomplexan parasites. *Curr Issues Mol Biol*. 2005; 7(1):57-79.

Wang Y, Huang Y, Wang J, Cheng C, Huang W, Lu P, Xu YN, Wang P, Yan N, Shi Y. Structure of the formate transporter FocA reveals a pentameric aquaporin-like channel. *Nature*. 2009; 462(7272):467-72.

Wassmer SC, Combes V, Grau GE. Pathophysiology of cerebral malaria: role of host cells in the modulation of cytoadhesion. *Ann N Y Acad Sci*. 2003; 992:30-8.

Wilson MC, Meredith D, Bunnun C, Sessions RB, Halestrap AP. Studies on the DIDS-binding site of monocarboxylate transporter 1 suggest a homology model of the open conformation and a plausible translocation cycle. *J Biol Chem*. 2009; 284(30):20011-21.

Worthington DJ, Rosemeyer MA. Glutathione reductase from human erythrocytes. Catalytic properties and aggregation. *Eur J Biochem*. 1976; 67(1):231-8.

Yasui M, Hazama A, Kwon TH, Nielsen S, Guggino WB, Agre P. Rapid gating and anion permeability of an intracellular aquaporin. *Nature*. 1999; 402(6758):184-7.

Publications

Rambow J, Wu B, Rönfeldt D, Beitz E. Aquaporins with anion/monocarboxylate permeability: mechanisms, relevance for pathogen-host interactions. *Front Pharmacol.* 2014; doi: 10.3389

Rambow J, Wu B, Bock S, Holm-Bertelsen J, Wiechert M, Blancke-Soares A, Spielmann T, Beitz E. Identity of a *Plasmodium* lactate/H+ symporter structurally unrelated to human transporters. *Nat. Commun.* 2015; currently under review

Acknowledgements

It is well-known that state of the art science is a multitasking challenge where well-rehearsed teams achieve goals that one alone could never accomplish. This team does not end at the doorstep of the workplace. Without all of you - your support, your care and your aid this thesis would have never been written. I am deeply grateful for this, thank you.

First of all I would like to thank my advisor Eric for giving me the opportunity to do what I love – gain knowledge in fields no one has ever explored before. His door is always open for asking questions and discussing problems and I never left his office without new ideas or a better understanding of my results.

Furthermore I would like to thank my colleagues for the good working atmosphere. We have a great team where everybody offers a helping hand when needed. My special thanks go to Ellen and Sinja, we had a great time together in the office.

Also I would like to thank Dirk Böhme. His ideas and inventions were not only helpful without him there would be no radioactive assay at all. And I had a lot of good chats with him.

Moreover I owe thanks to my colleagues who took care of the students in the second semester with me. Each semester, after the first days when we were more or less certain that none of the students would cause a major explosion, we enjoyed the time together. I will certainly miss the days when we got handed over the record cards for each semester.

In addition I would like to thank my friends, those which I had before I started my thesis and those which I met during doing it. I will always keep good memory of going out for lunch at the mensa with a coffee afterwards or having a party.

Last but not least I thank my family, my parents and my little brother. You not only supported me in every way, you are my backbone and my home. I love you with all my heart.

Curriculum Vitae

Janis Rambow
geboren am: 13.03.1984
geboren in: Kiel
Nationalität Deutsch

Schule und Studium

2004 Abitur, Hebbelschule Kiel
2005 Zivildienst, mobile Frühförderung Kiel
2009 zweites Staatsexamen Pharmazie, Universität zu Kiel
2010 Apotheker im praktischen Jahr, Planton GmbH Kiel
2010 Apotheker im praktischen Jahr, Esmarch Apotheke Kiel
2011 Approbation als Apotheker

Promotion

seit 2011 Wissenschaftlicher Mitarbeiter am pharmazeutischen Institut unter Leitung von Prof. Dr. E. Beitz,
Abteilung pharmazeutische und medizinische Chemie,
Christian-Albrechts-Universität zu Kiel

Eidesstattliche Erklärung

Hiermit versichere ich, dass ich die vorliegende Abhandlung, abgesehen von der Beratung durch den Betreuer, selbstständig verfasst und keine anderen als die angegebenen Quellen und Hilfsmittel benutzt habe, dass alle Stellen der Arbeit, die wörtlich oder sinngemäß aus anderen Quellen übernommen wurden, als solche kenntlich gemacht sind. Die Arbeit wurde bisher in gleicher oder ähnlicher Form noch keiner Prüfungsbehörde vorgelegt.

Die Arbeit ist unter Einhaltung der Regeln zur guten wissenschaftlichen Praxis der Deutschen Forschungsgemeinschaft entstanden.

Kiel, den 06. Januar 2015
Janis Rambow